IRPL-R24

RELATIONS BETWEEN BAND WIDTH, PULSE SHAPE AND USEFULNESS OF PULSES IN THE LORAN SYSTEM

ISSUED

12 OCTOBER, 1945

PREPARED BY INTERSERVICE RADIO PROPAGATION LABORATORY
National Bureau of Standards
Washington , D. C.

IRPL-R24 INTERSERVICE RADIO PROPAGATION LABORATORY
NATIONAL BUREAU OF STANDARDS
WASHINGTON, D.C.
Organized under Joint U.S. Communications Board

Issued
10 Oct. 1945

RELATIONS BETWEEN BAND WIDTH, PULSE SHAPE, AND USEFULNESS OF PULSES IN THE LORAN SYSTEM.

Contents

I. Introduction

a. The National Bureau of Standards was requested by letter of 19 January 1945 (Serial C-935-1178a) from the Bureau of Ships, U.S. Navy Department, to study certain transmitter and receiver problems directly applicable to the design of Loran equipment. This report covers the results of the work done on this project, as of the date of this report.

The problems specifically outlined in the Bureau of Ships' letter of 19 January (paragraph 3) are as follows:

> "(a) Using as a standard, the pulse pattern as observed with present equipment, determine the extent to which the emitted frequency band may be restricted without appreciably affecting the leading edge of the pulse.
>
> "(b) With the same pulse pattern as a standard, determine the extent to which the receiver band width may be restricted without appreciably affecting the precision of measurement.
>
> "(c) As a more general problem, determine the optimum pulse pattern (particularly the leading edge) for maximum accuracy commensurate with minimum interference and maximum signal to noise ratio.
>
> "(d) Improvement of the emission characteristic of transmitters now in service. (It is hoped that sufficient circuit design information might result from this work to enable the problem of equipment modification design to be turned over to a commercial firm)."

b. A more detailed discussion of factors involved in these problems is contained in the Bureau of Ships memorandum of 16 November 1944 (Serial M-935-987a), "Notes of General Problem of Optimum Emitted Loran Pulse Shape and Receiver Band Width." The practical application, to the Loran system, of the information desired from this investigation is summarized under the section entitled "Trace Stability" of the above memorandum, and is herewith quoted.

> "The principal transmission factors which result in instability of the Loran traces are radio noise and interference. Usually the duration of such interfering noise and signals is long, or at least comparable with the duration of the Loran pulse signals so that the result is an upward displacement of the pulse. If, now, the leading edge of the pulse were vertical, there would not be any horizontal translation of the trace. At angles other than vertical, there will however be a translation proportional to the cosine of the angle.
>
> "In general, it is desired to obtain as steep a slope as possible of the leading edge of the pulse and at the same time

reduce the effect of noise and interference. Unfortunately these two cannot be obtained entirely independent of each other. The steepness of the slope of the leading edge of the pulse trace is in part due to the shape of the emitted pulse and in part due to the shaping by the receiver-indicator. However, with a given emitted pulse, narrowing the receiver band to reduce noise will tend to widen out the pulse shape and reduce the steepness of the pulse.

"Linked with the steepness of the emitted pulse is the important consideration of the amplitude-frequency distribution of the radio frequency components which contribute to the shape of the pulse, viz, the steeper the pulse, the greater the space occupied in the frequency spectrum.

"The overall problem involves therefore both the receiver and the transmitter characteristics. From the receiver standpoint it is desired to restrict the band so as to keep noise and interference to a minimum and yet keep the band sufficiently wide so as not to reduce the pulse slope and impair the measurement accuracy. From the standpoint of the transmitter, it is desired to restrict the frequency band of the radiated components so as to avoid interference with other Loran channels and other services and yet wide enough to provide a satisfactory pulse shape and also not to complicate the transmitter equipment unduly."

II. Description of Special Equipment.

a. Radio-frequency pulse generator.

In order to proceed with the investigation of the Bureau of Ships problem it was deemed necessary to design and construct a pulse generator, capable of producing radio-frequency pulses of various lengths and shapes, and a radio-frequency receiver from which various radio-frequency band widths could be obtained.

The radio-frequency pulse generator was modeled after the regular Loran transmitters. It consisted of an exciter, a modulator, and a self-excited oscillator. Photographs of this equipment are shown in Figs. 1 and 2.

The exciter produced a d-c pulse, of approximately 450 volts amplitude. The pulse length could be controlled over a range of from 20 to 100 microseconds. The recurrence of the exciter pulse was precisely maintained by means of a Model B-1 Loran timer. A circuit diagram of the exciter unit is shown in Fig. 3. Circuit constants and operating voltages are shown in Tables I and II.

Radio-frequency pulses were produced by a tuned-grid tuned-plate oscillator, keyed in the cathode circuit by means of a modulator tube, which in turn was controlled by the exciter output. The circuit diagram

of the modulator and oscillator is shown in Fig. 4. Circuit constants and operating voltages are given in Tables III and IV.

The equipment was made adjustable to a variety of pulse shapes by employing variable controls and adding additional circuit components. Adjustable controls, most of which were of the screwdriver type, are shown in Fig. 1, and may be located on the schematic diagrams in Figs. 3 and 4 by referring to Table 5. Control "A" was provided to adjust the output amplitude of the d-c pulses from the exciter unit. The control grid-bias voltage on the oscillator tubes was varied by adjusting control "D". Adjustment "E" was provided for changing the oscillator feedback voltage. The loading on the oscillator could be changed by adjusting control "F".

The length of the pulse could be adjusted in steps by changing the position of the taps on inductance "L_1" in Fig. 3. As more inductance was added the pulse length became greater. Vernier adjustment of the pulse length could be obtained by varying control "A".

The top and bottom of rectangular pulses could be made almost parallel with the base line or slanted by changing the value of storage capacitor "C_g" in Fig. 4. The lower the capacitance used at this point, the greater was the slant of the top and bottom of the radio-frequency pulse. A capacitance of 2 microfarads provided almost a perfect rectangular pulse.

The circuit components in the diagrams of Figs. 3 and 4 were used to obtain the regular Loran-type pulses. The leading edge of this pulse could be rounded a small amount by adjustment of the oscillator feedback control "D". More rounding could be obtained by inserting a choke coil in the cathode circuit of the oscillator as shown in Fig. 6A. The leading edge of the pulse could be made less round and the rise time reduced to approximately 2.5 microseconds by changing the 6J5 tubes, V2 and V3 (Fig. 4), to 6L6 tubes, triode-connected.

The lagging edge of the pulse could be rounded by inserting a choke coil and capacitor network in the input of the modulator circuit. This arrangement is shown in Fig. 6B. The length of the tail on the lagging edge of the pulse could be changed by means of the load coupling control "F", or by changing the value of the load resistor "R_{15}" in Fig. 4.

Table I

Parts List of Exciter Unit of Radio-Frequency Pulse Generator

Resistors

Symbol No.	Description	
	Ohms	Watt
R1	100	1
R2	50000	1
R3	50000	1
R4	50000	1
R5	200	1

Table I (continued)

Resistors (continued)

Symbol No.	Description	
	Ohms	Watt
R6	20000	1
R7	100000	1
R8	100000	1
R9	100000	1
R10	100000	1
R11	500	1
R12	1000000	1
R13	25000	1
R14	50	1
R15	100000	1
R16	250000	1
R17	50	1
R18	10000	1
R19	50000	1
R20	1000000	1
R21	1000000	1
R22	2000 - potentiometer	
R23	200	1
R24	250000	1
R25	250000	1
R26	100000	1
R27	100000	1
R28	150000	1
R29	100000 adjustable	25
R30	150000	1
R31	150000	1
R32	50000	1
R33	50000	1
R34	500000	1
R35	50000	1

Capacitors

		Volt
C1	100 μμf	600
C2	0.01 μf	600
C3	25 μf	25
C4	0.01 μf	600
C5	0.01 μf	600
C6	0.01 μf	600
C7	0.022 μf	600
C8	50 μμf	600
C9	0.005 μf	1000
C10	0.01 μf	600
C11	1 μf	1000
C12	2 μf	1000
C13	2 μf	1000
C14	2 μf	600
C15	0.5 μf	600
C16	0.5 μf	600

Table I (continued)

Tubes

Symbol No.	Description
V1	Type 6SN7
V2	Type 6X5
V3	Type 2050
V4	Type 807
V5	Type 5Y3
V6	Type 5Y3

Coils

L1	40 mh total, taps at every 8 mh

Transformers

T1	Primary 110 v, secondary 5-v winding, 6.3-v winding, 600-v winding center tapped.
T2	Primary 110 v, secondary 5 v
T3	Primary 110 v, secondary 6.3 v.

Miscellaneous

S1	D.P.S.T. switch
F1	1-amp. fuse
K1	Input testing phone jack
K2	Output testing phone jack

Table II

Typical Operation Voltages for Exciter Unit

All measurements made with a vacuum-tube voltmeter and are positive with respect to ground unless otherwise indicated.

Tube Symbol	Tube Type	Pin No.	Direct-Current Voltage
V1	6SN7	1	0
		2	137
		3	3.4
		4	0
		5	190
		6	3.4

Table II (continued)

Tube Symbol	Tube Type	Pin No.	Direct-Current Voltage
V2	6X5	3, 4 and 8	-220 (varies from -200 to -240 with setting of bias control R33)
V3	2050	3	470
		5	-220 (varies from -200 to -240 with setting of bias control R33)
		6 and 8	-167
V4	807	T.C.	680
		2	565
		3	-580
		4	-172
V5	5Y3	2 and 8	-175
		4 and 6	-625
V6	5Y3	2 and 8	710
		4 and 6	-175

Table III

Parts List of Oscillator and Modulator Unit of Radio-Frequency Pulse Generator.

Symbol	Description		
	Resistors	Ohms	Watt
R1		150000	1
R2		50	1
R3		20000	1
R4		50	1
R5		150000	1
R6		500	1
R7		2000	1
R8		300	1
R9		100	1
R10		50	1
R11		50	1
R12		50	1
R13		50	1
R14		2000	1
R15		50	1
	Condensers		
			Volts
C1		0.01 μf	600
C2		1.0 μf	600
C3		1.0 μf	600
C4		1.0 μf	1000

Table III (continued)

Symbol	Description	
	Condensers (continued)	
		Volts
C5	0.005 µf	600
C6	2-gang variable, 100 µµf per section	
C7	split stator, 100 µµf per section	
C8	0.15 µf	600
C9	2-gang variable, 100 µµf per section	
C10	0.0004 µµf	1000
C11	0.1500 µµf	1000
C12	0.0004 µµf	1000
C13	200 µµf variable	
C14	0.0008 µf	1000
	Transformers	
T1	Primary 110 v, secondary 6.3 v	
T2	Primary 110 v, secondary 6.3 v	
	Coils	
L1	100 µh	
L2	40 µh	
L3	6.8 µh	
L4	10 µh	
L5	4 mh	
L6	40 mh	
L7	1.2 µh	
L8	1.2 µh	
	Tubes	
	Type	
V1	807	
V2	6J5	
V3	6J5	

Table IV

Typical Operating Voltages for Oscillator and Modulator Unit

All measurements made with a vacuum-tube voltmeter and are positive with respect to ground unless otherwise indicated.

Tube Symbol	Tube Type	Pin No.	Direct-Current Voltage
V1	807	TC	45
		2	45
		3	-170
		4	0

Table IV (continued)

Tube Symbol	Tube Type	Pin No.	Direct-Current Voltage
V2 and V3	6J7	3	600
		5	5.5 (varies from 0 to 112 with setting of bias control R16)
		8	60 (varies from 47 to 142 with setting of bias control R16)

Table V

Adjustable Controls on the Radio-Frequency Pulse Generator

Symbol on Photograph in Fig. 1	Symbol on Schematic Diagram	Function
A	R22 in Fig. 3	Exciter output amplitude.
B	R3 in Fig. 3	Exciter input amplitude.
C	R33 in Fig. 3	2050 tube grid-bias voltage.
D	R16 in Fig. 4	Grid-bias voltage on 6J5 tubes.
E	C6 in Fig. 4	Oscillator feedback voltage.
F	L3 and L4 in Fig. 4	Oscillator loading.
G	C9 in Fig. 4	Oscillator plate tuning.
H	C7 in Fig. 4	Oscillator grid tuning

b. Variable band-width receiver.

A National NC100 receiver was modified to permit varying the radio-frequency band width from approximately 10 to 80 kilocycles, at the half-power point. The major change was the replacement of the regular intermediate-frequency transformers with variable coupling intermediate-frequency transformers and the provision for damping resistors across all tuned circuits. In order to maintain a reasonable receiver gain at the wide band widths it was found desirable to add an extra intermediate-frequency stage to the original receiver. A circuit diagram of the modified receiver is shown in Fig. 7. The receiver output, from the second detector, was fed to the grid of the video state of a Fada Model LRN-1 receiver and through the regular circuits to the oscilloscope of an LRN-1A indicator.

Different receiver band widths were obtained by varying the coupling of the intermediate-frequency transformer windings and the damping across the tuned circuits. As the coupling was increased, wider band widths were obtained. Tendencies toward double-humped response curves were minimized by reducing the resistance of the damping resistors as the coupling was increased.

III. Method of Investigation.

a. Transmitter pulse shape.

1. Fourier analysis of frequency components.- The frequency components of a few simple d-c pulses, comparable in length and recurrence rate to the pulses transmitted by the regular Loran installations, were calculated by means of Fourier expansions. These frequencies were assumed to represent the deviations, from the carrier frequency, of the side-band frequencies of a radio-frequency pulse having an envelope identical in shape to each of the calculated d-c pulses. The relative amplitudes of the side-band currents were plotted for frequencies above and below the carrier frequency, illustrating the effect of pulse shape upon side-band radiation.

The pulse-frequency components were calculated from the following relationships:

$$f(x) = 1/2\ A_0 + A_1 \cos x + A_2 \cos 2x + A_3 \cos 3x + \ldots\ldots A_n \cos nx + B_1 \sin x + B_2 \sin 2x + B_3 \sin 3x + \ldots\ldots B_n \sin nx$$

where:

$$A_n = \frac{1}{\pi} \int_{-\pi}^{\pi} f(x) \cos nx \ dx \qquad \text{for: } n = 0, 1, \ldots\ldots$$

$$B_n = \frac{1}{\pi} \int_{-\pi}^{\pi} f(x) \sin nx \ dx \qquad \text{for: } n = 1, 2, \ldots\ldots$$

and:

$$f(x) = K_0 + K_1 \sin (x + \theta_1) + K_2 \sin (2x + \theta_2) + \ldots K_n \sin (nx + \theta_n)$$

where:

$$K_0 = 1/2\ A_0$$

$$K_n = \sqrt{A_n^2 + B_n^2}$$

$$\theta_n = \tan^{-1} \left[\frac{A_n}{B_n}\right]$$

2. Measurement of frequency components.- Pulses of different shapes were produced by the radio-frequency pulse generator, and the frequency components were measured by means of a National HRO receiver. The values so obtained were compared with frequency components calculated in the manner previously described.

The amplitudes of the side bands of a pulse approaching as nearly as possible the shape of the regular Loran transmitter pulses were measured with the HRO receiver and compared with similar measurements made on the same pulse after passing through a radio-frequency filter.

b. Receiver band-width characteristics.

Various receiver band width were obtained and tracings, from the indicator oscilloscope, were made of the pulse patterns obtained by using (a) a rounded pulse produced by adjustment of the oscillator circuit constants, (b) a pulse simulating the regular Loran pulse, and (c) the regular Loran pulse of (b) after passing through a radio-frequency filter. The tracings were scaled for (a) rise time, representing the length from the beginning of the pulse to the point of maximum amplitude, (b) the length of the pulse at one-half amplitude, and (c) the base length of the pulse. These values were plotted against receiver band width.

The amplitudes of the receiver input and output pulses were held constant and the receiver gain (C.W. sensitivity) measured at different band widths. These values were plotted against receiver band width.

A study of signal-noise ratio and its effect upon the accuracy of Loran measurements was made by using a brush-type electric motor as a noise generator. Signal-noise ratio was measured at the oscilloscope indicator at two different noise levels: (1) the noise peaks that reached the highest amplitude, which will be referred to as the maximum noise peaks, and (2) the level of the amplitude of the average noise peaks. Signal-noise ratios were measured on the maximum noise peaks, at the input of the oscillograph indicator, by placing the signal and noise separately on the receiver and using their respective amplitudes to trip a type 2050 gas tube. The ratios of the two different control grid-bias voltages that were on the grid at the point of tripping were taken as the signal-noise ratios. The relative amplitudes of the signal and noise were scaled directly from the indicator oscilloscope for the signal-noise ratio on the average noise peaks.

The noise sensitivity curve in Fig. 43 was obtained by holding the receiver C.W. sensitivity constant for various band widths and measuring the relative noise on the maximum noise peaks.

The curves of Fig. 45, showing the effect of signal-noise ratio on "signal merit", were obtained by picking up the constant noise from the noise generator on the receiver by means of a short antenna, connected to the receiver and placed close to the noise generator. The pulse from the pulse generator was picked up on the same receiving antenna. The amplitude of the pulse at the receiver input was varied by changing the length of a radiating antenna which was connected to the pulse generator. For each value of signal-noise ratio the signal merit was estimated visually.

The values representing receiver band widths were obtained in the following manner:

(a) The receiver was tuned to an approximate frequency of 1,950 kilocycles. A radio-frequency voltage, with 400-cycle modulation, from a Model LP-3 General Radio signal generator, was fed

to the input terminals of the receiver. The receiver gain was adjusted to provide a suitable deflection on the indicator oscilloscope for the modulation pattern. The frequency of the signal generator was varied and the receiver input voltage, necessary to maintain a constant output deflection at the oscilloscope, was determined over a suitable frequency range. These values were plotted to obtain the radio-frequency response curve. The radio-frequency band width was obtained by scaling the width of the radio-frequency response curve at the half-power point.

(b) The video response curve was determined by connecting a signal generator to the second detector circuit of the receiver, as indicated in Fig. 8, and measuring the voltage necessary to maintain a constant deflection at the indicator oscilloscope as the signal-generator frequency was varied between 400 and 100,000 cycles. The diode filament voltage was disconnected during this operation.

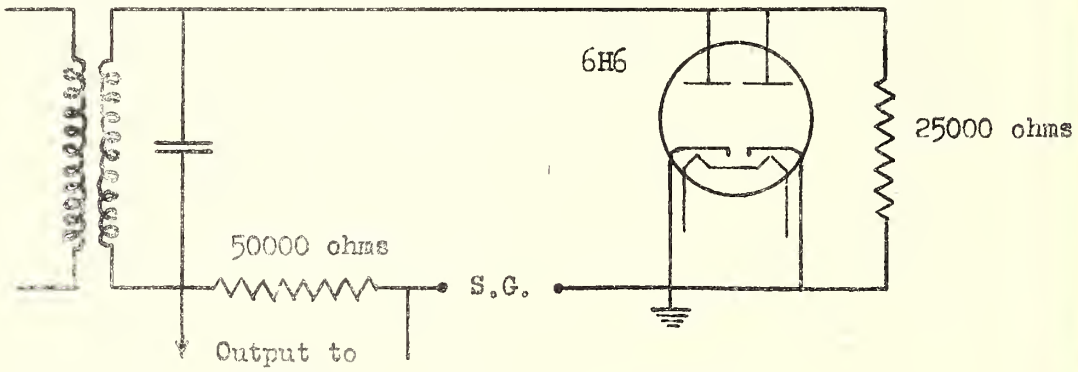

Fig. 8.

(c) The overall band width was obtained graphically by correcting the radio-frequency response curve by the amounts indicated on the video response curve.

A sample of each of the three type response curves, with band-width determinations, is illustrated in Fig. 9.

IV. Discussion of Data

a. Transmitter pulse shapes.

1. Calculated frequency components.- Frequency components were calculated for the following simple pulses, having steep leading edges:

(a) square-wave pulse
(b) cosine pulse
(c) exponential pulse of the spark-transmitter type
(d) exponential filter-type pulse.

(a) Calculation for a square-wave pulse:

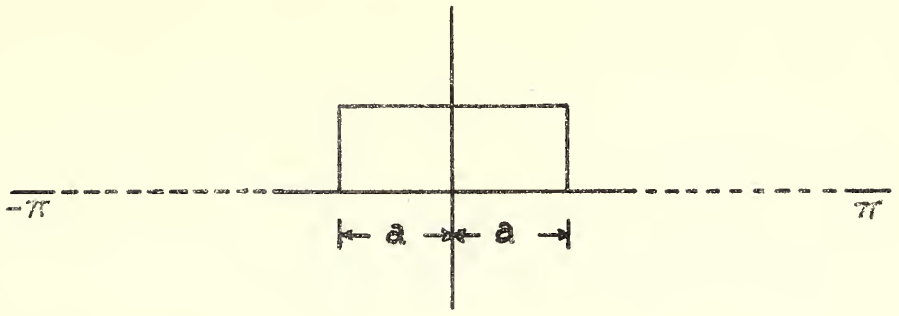

$f(x) = 0$ for interval: $-\pi < x < -a$

$f(x) = 1$ " " $-a < x < a$

$f(x) = 0$ " " $a < x < \pi$

$$A_n = \frac{1}{\pi} \int_{-a}^{a} \cos nx \, dx$$

$$= \frac{1}{n\pi} \left[\sin nx\right]_{-a}^{a}$$

$$\frac{2}{n\pi} \sin an$$

$$B_n = 0$$

$$f(x) = \frac{2}{\pi} \left[\frac{1}{2} + \sin a \cos x + \frac{1}{2} \sin 2a \cos 2x + 1/3 \sin 3a \cos 3x + \ldots\ldots 1/n \sin an \cos nx\right]$$

The amplitude of the frequency components of a square-wave pulse is thus proportional to: $1/n \sin an$. The envelope of the side-band current amplitudes, for a square-wave radio-frequency pulse, may be expressed in terms of frequency separation from the carrier frequency as follows:

$$I = kr \left[\frac{1}{f} \sin \frac{2\pi af}{10^6}\right] \qquad \text{for:} \quad f \geqslant r$$

where:

I = the amplitude of the side-band envelope.
f = separation from the carrier frequency, in cycles per second.
a = one-half the pulse length, in microseconds.
r = recurrence rate, in cycles per second.
$k = \frac{2}{\pi}$

The ratio (R_f) of amplitude of side-band envelope, at a frequency separation from the carrier frequency of f cycles, to the amplitude of the en-

velope at a frequency separation equal to the recurrence rate of the pulse, is given below.

$$R_f = \frac{\frac{r}{f}\sin\frac{2\pi fa}{10^6}}{\sin\frac{2\pi ra}{10^6}} \qquad \text{for: } f \geqslant r$$

If the angle in the denominator is small, as is the case with a 40-microsecond pulse with a recurrence rate of 25 cycles per second, this expression becomes:

$$R_f = \frac{10^6}{2\pi fa}\sin\frac{2\pi fa}{10^6} \qquad \text{for: } f \geqslant r$$

The amplitude of the side bands, therefore, varies approximately inversely with the product of the frequency separation from the carrier frequency and the pulse length. However, it will be noted that nulls are obtained at all points at which $2af = 10^6$, or a multiple of 10^6. This condition occurs at intervals of 25 kilocycles in the case of a 40-microsecond pulse.

The amplitude of the side-band envelope, for a 40-microsecond square-wave radio-frequency pulse, as a function of frequency separation from the carrier frequency, is shown in Fig. 10. Points measured with a National HRO receiver from an approximate 40-microsecond square-wave pulse, produced by the radio-frequency pulse generator previously described, are shown in this Fig. for comparison with the calculated values. The measured values are recognized as running sums of the pulse frequency components falling under the response curve (see Fig. 11) of the HRO receiver. However, it is believed that the correlation obtained between the calculated and experimental points is sufficient to justify the use of either method for determination of the frequency components present in pulse transmissions, for practical purposes.

(b) Calculation for a cosine pulse:

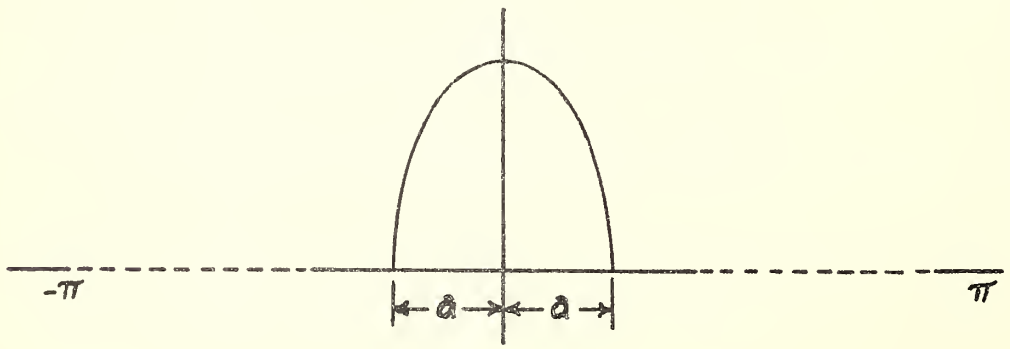

$f(x) = 0$ for interval: $-\pi < x < -a$

$f(x) = \cos \frac{\pi x}{2a}$ " " $-a < x < a$

$f(x) = 0$ " " $a < x < \pi$

$$A_n = \frac{1}{\pi} \int_{-a}^{a} \cos \frac{\pi x}{2a} \cos nx \, dx$$

$$= \frac{1}{2\pi} \int_{-a}^{a} \left[\cos \left(n - \frac{\pi}{2a}\right)x + \cos \left(n + \frac{\pi}{2a}\right)x\right] dx$$

$$= \frac{1}{2\pi} \left[\frac{\sin \left(n - \frac{\pi}{2a}\right)x}{n - \frac{\pi}{2a}} + \frac{\sin \left(n + \frac{\pi}{2a}\right)x}{n + \frac{\pi}{2a}}\right]_{-a}^{a}$$

$$A_n = \frac{\cos an}{a\left[n^2 - \left(\frac{\pi}{2a}\right)^2\right]}$$

$B_n = 0$

The envelope of the side-band amplitudes for a cosine-wave radio-frequency pulse may be expressed in terms of the frequency separation from the carrier frequency as follows:

$$I = \frac{kr}{a}\left[\frac{\cos \frac{2\pi fa}{10^6}}{f^2 - \left(\frac{10^6}{4a}\right)^2}\right] \qquad \text{for: } f \geq r$$

where:

I = the amplitude of the side-band envelope.
f = separation from the carrier frequency, in cycles per second.
a = one-half the pulse base length, in microseconds.
r = recurrence rate, in cycles per second.
$k = \frac{10^6}{2\pi}$

The ratio (R_f) of the amplitude of the side-band envelope, at a frequency separation from the carrier frequency of f cycles, to the amplitude of the envelope at a frequency separation equal to the recurrence rate of the pulse, is given below.

$$R_f = \frac{r^2 + \left(\frac{10^6}{4a}\right)^2}{f^2 + \left(\frac{10^6}{4a}\right)^2} \cos \frac{2\pi fa}{10^6} \qquad \text{for: } f \geq r$$

If $(r)^2$ is $<< \left(\frac{10^6}{4a}\right)^2$, as in the case of a 40-microsecond pulse with a recurrence rate of 25 cycles per second, the above expression becomes:

$$R_f \doteq \frac{(10^6)^2}{(4af)^2 + (10^6)^2} \cos \frac{2\pi fa}{10^6}$$

The envelope of the side-band amplitudes, for a cosine-wave radio-frequency pulse, with a 40-microsecond base length, is shown in Fig. 12. It will be observed that, after the first 30 kilocycles, the amplitudes of the frequency components fall off faster than those of a square wave. However, this is accomplished at the expense of the leading edge, which requires approximately 14 microseconds to reach 90 percent of full amplitude.

(c) Calculation for an exponential pulse of the spark-transmitter type:

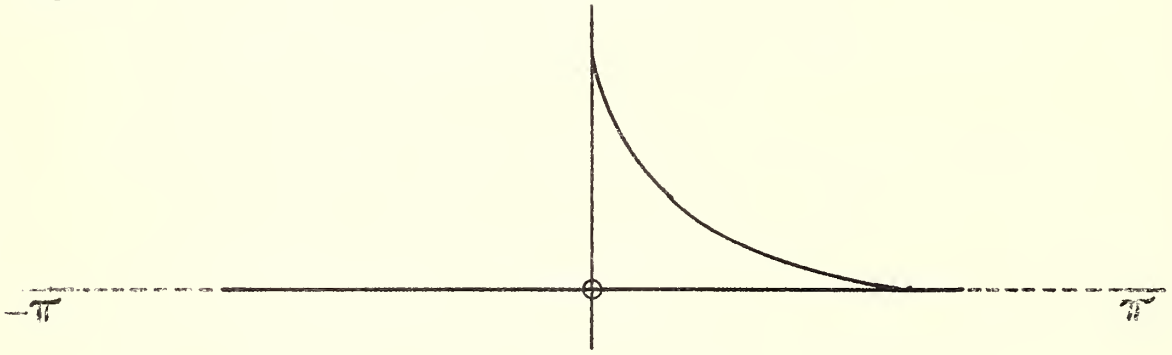

$f(x) = 0$ for interval: $-\pi < x < 0$

$f(x) = e^{-ax}$ " " $0 < x < \pi$

$$A_n = \frac{1}{\pi}\int_0^{\pi} e^{-ax} \cos nx \quad dx$$

$$= \frac{1}{\pi}\left[\frac{e^{-ax}(n \sin nx - a \cos nx)}{a^2 + n^2}\right]_0^{\pi}$$

$$= \frac{1}{\pi}\left[\frac{a}{a^2 + n^2}\ (1 - e^{-a\pi} \cos \pi n)\right]$$

Where: $a > 100$

$$A_n \doteq \frac{1}{\pi}\left[\frac{a}{a^2 + n^2}\right]$$

$$B_n = \frac{1}{\pi}\int_0^{\pi} e^{-ax} \sin nx \quad dx$$

$$= \frac{1}{\pi}\left[\frac{-e^{-ax}(n \cos nx + a \sin nx)}{a^2 + n^2}\right]_0^{\pi}$$

$$B_n = \frac{1}{\pi}\left[\frac{n}{a^2 + n^2}\ (1 - e^{-a\pi} \cos n\pi)\right]$$

Where: a is $>$ 100

$$B_n \doteq \frac{1}{\pi}\left[\frac{n}{a^2 + n^2}\right]$$

$$K_n = \sqrt{A_n^{\,2} + B_n^{\,2}}$$

$$= \frac{1}{\pi}\,\frac{1}{\sqrt{a^2 + n^2}}$$

The envelope of the side-band amplitudes for this type radio-frequency pulse may be expressed in terms of the frequency separation from the carrier frequency as follows:

$$I = \frac{rk}{\sqrt{f^2 + (ra)^2}} \qquad \text{for: } f \geq r$$

Where:

I = the amplitude of the side-band envelope.
f = the separation from the carrier frequency, in cycles per second.
a = exponent determining the rate at which the amplitude of the pulse drops with time.
r = recurrence rate, in cycles per second.
$k = \frac{1}{\pi}$

The ratio (R_f) of the amplitude of the side-band envelope, at a frequency separation from the carrier frequency of f cycles, to the amplitude of the envelope at a frequency separation equal to the recurrence rate of the pulse, is given below.

$$R_f = \frac{r\sqrt{1 + a^2}}{\sqrt{f^2 + (ra)^2}} \qquad \text{for: } f \geq r$$

Where: a is $>$ 100

$$R_f \doteq \frac{ra}{\sqrt{f^2 + (ra)^2}}$$

The shape of the envelope of the side-band amplitudes, with respect to frequency separation from the carrier frequency, for this type pulse (a = 250) is shown in Fig. 13. Under this condition, the amplitude of the pulse drops to approximately 22.5 percent of full amplitude in 40 microseconds. It will be observed that this pulse provides approximately the same frequency spectrum as does the square-wave pulse of Fig. 10, except for the absence of the peaks and nulls present in the square-wave pattern.

(d) Calculation for an exponential filter-type pulse:

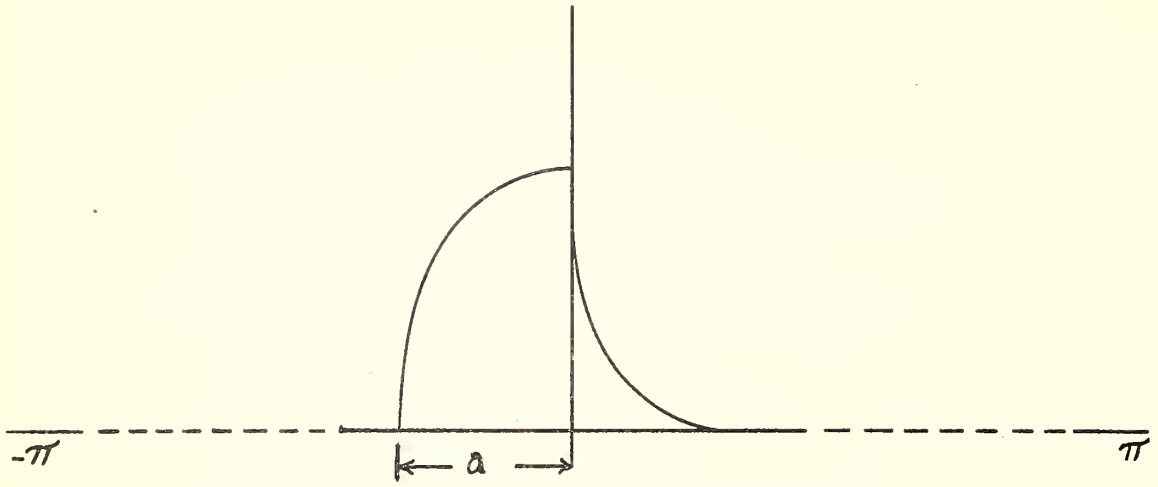

$f(x) = 0$ for interval: $-\pi < x < -a$

$f(x) = 1 - e^{-\alpha}(x + a)$ for interval: $-a < x < 0$

$f(x) = \left[1 - e^{-a\alpha}\right] e^{-\alpha x}$ for interval: $0 < x < \pi$

$$A_n = \frac{1}{\pi}\left\{\int_{-a}^{0}\left[1 - e^{-\alpha(x+a)}\right]\cos nx\ dx + \int_{0}^{\pi}\left[1 - e^{-a\alpha}\right] e^{-\alpha x}\cos nx\ dx\right\}$$

$$A_n = \frac{1}{\pi}\left\{\left[\frac{1}{n}\sin nx\right]_{-a}^{0} - \left[\frac{e^{-\alpha(x+a)}}{n^2 + \alpha^2}(n\sin nx - \alpha\cos nx)\right]_{-a}^{0}\right.$$

$$\left. + \left[\frac{1 - e^{-a\alpha}}{n^2 + \alpha^2}(e^{-\alpha x})(n\sin nx - \alpha\cos nx)\right]_{0}^{\pi}\right\}$$

$$= \frac{\alpha}{\pi}\left\{\frac{\alpha}{n(n^2 + \alpha^2)}\sin an + \frac{1}{n^2 + \alpha^2}(1 - \cos an)\right.$$

$$\left. \frac{e^{-\alpha\pi}(1 - e^{-a\alpha})}{n^2 + \alpha^2}\cos n\pi\right\}$$

Where: $\alpha > 100$

$$A_n = \frac{\alpha}{\pi}\left[\frac{1}{n(n^2 + \alpha^2)}\right]\left[\alpha\sin an + n(1 - \cos an)\right]$$

$$B_n = \frac{1}{\pi}\left\{\int_{-a}^{0}\left[1 - e^{-\alpha(x+a)}\right]\sin nx\ dx\right.$$

$$\left. + \int_{0}^{\pi}\left[1 - e^{-a\alpha}\right] e^{-\alpha x}\sin nx\ dx\right\}$$

$$= \frac{1}{\pi}\left\{\left[\frac{1}{n}\cos nx\right]_{0}^{-a} - \left[\frac{e^{-\alpha(x+a)}}{n^2+\alpha^2}(n\cos nx + \alpha \sin nx)\right]_{0}^{-a} + \left[\frac{e^{-\alpha x}}{n^2+\alpha^2}(n\cos nx + \alpha \sin nx)(1 - e^{-a\alpha})\right]_{\pi}^{0}\right\}$$

$$= \frac{1}{\pi}\left\{\frac{\alpha^2}{n(n^2+\alpha^2)}(\cos an - 1) + \frac{\alpha}{n^2+\alpha^2}\sin an - \frac{e^{-\alpha\pi}}{n^2+\alpha^2}\, n\,(1 - e^{-a\alpha})\cos n\pi\right\}$$

Where: $\alpha > 100$

$$B_n = \frac{\alpha}{\pi}\left[\frac{1}{n(n^2+\alpha^2)}\right]\left[n \sin an - \alpha(1 - \cos an)\right]$$

$$K_n = \sqrt{A_n^2 + B_n^2}$$

$$= \frac{2\alpha}{\pi n\sqrt{n^2+\alpha^2}} \sin\frac{an}{2}$$

The envelope of the side-band amplitudes for this type radio-frequency pulse may be expressed in terms of the frequency separation from the carrier frequency as follows:

$$I = \frac{k\alpha r^2}{f\sqrt{f^2 + (r\alpha)^2}} \sin\frac{\pi fa}{10^6} \qquad \text{for: } f \geqslant r$$

Where:

I = the amplitude of the side-band envelope.
f = the separation from the carrier frequency, in cycles per second.
α = exponent determining the rate at which the amplitude of the pulse rises and falls with time.
r = recurrence rate, in cycles per second.
a = the rise time of the pulse, in microseconds.
$k = \frac{2}{\pi}$

The ratio (R_f) of the amplitude of the side-band envelope, at a frequency separation from the carrier frequency of f cycles, to the amplitude of the envelope at a frequency separation equal to the recurrence rate of the

pulse, is given below:

$$R_f = \frac{10^6 r \sqrt{1+\alpha^2}}{\pi af\sqrt{f^2+(r\alpha)^2}} \sin\frac{\pi fa}{10^6} \quad \text{for: } f \geqslant r$$

Where: $\alpha^2 \gg 1$

$$R_f = \frac{10^6 r \alpha}{\pi af\sqrt{f^2+(r\alpha)^2}} \sin\frac{\pi fa}{10^6}$$

The envelope of the side-band amplitudes for an exponential pulse, of the filter type, with 40-microseconds rise time (α = 1000) and a recurrence rate of 25 cycles per second, is shown in Fig. 14. The leading edge of this pulse is sufficiently steep to reach approximately 90 percent of full amplitude in 15 microseconds.

For frequencies sufficiently removed from the carrier frequency, say 100 kilocycles or more in the illustration of Fig. 14, so that $f^2 \gg (r\alpha)^2$, the amplitude of the side-band envelope varies approximately inversely with the square of the frequency separation, as compared with the first power of the frequency separation indicated for a square-wave pulse. Under this condition ($f^2 \gg (r\alpha)^2$) the amplitude of the side-band envelope, varies approximately inversely with the pulse length and directly with the product of the recurrence rate (r) and the exponential time constant (α).

The nulls of the exponential filter-type pulse are found at all points at which $fa = 10^6$, or any multiple of 10^6. In the case of the pulse illustrated in Fig. 14, this condition is obtained at 25-kilocycle intervals, beginning at 25 kilocycles from the carrier frequency. The nulls are obtained in the cosine-wave pulse at all points at which $fa = (1/4)10^6$, or odd multiples of $(1/4)10^6$. These nulls are found at intervals of 25 kilocycles, beginning at 12.5 kilocycles from the carrier frequency in the illustration of Fig. 12. Thus the nulls of one of these pulses appear at the same frequency as the peaks of the other type pulse for a frequency separation more than 12.5 kilocycles from the carrier frequency. It would therefore appear that the best pulse shape, from a standpoint of frequency components, consistent with a steep leading edge and reasonably narrow pulse length, would be a combination of a cosine wave and a filter-type exponential pulse.

2. Measured frequency components.- The frequency components of a smooth shaped radio-frequency pulse, produced by adjustment of the pulse generator circuit constants, without the use of special radio-frequency filters, measured with a National HRO receiver, are shown in Fig. 15. The measured frequency components of a radio-frequency pulse, approaching as nearly as possible the shape of the pulses emitted by the regular Loran transmitting stations, are shown in Fig. 16. The frequency components of the regular Loran pulse, after passing through a radio-

frequency filter, are shown in Fig. 17. The shape of the radio-frequency envelope of each of these pulses is shown in Fig. 18.

The measured frequency components of the filtered pulse are easily the most favorable, from a standpoint of reduction in side-band radiation from the regular Loran transmitting stations, of any of the measured or calculated pulses. The amplitudes of the side-band currents, at 100 kilocycles from the carrier frequency, are approximately 0.01 of the regular Loran pulse (40 db down.)

The frequency components of a number of various shaped radio-frequency pulses, without the use of special filters, were measured. These values fell between those obtained for the smooth-shaped pulse of Fig. 15, and the square-wave points illustrated in Fig. 10. It therefore appears that the most practicable method of shaping a radio-frequency pulse, for use in the Loran system, is by means of a radio-frequency filter. The effect upon the leading edge of a pulse, so shaped, as it appears on the indicator oscilloscope after passing through the receiver, will be discussed and illustrated under "Receiver band-width characteristics", below.

b. Receiver band-width characteristics.

1. Receiver response curves.- A number of typical radio-frequency receiver response curves, obtained for receiver adjustments used in comparing pulse shapes, are shown in Fig. 19. The band widths, before correcting for the effect of the video amplifier, are indicated on the response curves. Response curves for the two video amplifiers used in conjunction with the variable band-width receiver are contained in Fig. 20. The relation between the radio-frequency band widths and the overall band widths, for each video amplifier, is illustrated in Fig. 21.

The three types of pulses examined with various receiver band widths were:

(1) a pulse simulating, as nearly as possible, the pulse emitted by the present Loran transmitting equipments which will be referred to as the Loran-type pulse;

(2) the Loran type pulse, after passing through the radio-frequency filter used to restrict the side-band components of the pulse as illustrated in Fig. 17;

(3) the approximate exponential filter-type pulse illustrated in Fig. 15.

2. Pulse shapes.- Tracings of representative pulse shapes for the Loran-type pulse are shown in Fig. 22, without filter, and in Fig. 23, with the filter inserted between the pulse generator and the receiver.

The pulse shapes at receiver band widths of 86.0, 75.5, 63.0 and 50.0 kc were obtained with the wide-band video amplifier (see Fig. 20).

Those at band widths of 37.0, 29.5, and 22.0 kc were obtained from the Fada video amplifier. The overall band width of 86.0 kc corresponds to the radio-frequency band width of 88.5 kc illustrated in Fig. 21. It will be observed that very little difference appears in the shape of the filtered pulse and the direct pulse as viewed on the indicator oscilloscope, at band widths less than 50.0 kc. Fig. 24 contains representative tracings of the exponential filter-type pulse, at various receiver band widths. All pulse patterns were obtained with Fada video amplifier.

All indicator oscilloscope pulse patterns were scaled for (a) rise time, representing the time required for the pulse to rise from zero to maximum amplitude, (b) pulse length at one-half amplitude, and (c) the base length of the pulse. These values are shown, as functions of receiver band width for each of the three type pulses in Figs. 25 to 33.

In general, the pulse rise time increases with reduced receiver band width. Therefore a reduction in receiver band width will be expected to be accompanied by a reduction in the steepness of the leading edge of the received pulse. For example, an increase in rise time from 25 microseconds to 50 microseconds may reasonably be expected with a receiver band-width change from 85.0 kc to 19 kc. The practical effect of inserting a radio-frequency filter between the pulse generator and the receiver is to increase the rise time of the pulse as it appears on the indicator oscilloscope. Reasonable estimates of this effect may be obtained from Figs. 25 and 28.

Figs. 26 and 29 indicate that the pulse length at one-half amplitude does not vary greatly at receiver band widths of 85.0 to 25.0 kc and should remain well below 50 microseconds over this range. The one-half amplitude length increases rapidly with decreasing receiver band widths below 15 kc.

The base length of the pulse, as viewed on the indicator oscilloscope, does not vary greatly at receiver band widths of 85.0 ot 25 kc. The base length increases rapidly at receiver band widths less than 15 kc. An increase in base length of from 10 to 20 microseconds was noted in pulse patterns obtained with the Fada video amplifier as compared with the wide-band video amplifier of the Dumont oscilloscope.

3. Effect of Method of Obtaining Band Width - Because of the scatter of the values, scaled from the pulse patterns in Figs. 25 to 33, it seems that the pulse patterns obtained were dependent upon the manner in which the overall band width was obtained, as well as upon the absolute value of the band width. An investigation was therefore made in which shapes were traced and scaled for various receiver band widths. Each band width was obtained by two different methods: (a) by damping the tuned circuits in the intermediate-frequency amplifier, and (b) by omitting the damping resistors. A comparison of the pulse shapes in the two cases is shown in Fig. 34 for the Loran-type pulse, and in Fig. 35 for the filtered Loran-type pulse. It will be

noted that the pulse shapes obtained under the two conditions for the same band width are substantially of the same shape, except for the ones made on the 34-kc band width. For this band width a double-humped receiver response characteristic (obtained by overcoupling) was used for the pulse obtained without the damping resistors, whereas overcoupling was kept to a minimum on the 33-kc damped band width. Comparisons of the pulse rise time, pulse length at one-half amplitude, and pulse base length, for both the Loran-type pulse and the filtered Loran type pulse, under these two conditions, are shown in Figs. 36 to 41. These Figs. indicate that, aside from the effects of overcoupling, which appeared to affect the base length of the pulse, the same results could be obtained by damping the tuned circuits in the intermediate-frequency amplifier as by obtaining the same radio-frequency band width without damping them.

4. Pulse sensitivity of receiver.- The relative receiver sensitivity to the Loran pulses for various band widths, using the narrow video amplifier, is shown in Fig. 42. The relative receiver pulse sensitivity, using the wide-band video amplifier, can be seen in Fig. 43. It will be noted that the sensitivity of the receiver to pulses changed appreciably more with band width when the narrow-band video amplifier was used than when the wide-band video amplifier was used. For example, a change in overall band width from 50 kc to 30 kc, using the narrow-band video amplifier, lowered the receiver sensitivity by a factor of about 1.30 (2.2 db); the same change in band width, using the wide-band video amplifier, lowered the receiver sensitivity by a factor of only about 1.14 (1.4 db).

5. Effect of band width on signal-noise ratio and accuracy of Loran measurements.- In Fig. 44 signal-noise ratio is shown as a function of overall receiver band width for both maximum noise peaks and average noise peaks. It will be noticed that the signal-noise ratio is, for an overall band width of 50 kc, about one-half (6 db lower) of its value for a 25-kc band width.

In Fig. 45 is shown the estimated "signal merit" as a function of signal-noise ratio. From this Fig. it appears that about an 8.5-db change in signal-noise ratio made a change of 1 in signal merit rating.

The pulses were found to be much easier to identify, under conditions of high noise, on the slow sweep of the indicator when narrow band widths were used than when wide band widths were used.

V. Conclusions

a. Transmitter pulse shape.

The side-band radiation from Loran transmitters can be considerably reduced below that for the present type pulse, without impairing the usefulness of the pulse for measurement purposes. The optimum pulse shape for emission by Loran transmitting stations, from the standpoint of minimum side-band radiation consistent with necessary steepness of the leading edge of the pulse, approximates an exponential filter-type pulse with sharp edges rounded. The most practical method for shaping such a pulse

seems to be by means of a radio-frequency filter in the transmitter circuit. This probably requires a master-oscillator power-amplifier type transmitting equipment. The side-band radiation, at 100 kilocycles off-frequency, can be reduced, by this method of shaping the transmitted pulse, to at least 0.001 (60 db down) of the fundamental, without appreciably affecting the accuracy of measurements made with receiving equipment in the field.

b. Receiver band-width characteristics.

The shape and amplitude of the pulse appearing on the oscilloscope screen of a Loran indicator is a function of the manner in which the receiver band width is obtained as well as of the absolute value of the overall band width. Considerable differences can be obtained in the rise time, pulse length and pulse amplitude, for the same radio-frequency band width obtained by different methods.

A narrow band width in the video amplifier contributes to attenuation of the high-frequency components of a pulse transmitted at the receiver radio frequency and therefore to the distortion of its pattern on the indicator oscilloscope while it does not contribute to the attenuation of low-frequency components of modulated C.W. or pulse transmissions on adjacent radio-frequency channels. A wide-band video amplifier is therefore desirable.

The optimum overall receiver band width recommended for use in the Loran system is 30 kilocycles, with a tolerance of ± 5 kilocycles. The overall band width should be determined, to as large an extent as reasonable design will permit, by the radio-frequency and intermediate-frequency stages of the receiver. The design of the radio-frequency and intermediate-frequency amplifier stages should be sufficiently damped with resistance to prevent overcoupling.

VI. Subjects Requiring Additional Investigation.

a. Transmitter pulse shape.

Further studies should be made of the possibility of reducing side-band radiation from Loran transmitters below those indicated in Fig. 17, by use of suitable radio-frequency filters, without seriously impairing the usefulness of the pulse for measurement purposes.

b. Receiver band-width characteristics.

Further studies should be made on signal-to-noise, as a function of receiver band width using natural noise. This may be done by making noise-sensitivity and pulse-sensitivity measurements in the manner shown in Fig. 43 and subtracting the attenuation of the pulse from the attenuation of the noise.

In view of the differences in the variation of receiver pulse sensitivity with different band widths between the wide video amplifier and the narrow video amplifier, it appears that a study should be made of the effect of the video amplifier on signal-noise ratio.

Figures

40. Comparison of the pulse length at one-half amplitude of a filtered Loran-type pulse with different adjustments of the receiver to obtain the same band widths.
41. Comparison of the base length of a filtered Loran-type pulse with different adjustments of the receiver to obtain the same band widths.
42. Receiver pulse sensitivity vs band width using narrow video amplifier.
43. Receiver pulse and noise sensitivity vs band width using wide video amplifier.
44. Signal-to-noise vs band width using wide video amplifier.
45. Signal merit vs signal-to-noise ratio.

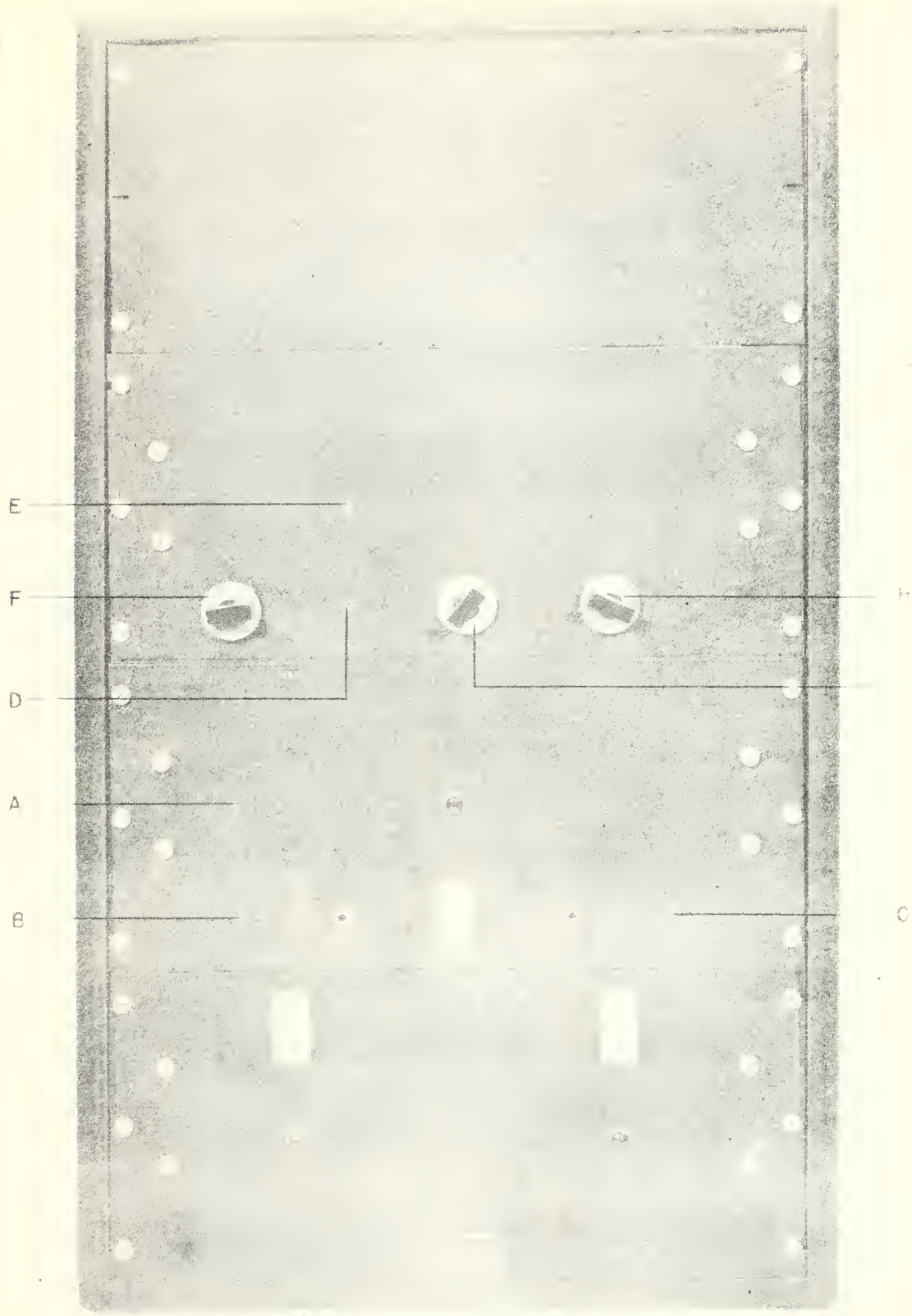

Fig 1- FRONT VIEW OF [illegible] FREQUENCY PULSE GENERATOR.


OSCILLATOR AND
MODULATOR UNIT
EXCITER UNIT
AUXILIARY
POWER SUPPLY

EXCITER UNIT FOR RADIO FREQUENCY PULSE GENERATOR

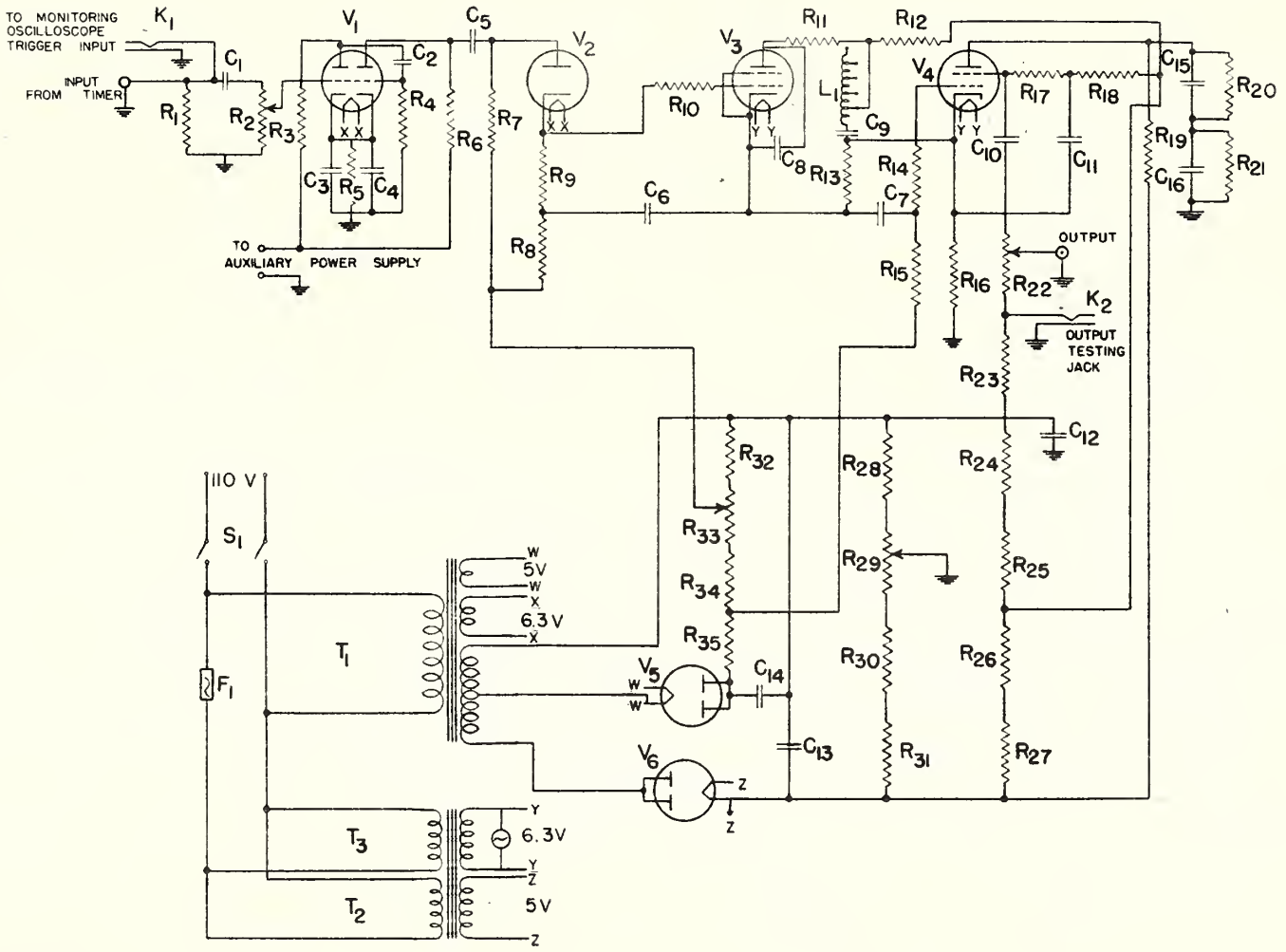

Fig. 3

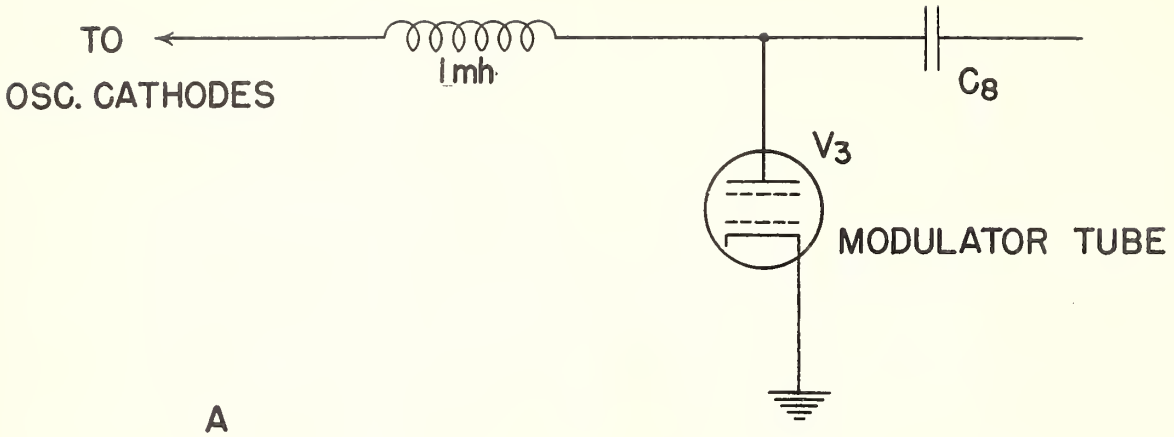

A

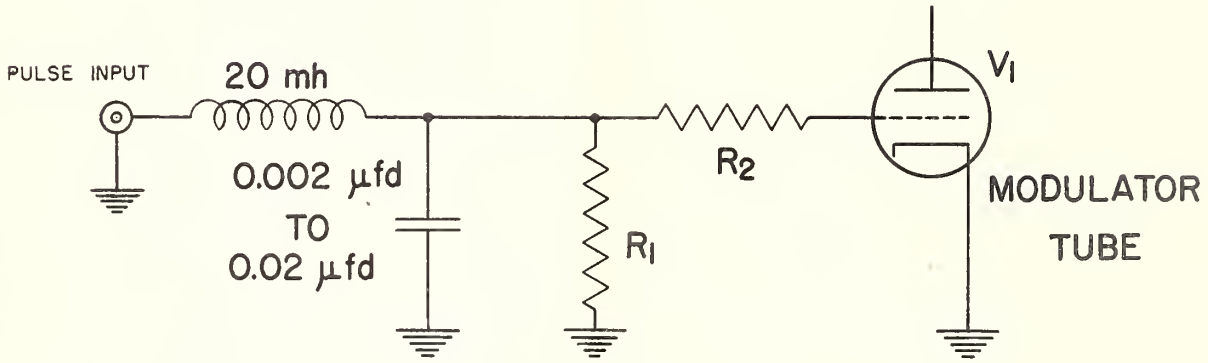

B

Fig. 6. ADDED COMPONENTS FOR ROUNDING LEADING AND LAGGING EDGES OF PULSES.

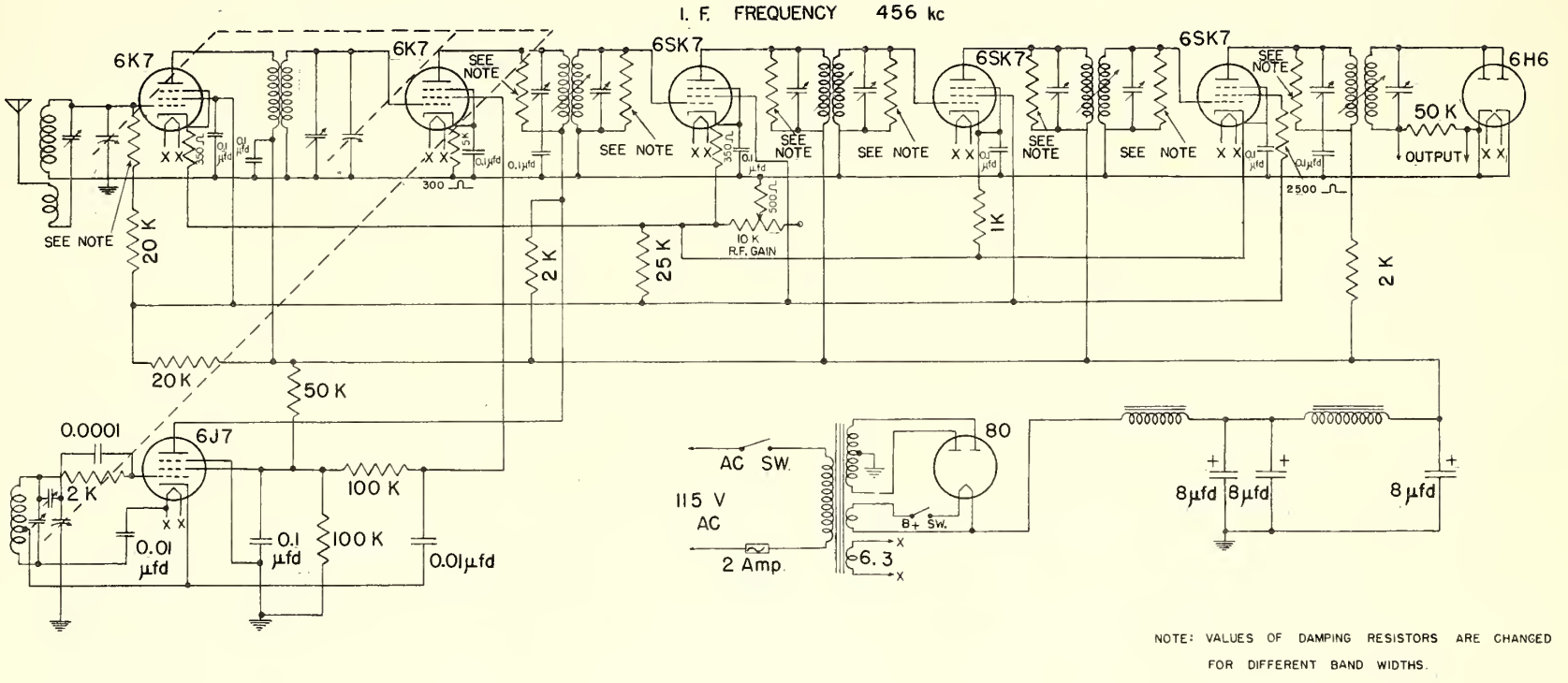

Fig. 7. CIRCUIT OF NC 100 RECEIVER AFTER IT WAS MODIFIED TO OBTAIN VARIABLE BAND WIDTH.

See page 12 of text for Fig. 8

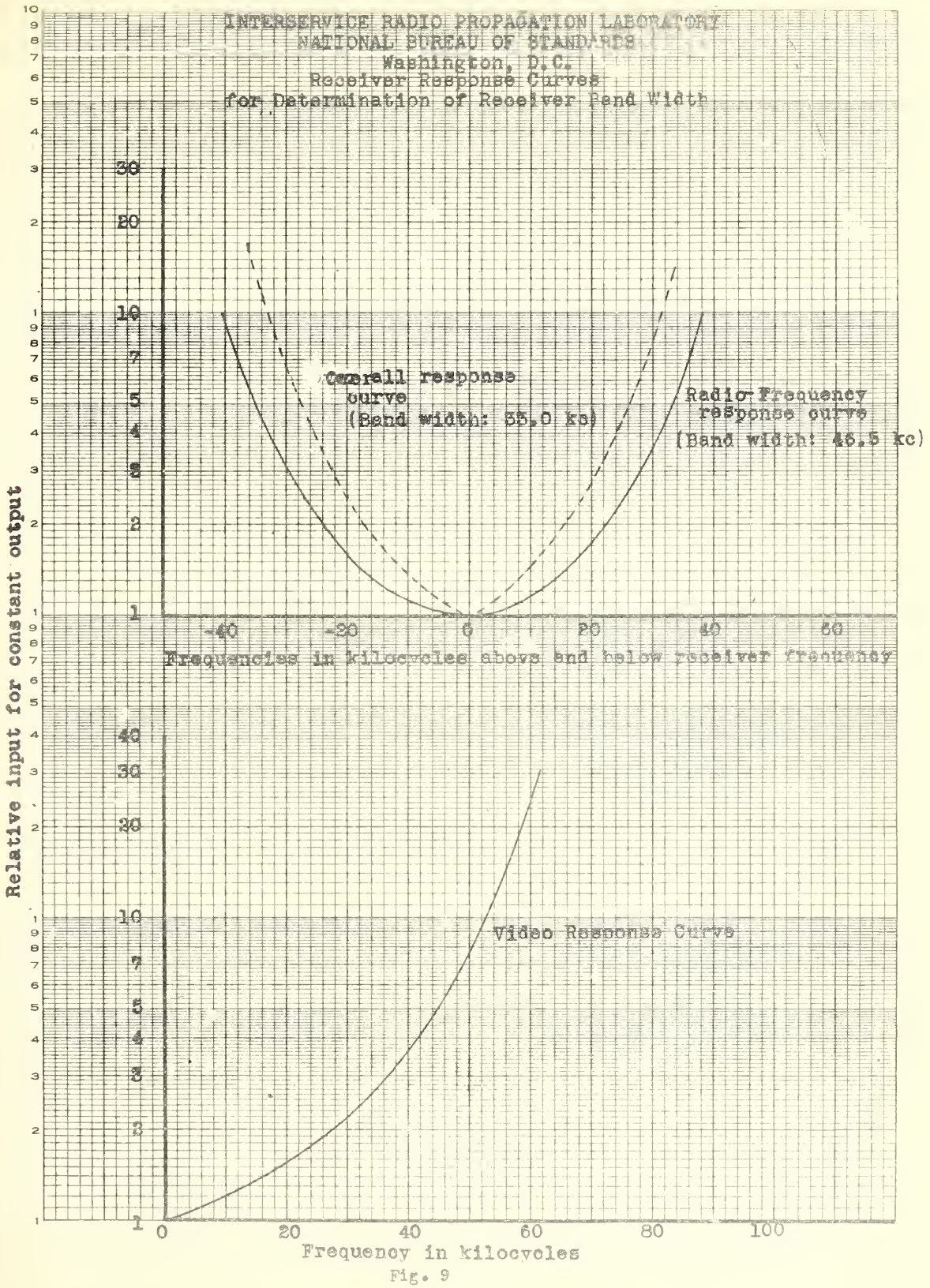
INTERSERVICE RADIO PROPAGATION LABORATORY
NATIONAL BUREAU OF STANDARDS
Washington, D.C.
Receiver Response Curves
for Determination of Receiver Band Width
Overall response curve
(Band width: 55.0 kc)
Radio-Frequency response curve
(Band width: 46.5 kc)
Frequencies in kilocycles above and below receiver frequency
Video Response Curve
Relative input for constant output
Frequency in kilocycles

Fig. 9

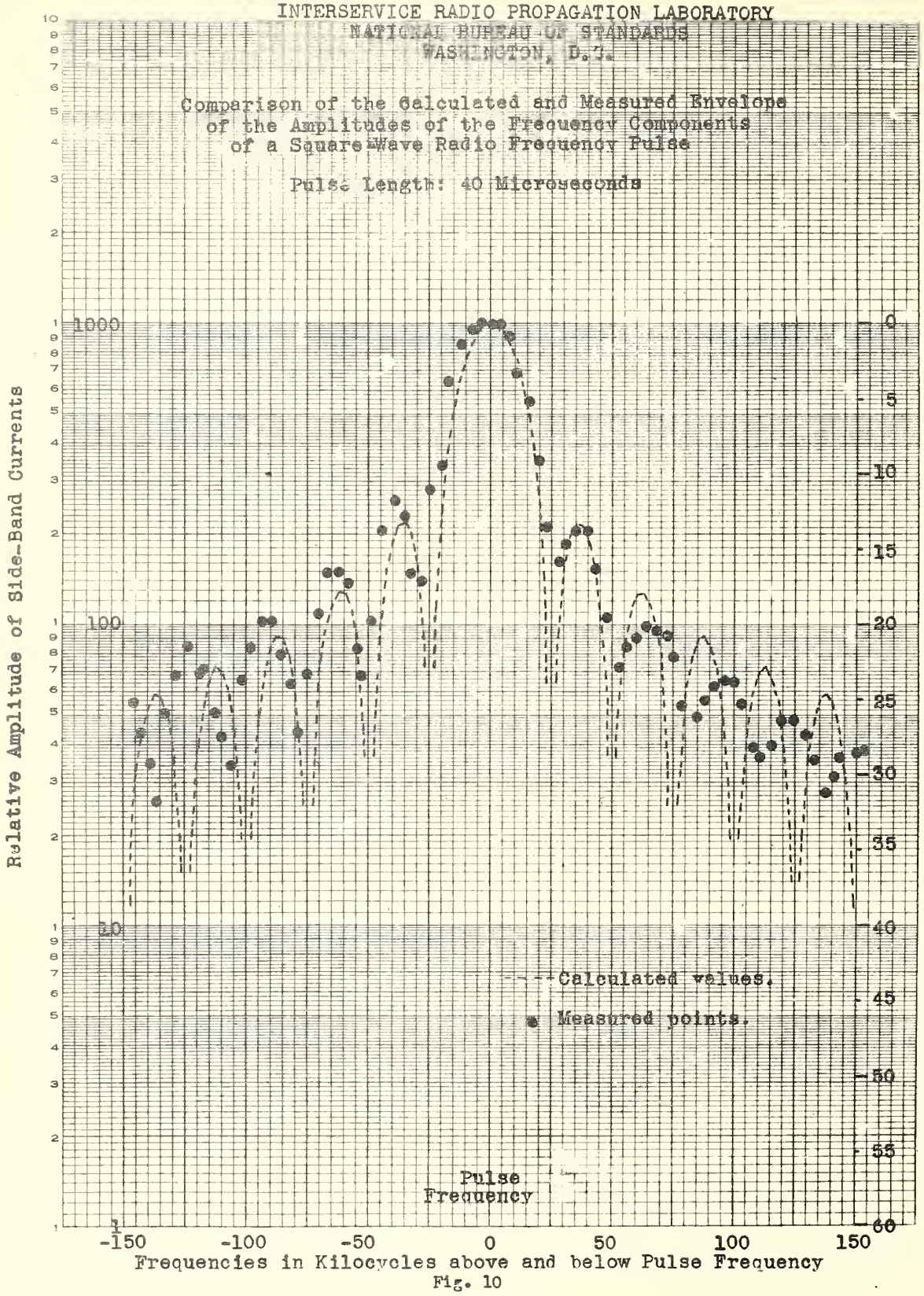
INTERSERVICE RADIO PROPAGATION LABORATORY
NATIONAL BUREAU OF STANDARDS
WASHINGTON, D.C.
Comparison of the Calculated and Measured Envelope
of the Amplitudes of the Frequency Components
of a Square Wave Radio Frequency Pulse
Pulse Length: 40 Microseconds
Relative Amplitude of Side-Band Currents
1000
100
10
Relative Amplitude - Db
0
5
10
15
20
25
30
35
40
45
50
55
60
Calculated values.
Measured points.
Pulse
Frequency
-150
-100
-50
0
50
100
150
Frequencies in Kilocycles above and below Pulse Frequency
Fig. 10

INTERSERVICE RADIO PROPAGATION LABORATORY
NATIONAL BUREAU OF STANDARDS
Washington, D.C.

Response Curve for National HRO Receiver
Used for Measurement of Frequency Components
of Radio-Frequency Pulses.

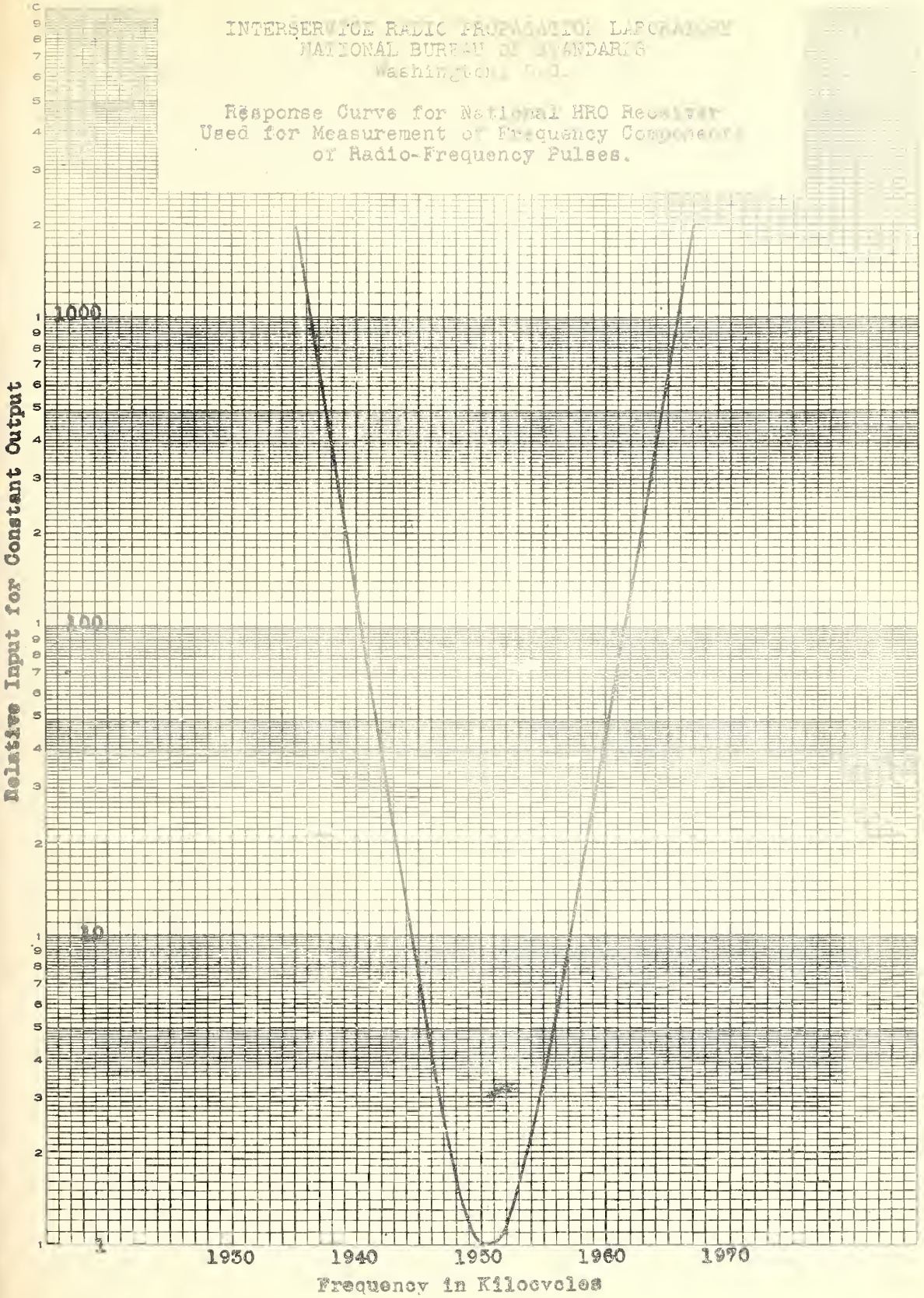

Fig. 11

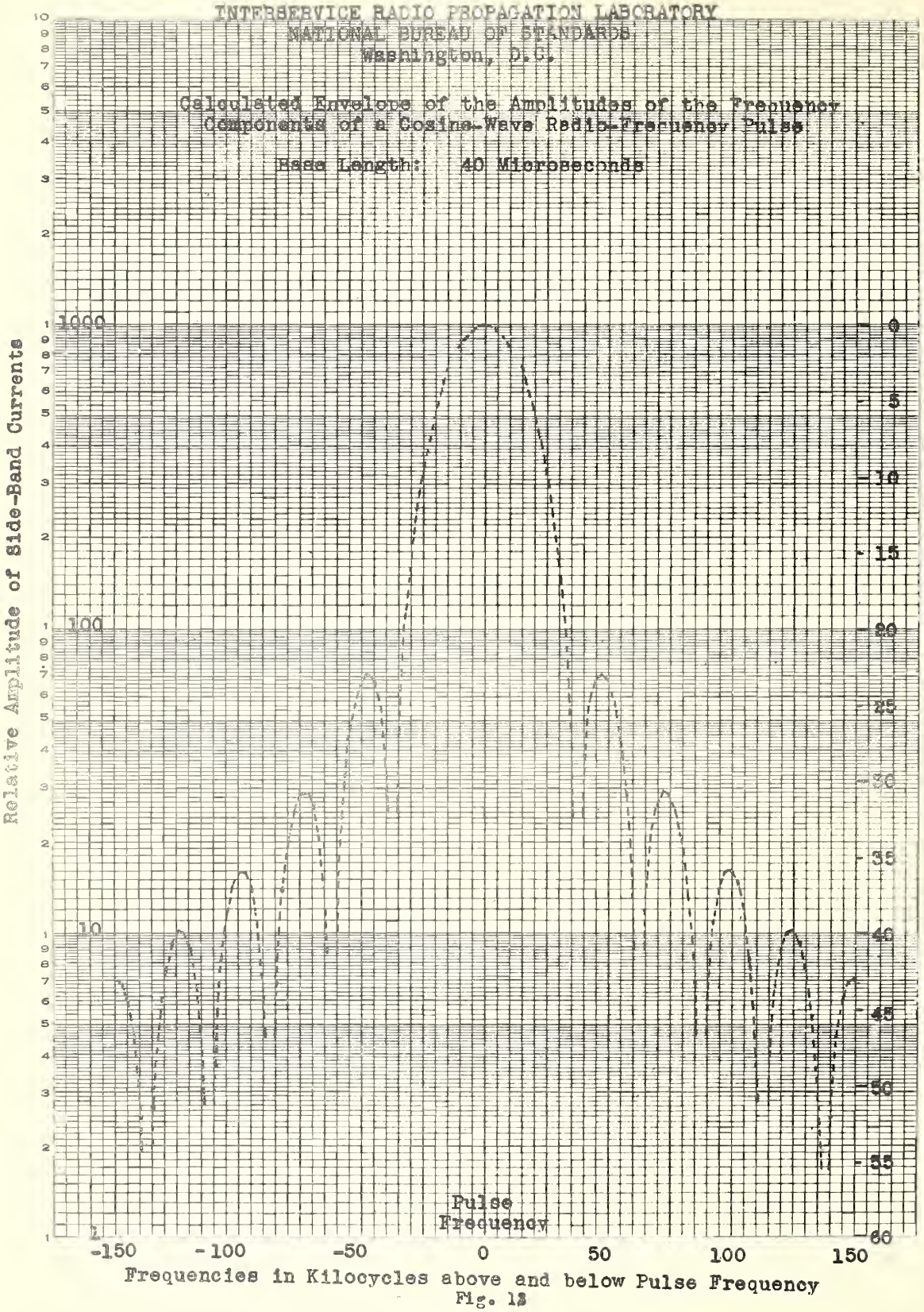
INTERSERVICE RADIO PROPAGATION LABORATORY
NATIONAL BUREAU OF STANDARDS
Washington, D.C.
Calculated Envelope of the Amplitudes of the Frequency Components of a Cosine-Wave Radio-Frequency Pulse
Base Length: 40 Microseconds
Relative Amplitude of Side-Band Currents
1000
100
10
1
0
5
10
15
20
25
30
35
40
45
50
55
60
Relative Amplitude - Db
Pulse Frequency
-150
-100
-50
0
50
100
150
Frequencies in Kilocycles above and below Pulse Frequency

Fig. 13

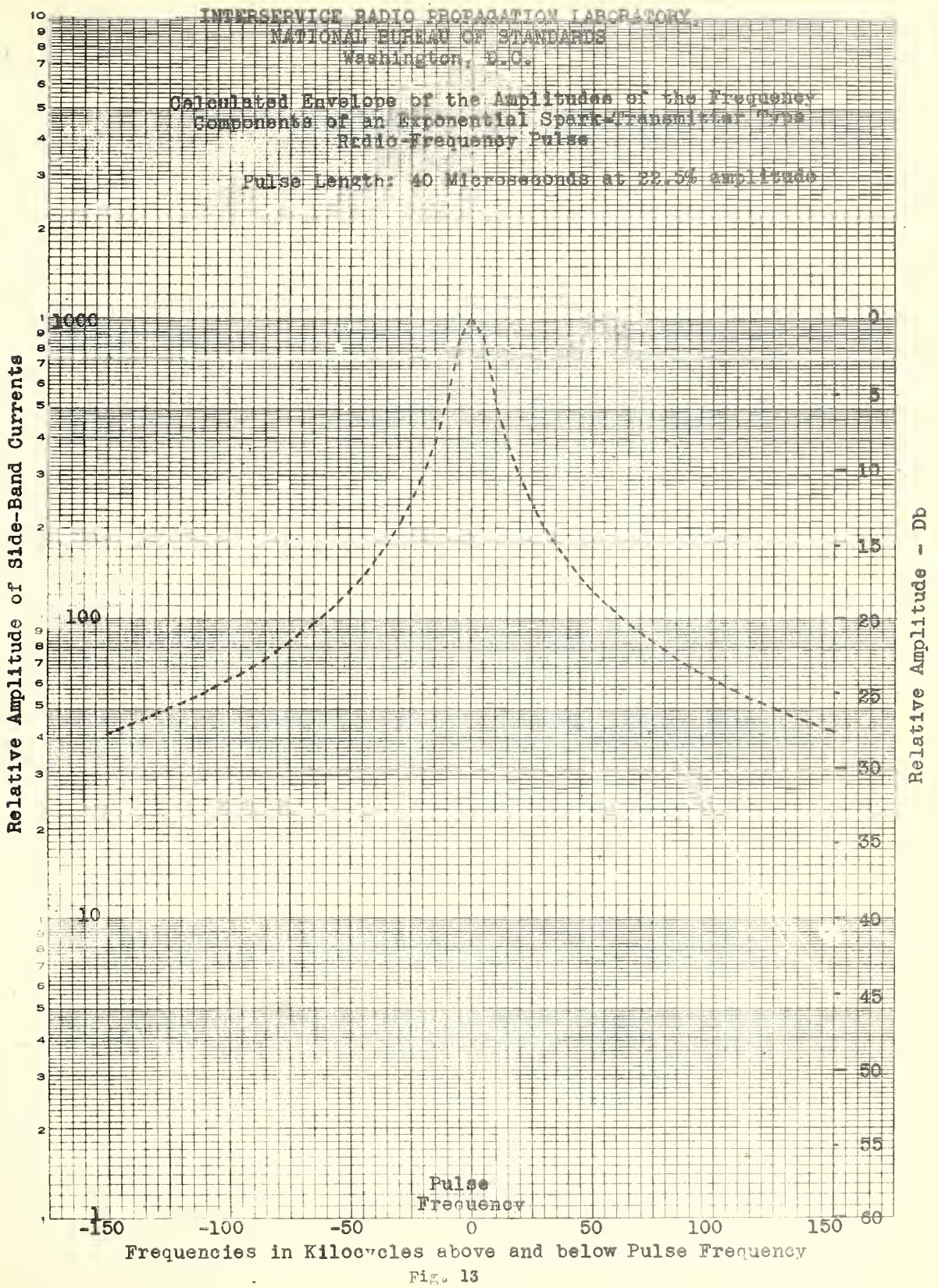
INTERSERVICE RADIO PROPAGATION LABORATORY
NATIONAL BUREAU OF STANDARDS
Washington, D.C.
Calculated Envelope of the Amplitudes of the Frequency Components of an Exponential Spark-Transmitter Type Radio-Frequency Pulse
Pulse Length: 40 Microseconds at 22.5% amplitude
Relative Amplitude of Side-Band Currents
Relative Amplitude - Db
1000
100
10
1
0
5
10
15
20
25
30
35
40
45
50
55
60
Pulse Frequency
-150
-100
-50
0
50
100
150
Frequencies in Kilocycles above and below Pulse Frequency

Fig. 13

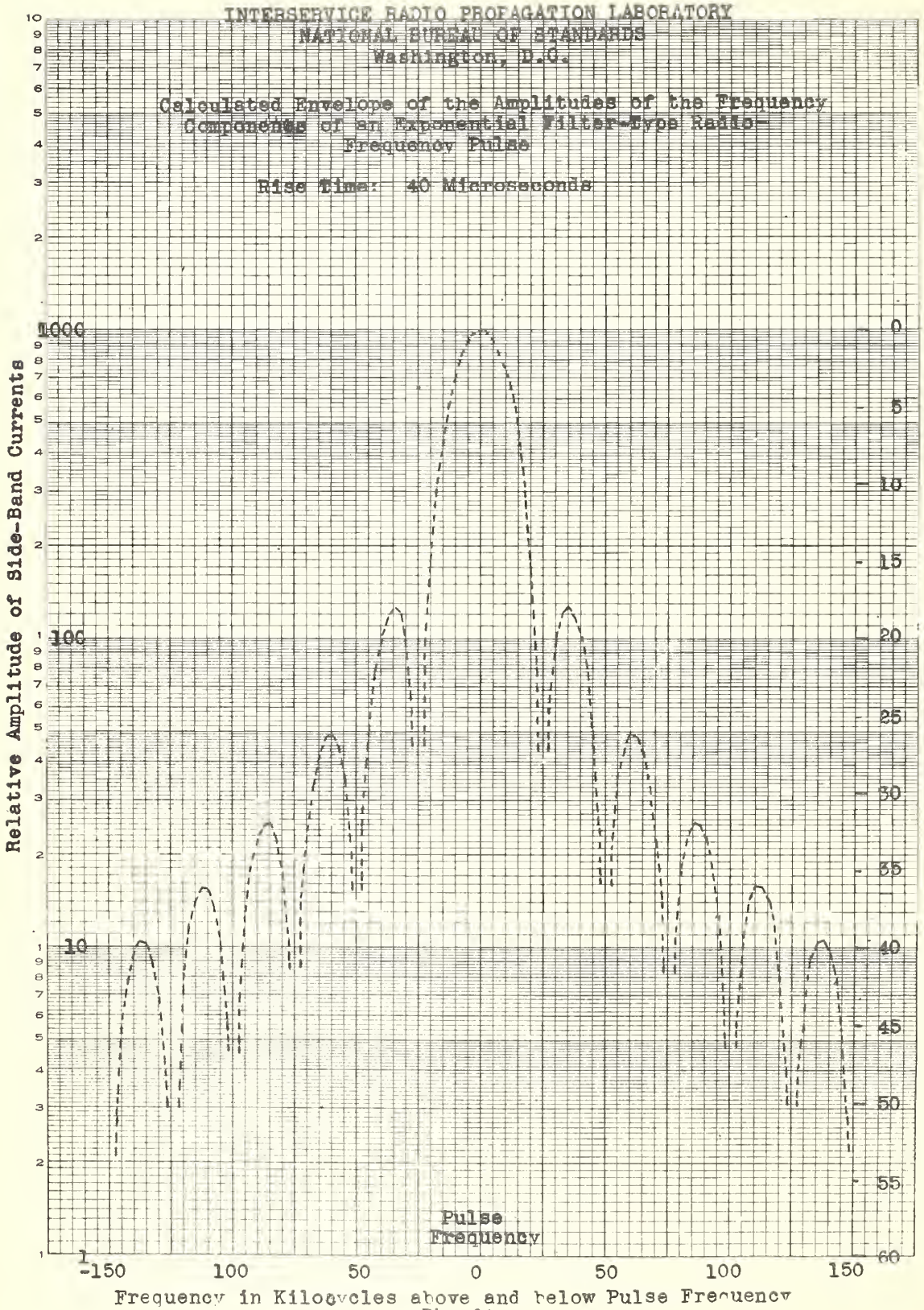
INTERSERVICE RADIO PROPAGATION LABORATORY
NATIONAL BUREAU OF STANDARDS
Washington, D.C.
Calculated Envelope of the Amplitudes of the Frequency Components of an Exponential Filter-Type Radio-Frequency Pulse
Rise Time: 40 Microseconds
Relative Amplitude of Side-Band Currents
1000
100
10
1
Relative Amplitude - Db
0
5
10
15
20
25
30
35
40
45
50
55
60
Pulse Frequency
-150
100
50
0
50
100
150
Frequency in Kilocycles above and below Pulse Frequency

Fig. 14

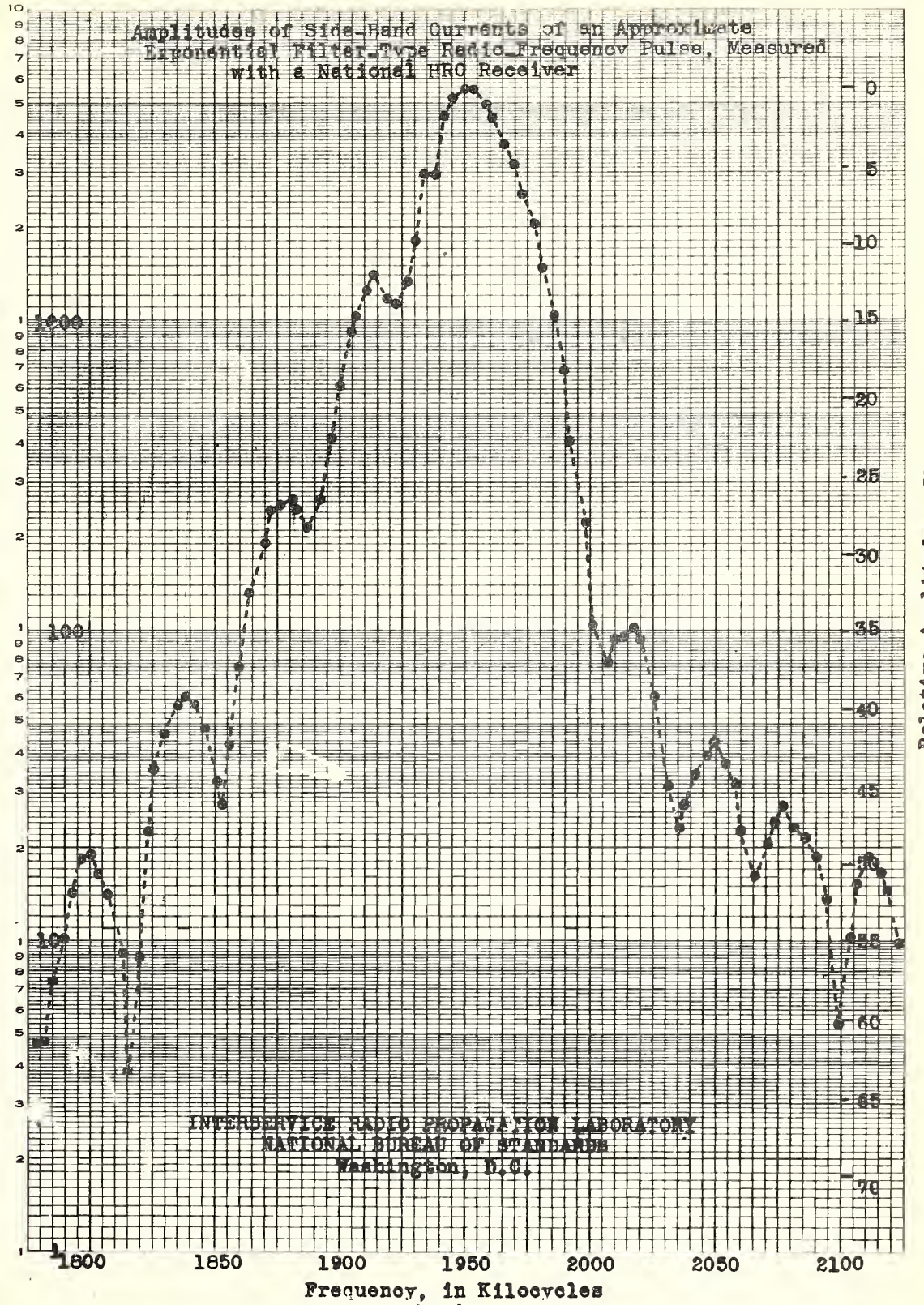
Amplitudes of Side-Band Currents of an Approximate
Exponential Filter-Type Radio-Frequency Pulse, Measured
with a National HRO Receiver
Relative Amplitude of Side-Band Currents
Relative Amplitude - Db
1000
100
10
1
0
5
10
15
20
25
30
35
40
45
50
55
60
65
70
1800
1850
1900
1950
2000
2050
2100
Frequency, in Kilocycles
INTERSERVICE RADIO PROPAGATION LABORATORY
NATIONAL BUREAU OF STANDARDS
Washington, D.C.

Fig. 15

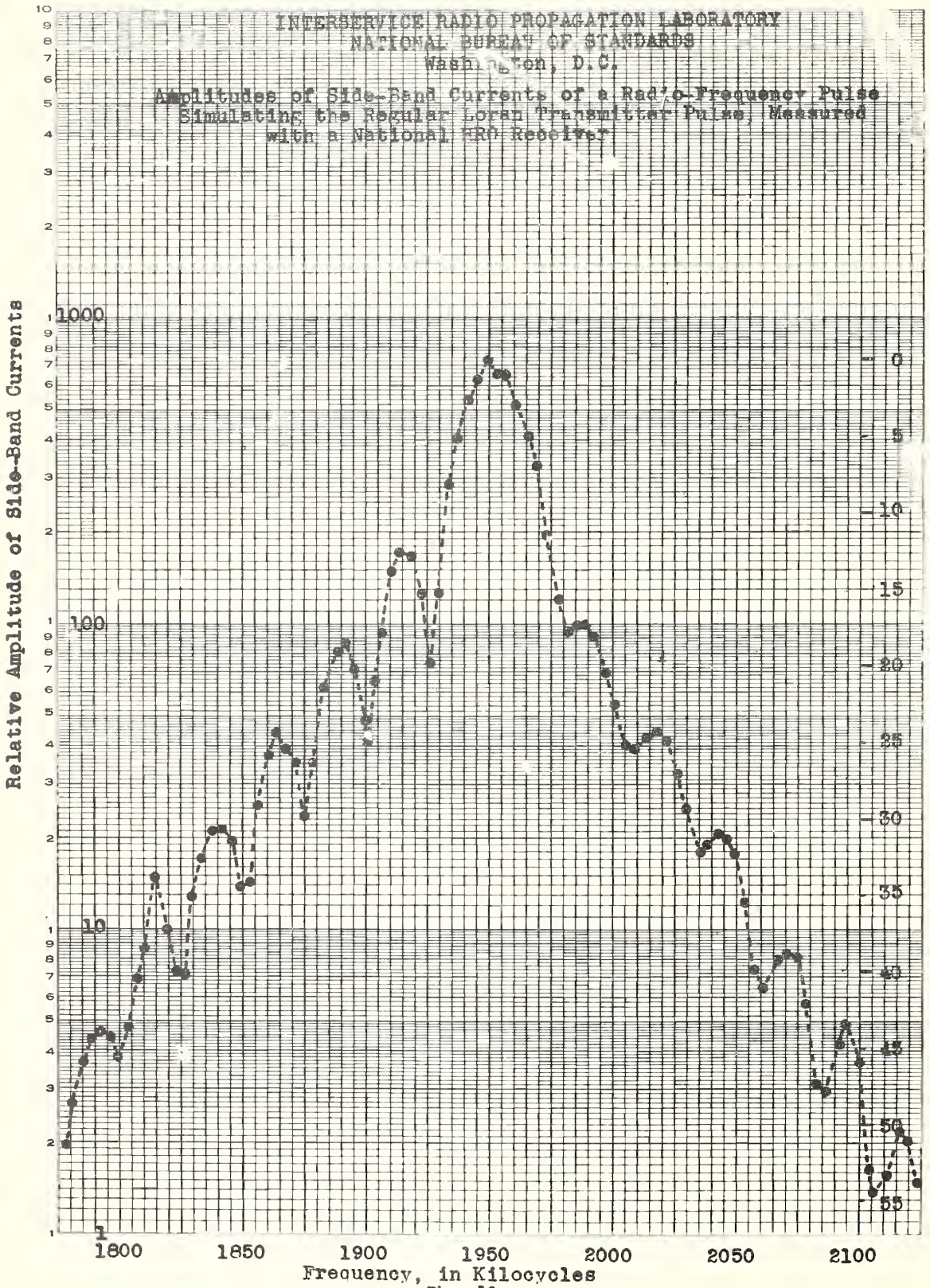
INTERSERVICE RADIO PROPAGATION LABORATORY
NATIONAL BUREAU OF STANDARDS
Washington, D.C.
Amplitudes of Side-Band Currents of a Radio-Frequency Pulse Simulating the Regular Loran Transmitter Pulse, Measured with a National HRO Receiver
Relative Amplitude of Side-Band Currents
1000
100
10
1
1800
1850
1900
1950
2000
2050
2100
Frequency, in Kilocycles
Relative Amplitude - Db
0
5
10
15
20
25
30
35
40
45
50
55

Fig. 16

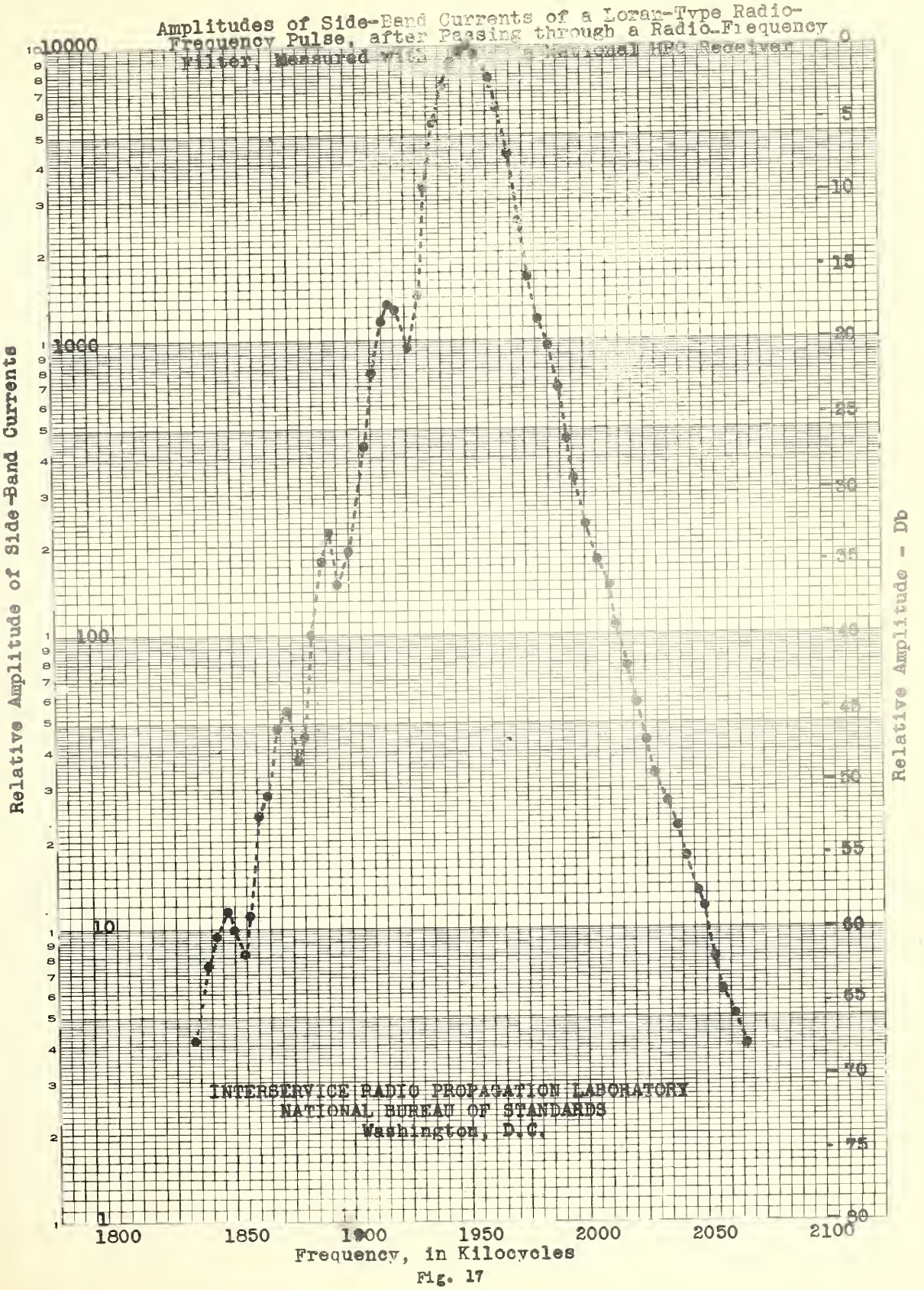
Amplitudes of Side-Band Currents of a Loran-Type Radio-Frequency Pulse, after Passing through a Radio-Frequency Filter, Measured with a Standard HRO Receiver
Relative Amplitude of Side-Band Currents
Relative Amplitude - Db
10000
1000
100
10
1
0
-5
-10
-15
-20
-25
-30
-35
-40
-45
-50
-55
-60
-65
-70
-75
-80
1800
1850
1900
1950
2000
2050
2100
Frequency, in Kilocycles
INTERSERVICE RADIO PROPAGATION LABORATORY
NATIONAL BUREAU OF STANDARDS
Washington, D.C.

Fig. 17

INTERSERVICE RADIO PROPAGATION LABORATORY
NATIONAL BUREAU OF STANDARDS
Washington, D.C.

Oscilloscope Tracings of Pulses
Measured for Frequency Components
(Radio-Frequency Envelope)

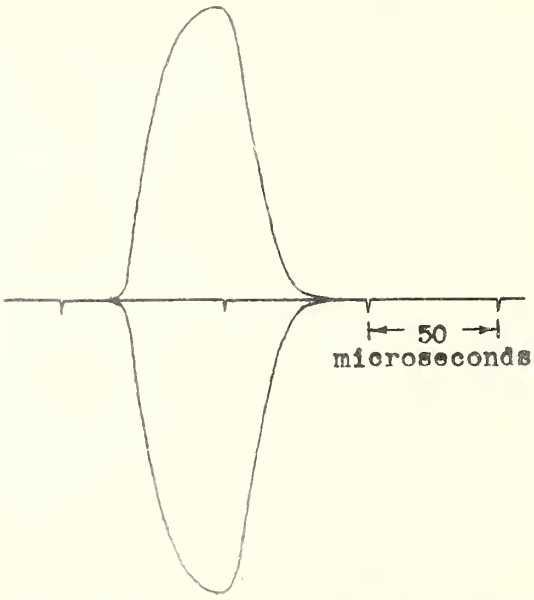

Approximate Exponential Filter-Type Pulse

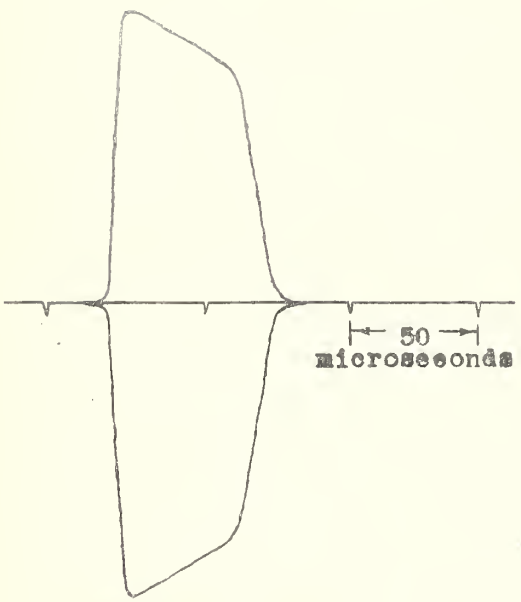

Loran Type Pulse

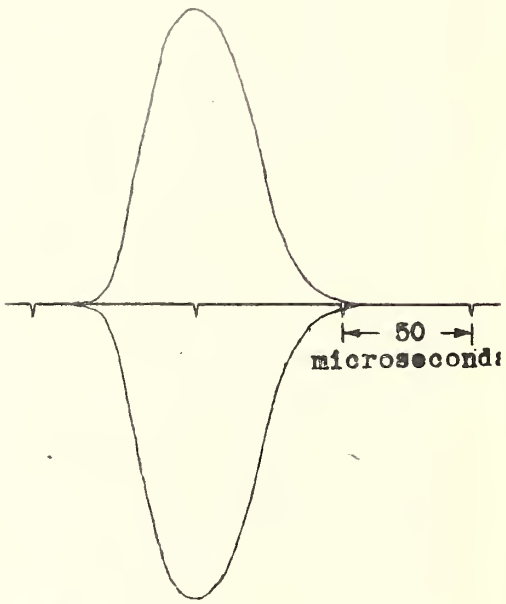

Loran Type Pulse after passing
through a radio-frequency filter

Fig. 18

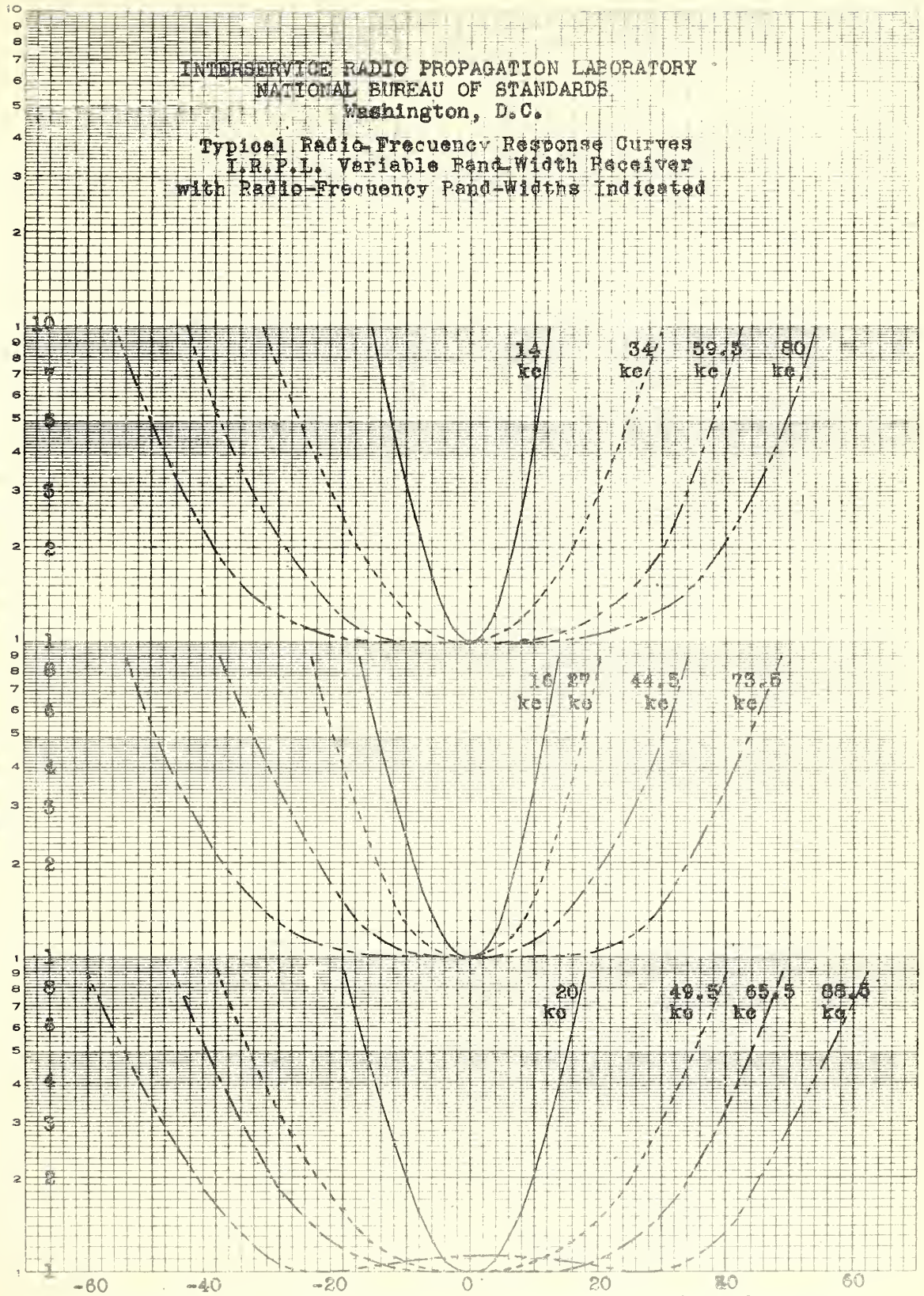
INTERSERVICE RADIO PROPAGATION LABORATORY
NATIONAL BUREAU OF STANDARDS
Washington, D.C.
Typical Radio-Frecuency Response Curves
I.R.P.L. Variable Band-Width Receiver
with Radio-Frequency Band-Widths Indicated
14 kc
34 kc
59.5 kc
80 kc
16 kc
27 kc
44.5 kc
73.5 kc
20 kc
49.5 kc
65.5 kc
88.5 kc
Relative input constant output
-60
-40
-20
0
20
40
60
Frequencies in kilocycles above and below receiver frequency

Fig. 19

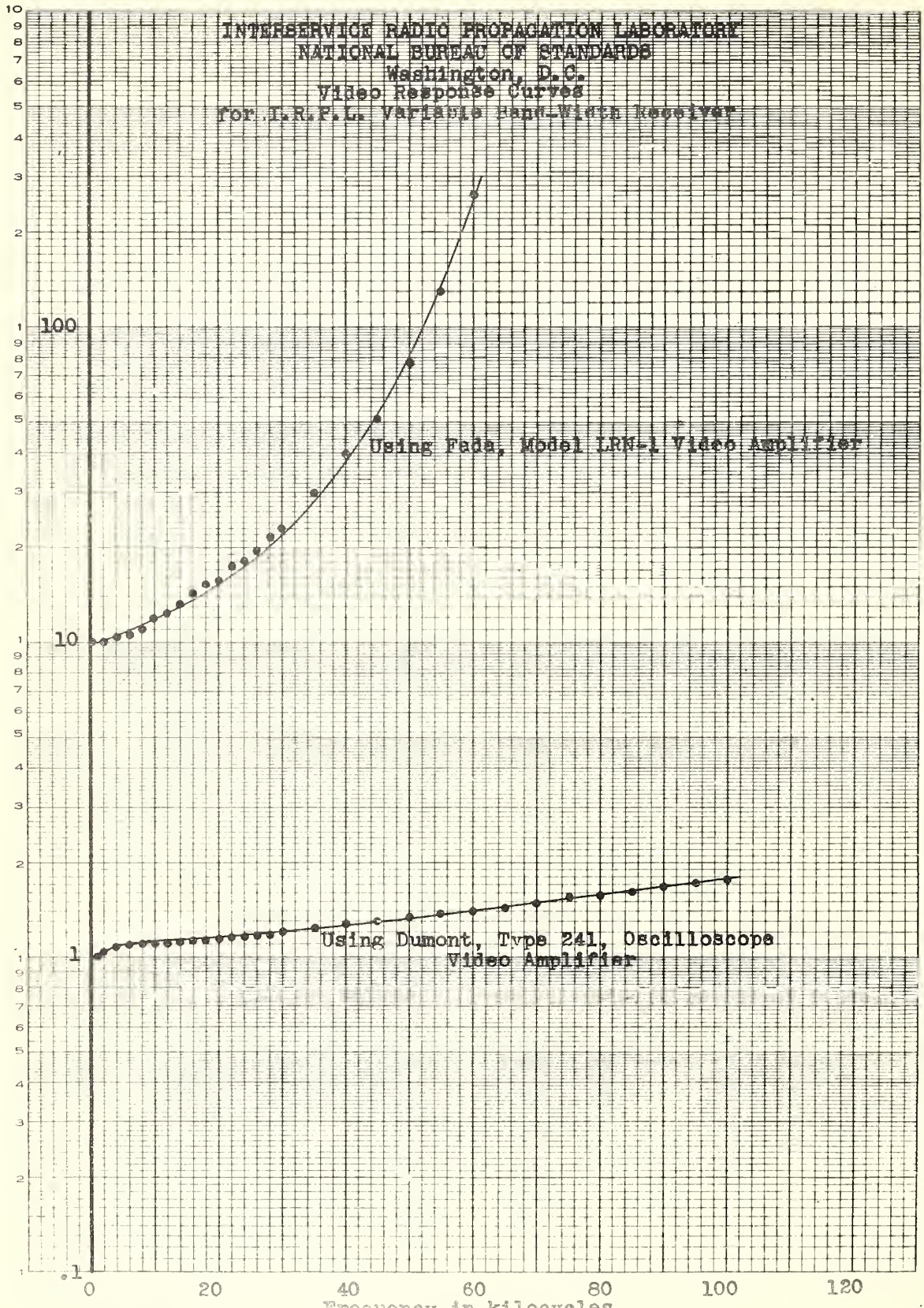
INTERSERVICE RADIO PROPAGATION LABORATORY
NATIONAL BUREAU OF STANDARDS
Washington, D.C.
Video Response Curves
for I.R.P.L. Variable Band-Width Receiver
Using Fada, Model LRN-1 Video Amplifier
Using Dumont, Type 241, Oscilloscope
Video Amplifier
100
10
1
.1
Relative input for constant output
0
20
40
60
80
100
120
Frequency in kilocycles

Fig. 20

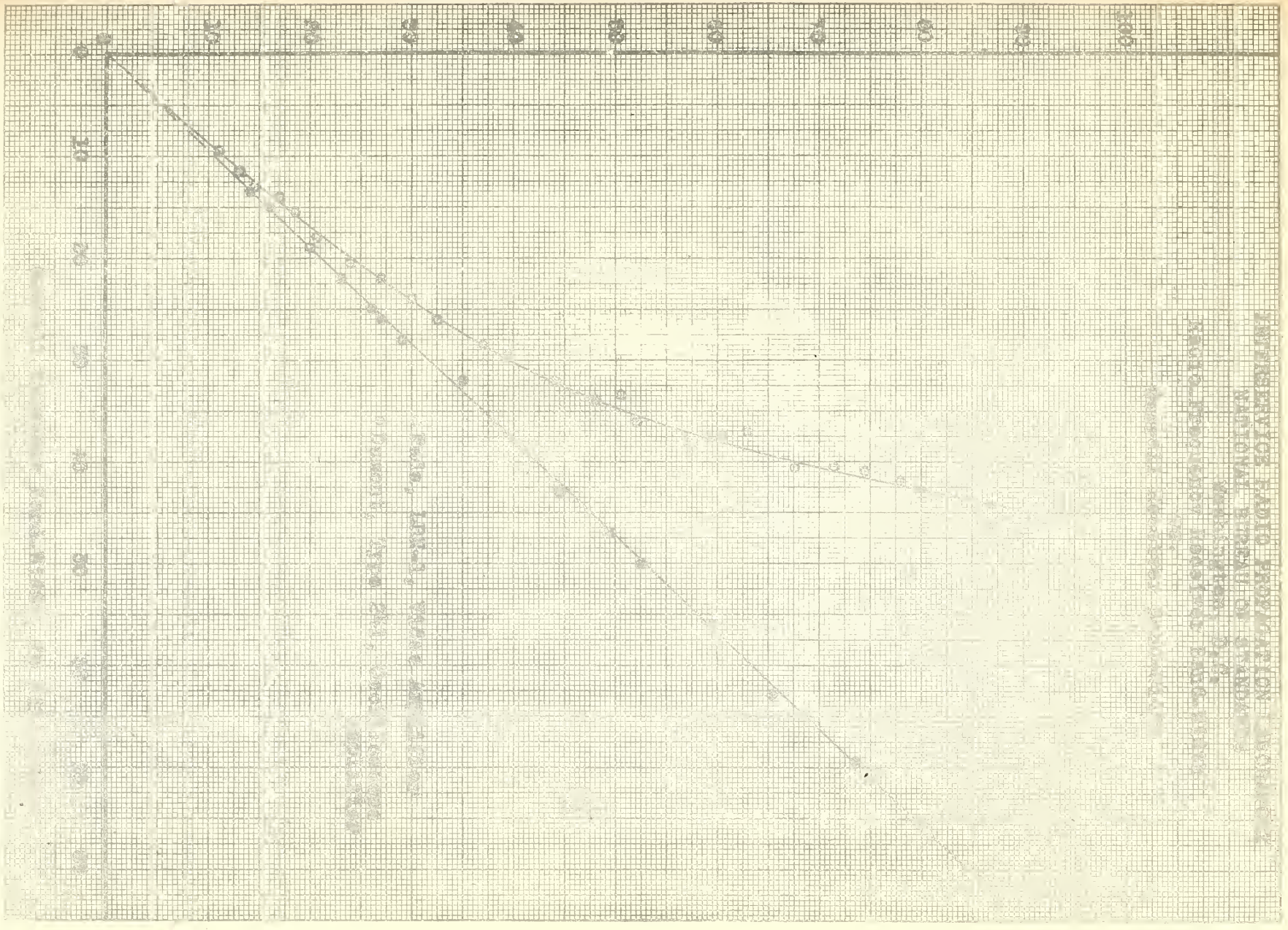
Radio-Frequency Receiver Band-Width, in Kilocycles

INTERSERVICE RADIO PROPAGATION LABORATORY
NATIONAL BUREAU OF STANDARDS
Washington, D.C.
Comparison of Pulse Shapes Obtained with Different
Receiver Band-Widths from the Regular Loran Pulse

(Markers indicate 50-microsecond intervals)

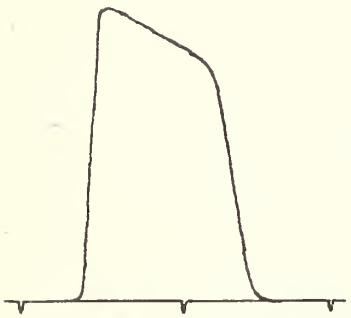

Receiver input pulse

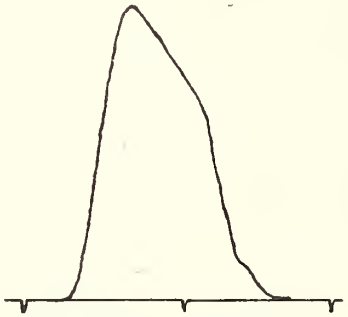

Overall band width
86.0 kc

Overall band width
75.5 kc

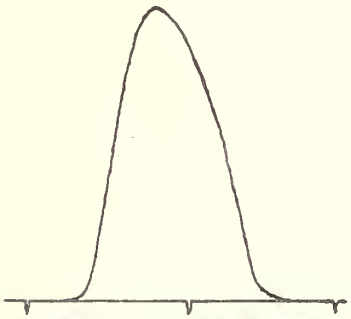

Overall band width
63.0 kc

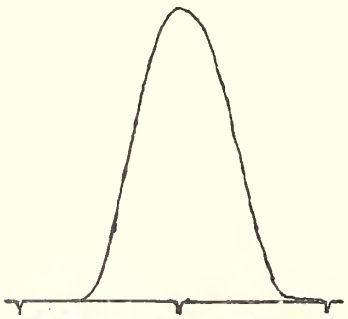

Overall band width
50.0 kc

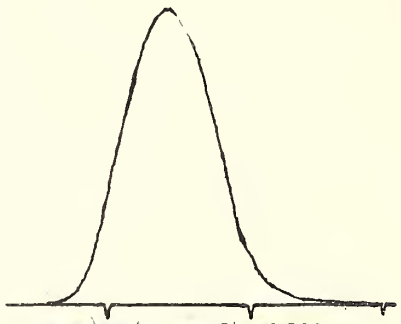

Overall band width
37.0 kc

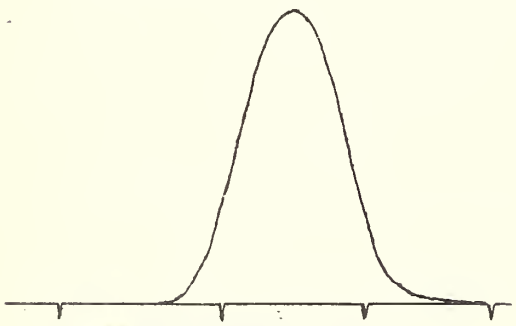

Overall band width
29.5 kc

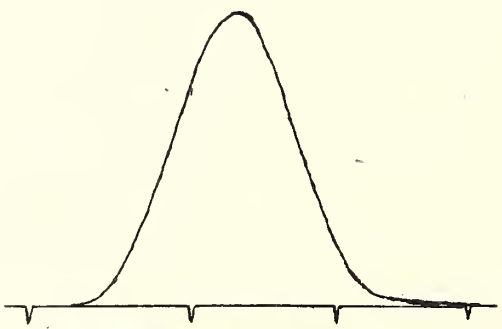

Overall band width
22.0 kc

Fig. 22

INTERSERVICE RADIO PROPAGATION LABORATORY
NATIONAL BUREAU OF STANDARDS
Washington, D.C.

Comparison of Pulse Shapes Obtained with Different Receiver Band-Widths from a Loran-Type Pulse with a Radio-Frequency Filter Inserted between the Pulse Generator and the Receiver
(Markers indicate 50-microsecond intervals)

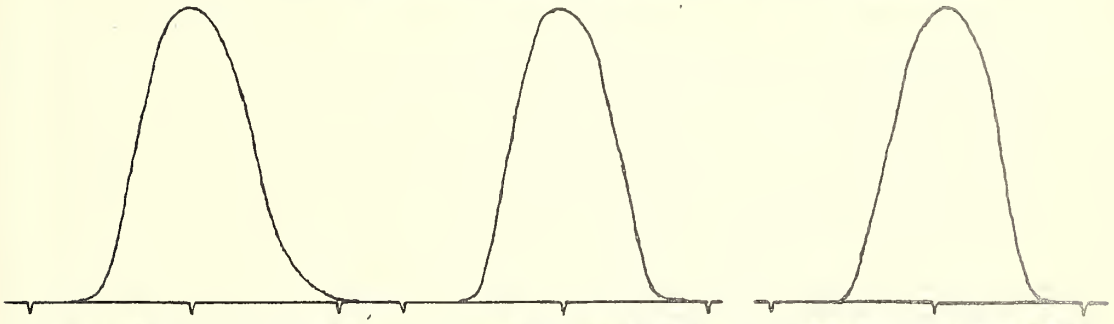

Receiver input pulse

Overall band width
86.0 kc

Overall band width
75.5 kc

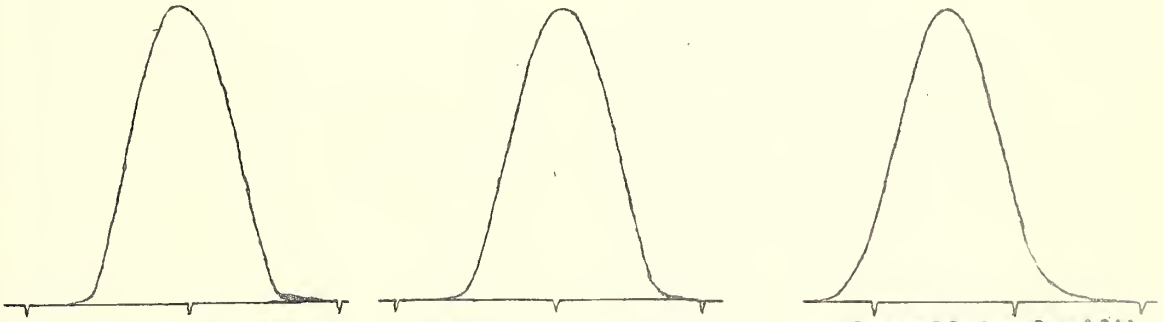

Overall band width
63.0 kc

Overall band width
50.0 kc

Overall band width
38.0 kc

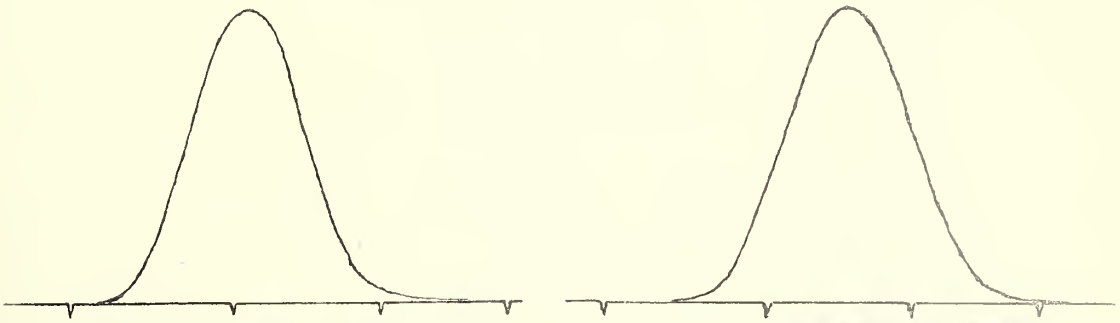

Overall band width
29.5 kc

Overall band width
22.0 kc

Fig. 23

INTERSERVICE RADIO PROPAGATION LABORATORY
NATIONAL BUREAU OF STANDARDS
Washington, D.C.

Comparison of Pulse Shapes Obtained with Different Receiver Band-Widths from an Approximate Exponential Filter-Type Pulse

(Markers indicate 50-microsecond intervals)

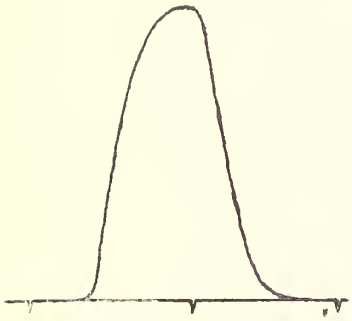

Receiver input pulse

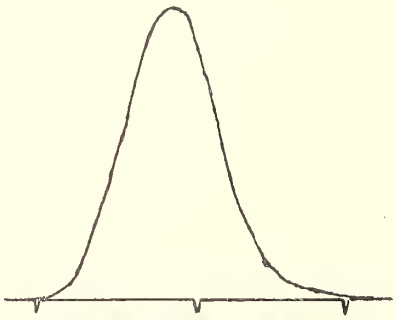

Overall band width
56.5 kc

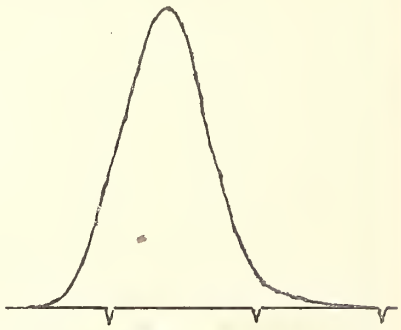

Overall band width
33.5 kc

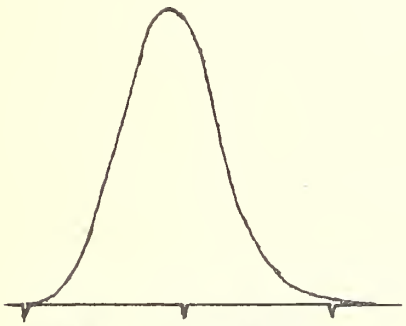

Overall band width
29.5 kc

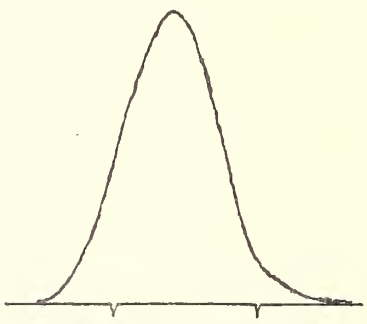

Overall band width
24.5 kc

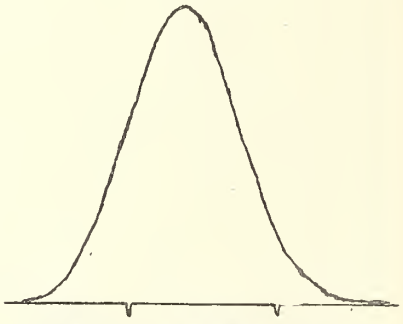

Overall band width
19.5 kc

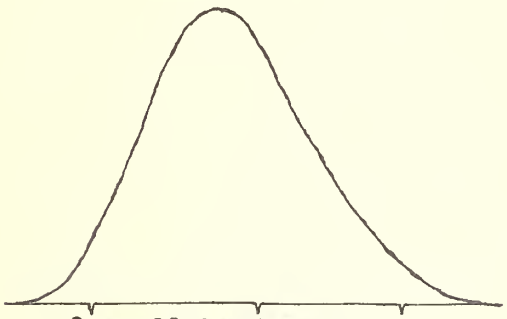

Overall band width
14.0 kc

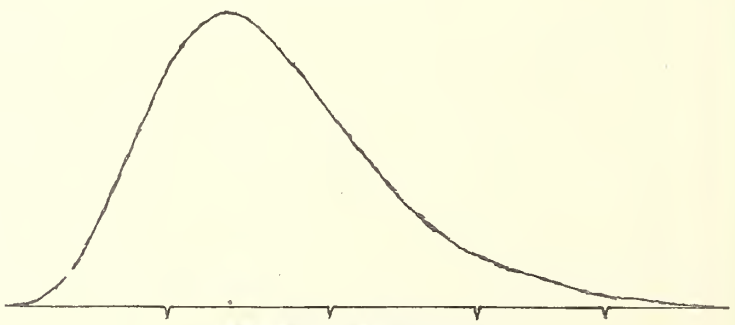

Overall band width
10.0 kc

Fig. 24

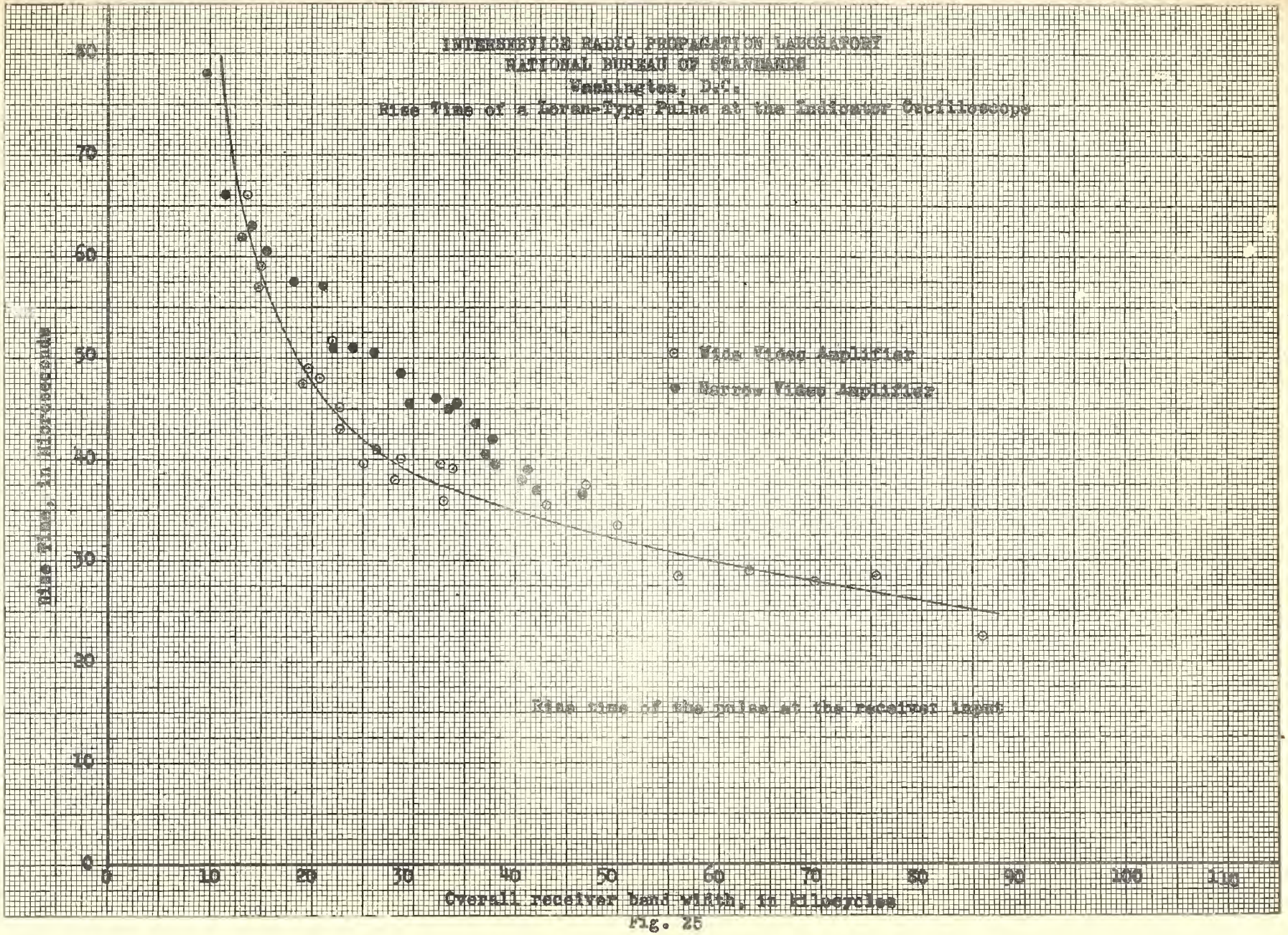
INTERSERVICE RADIO PROPAGATION LABORATORY
NATIONAL BUREAU OF STANDARDS
Washington, D.C.
Rise Time of a Loran-Type Pulse at the Indicator Oscilloscope
Rise time, in microseconds
80
70
60
50
40
30
20
10
0
Wide Video Amplifier
Narrow Video Amplifier
Rise time of the pulse at the receiver input
0
10
20
30
40
50
60
70
80
90
100
110
Overall receiver band width, in kilocycles

Fig. 25

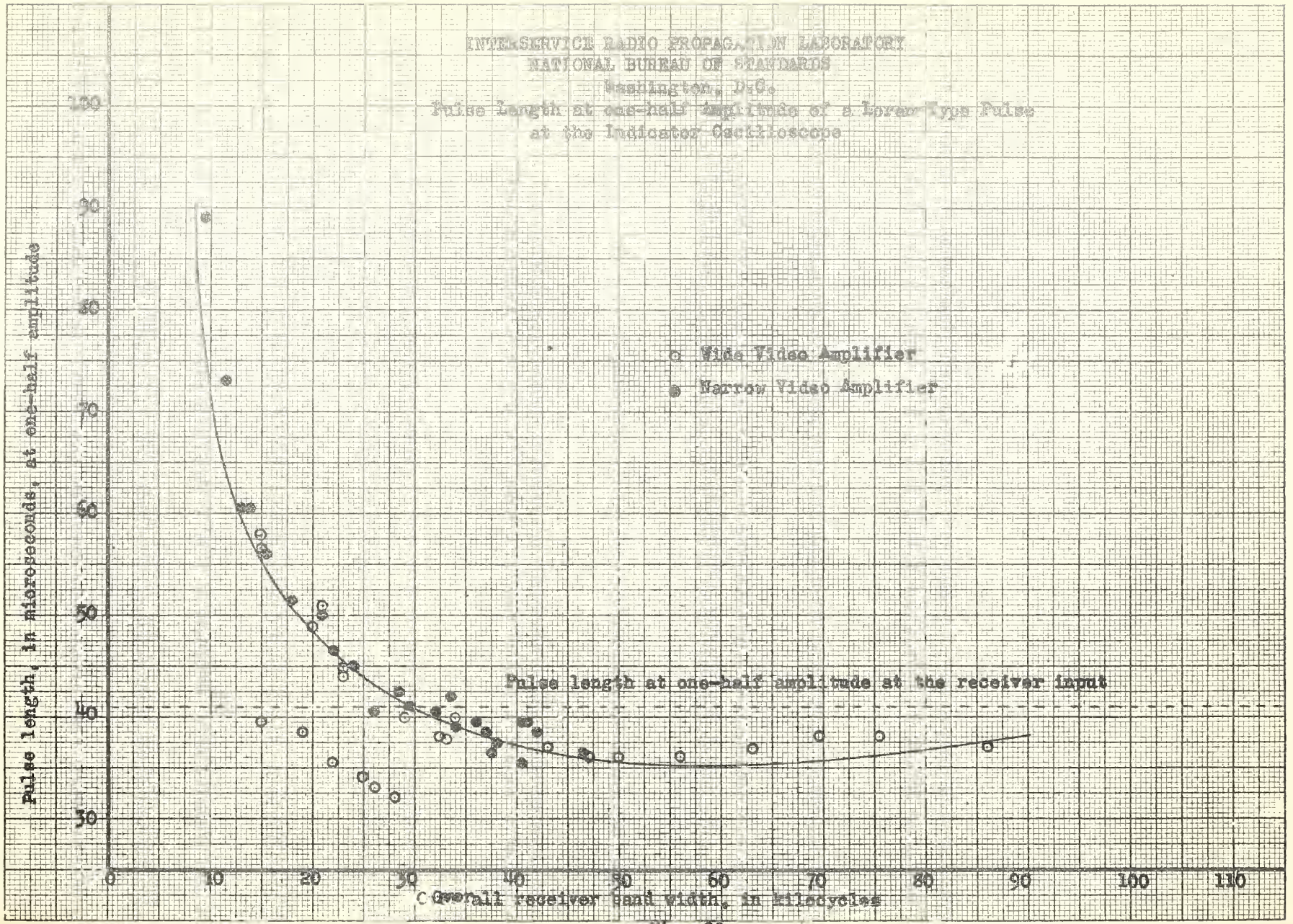
INTER-SERVICE RADIO PROPAGATION LABORATORY
NATIONAL BUREAU OF STANDARDS
Washington, D.C.
Pulse Length at one-half Amplitude of a Lower Type Pulse
at the Indicator Oscilloscope
o Wide Video Amplifier
● Narrow Video Amplifier
Pulse length at one-half amplitude at the receiver input
Pulse length, in microseconds, at one-half amplitude
100
90
80
70
60
50
40
30
0
10
20
30
40
50
60
70
80
90
100
110
Overall receiver band width, in kilocycles

Fig. 26

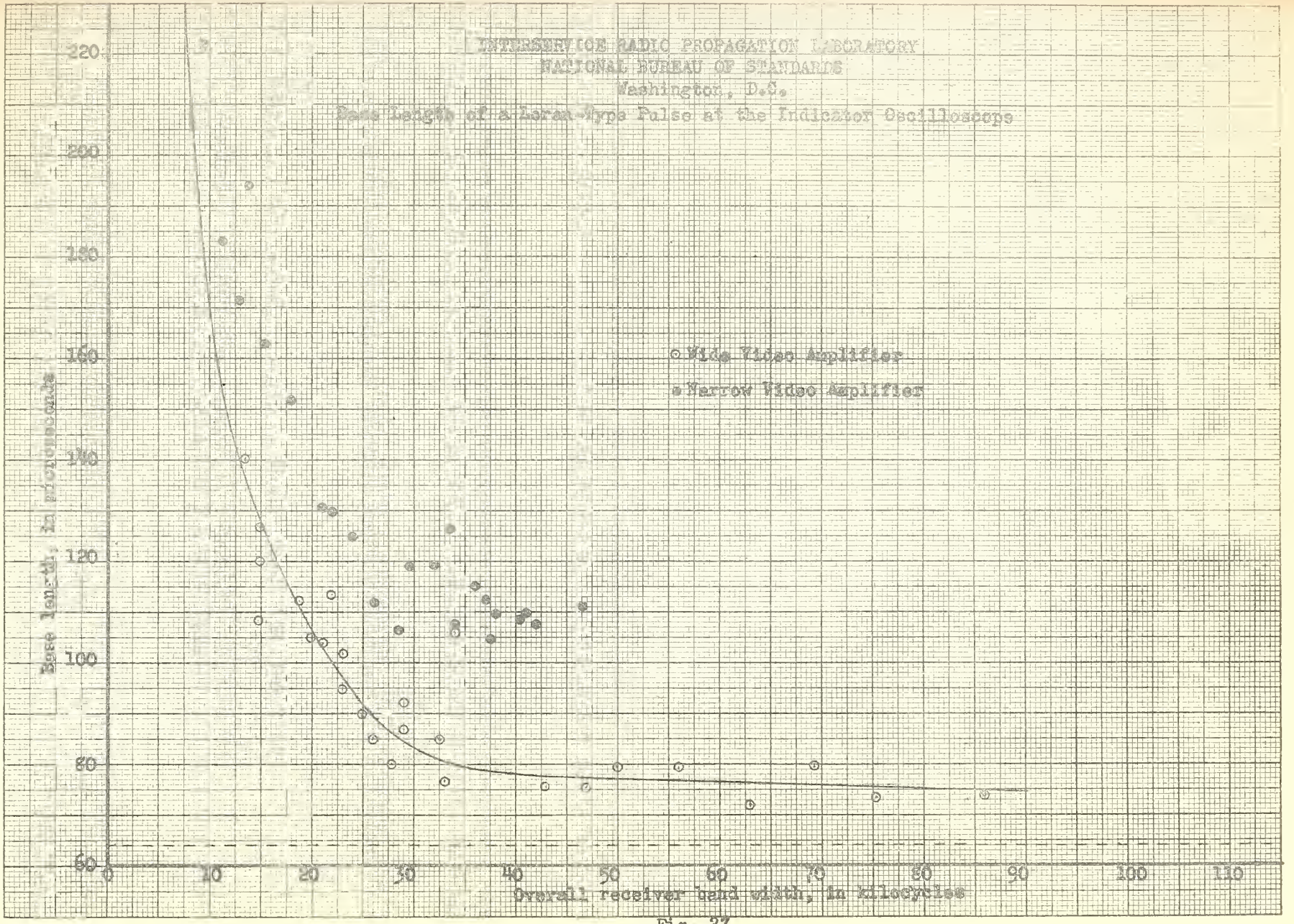
INTERSERVICE RADIO PROPAGATION LABORATORY
NATIONAL BUREAU OF STANDARDS
Washington, D.C.
Pulse Length of a Loran-Type Pulse at the Indicator Oscilloscope
Wide Video Amplifier
Narrow Video Amplifier
Pulse length, in microseconds
Overall receiver band width, in kilocycles
220
200
180
160
140
120
100
80
60
0
10
20
30
40
50
60
70
80
90
100
110

Fig. 27

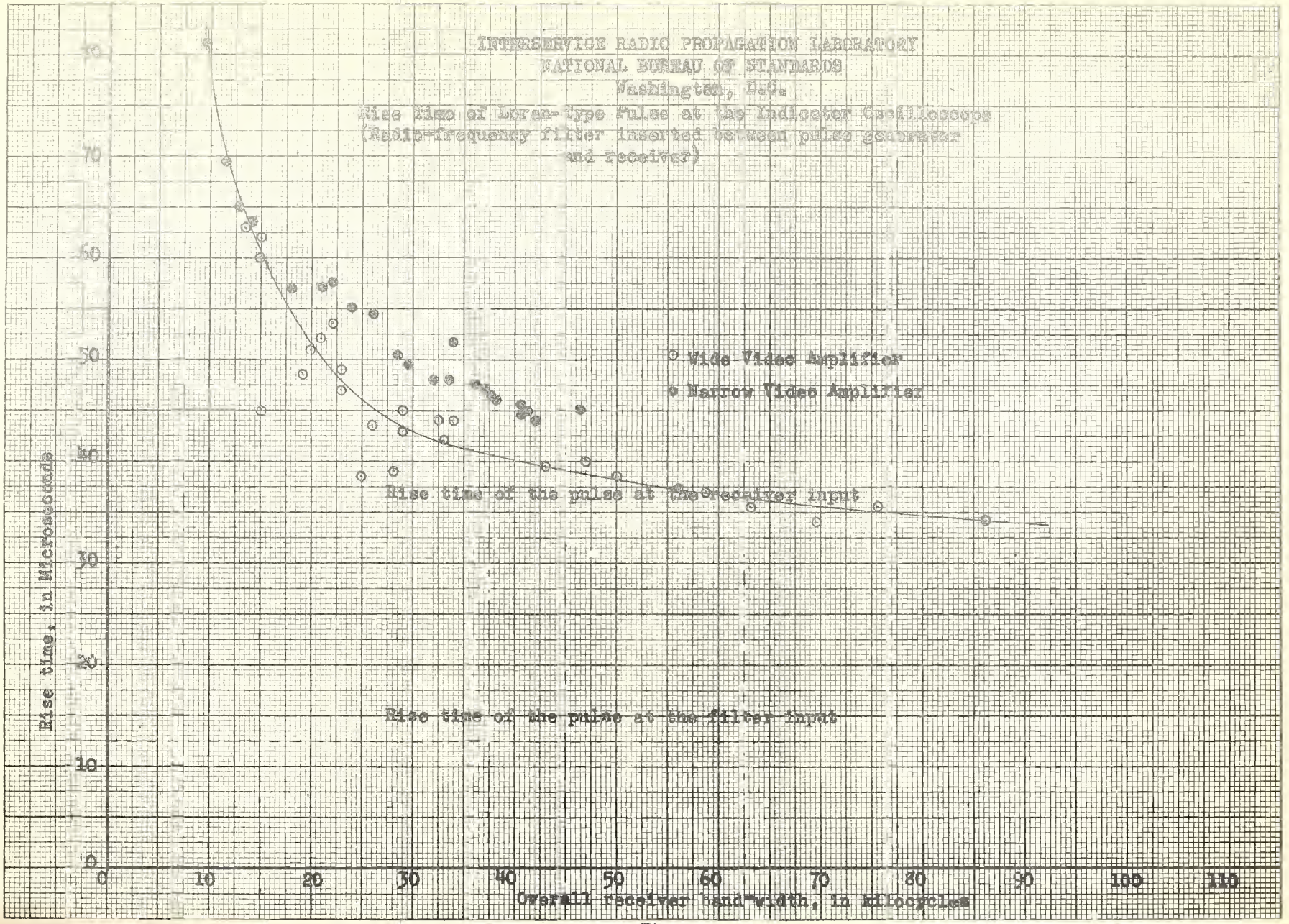
INTERSERVICE RADIO PROPAGATION LABORATORY
NATIONAL BUREAU OF STANDARDS
Washington, D.C.
Rise Time of Loran-Type Pulse at the Indicator Oscilloscope
(Radio-frequency filter inserted between pulse generator and receiver)
Wide Video Amplifier
Narrow Video Amplifier
Rise time of the pulse at the receiver input
Rise time of the pulse at the filter input
Rise time, in Microseconds
Overall receiver band-width, in Kilocycles
0
10
20
30
40
50
60
70
80
90
100
110

Fig. 28

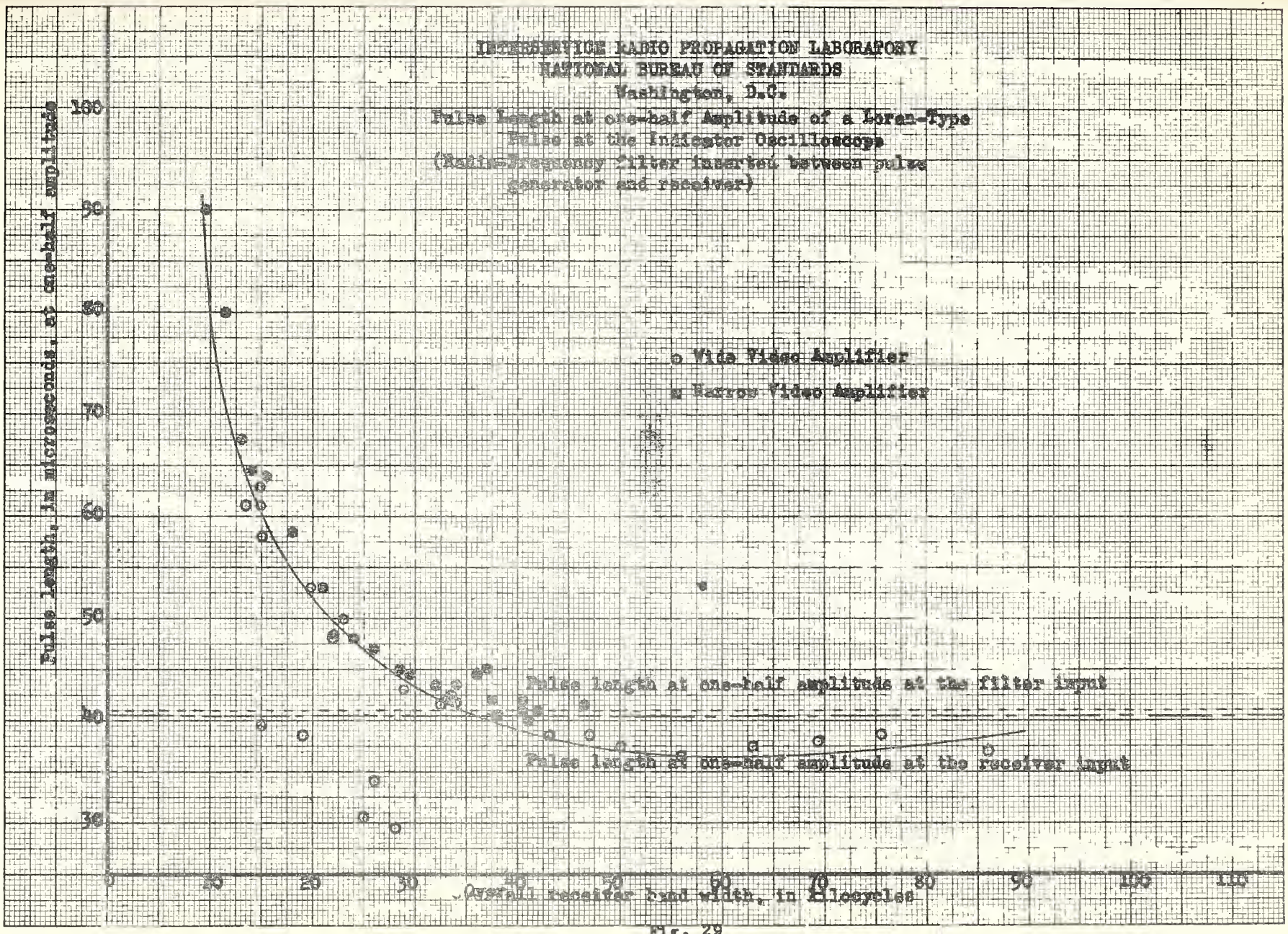
INTERSERVICE RADIO PROPAGATION LABORATORY
NATIONAL BUREAU OF STANDARDS
Washington, D.C.
Pulse Length at one-half Amplitude of a Loran-Type Pulse at the Indicator Oscilloscope
(Radio-frequency filter inserted between pulse generator and receiver)
Pulse length, in microseconds, at one-half amplitude
100
90
80
70
60
50
40
30
0
10
20
30
40
50
60
70
80
90
100
110
Overall receiver band width, in kilocycles
o Wide Video Amplifier
x Narrow Video Amplifier
Pulse length at one-half amplitude at the filter input
Pulse length at one-half amplitude at the receiver input

Fig. 29

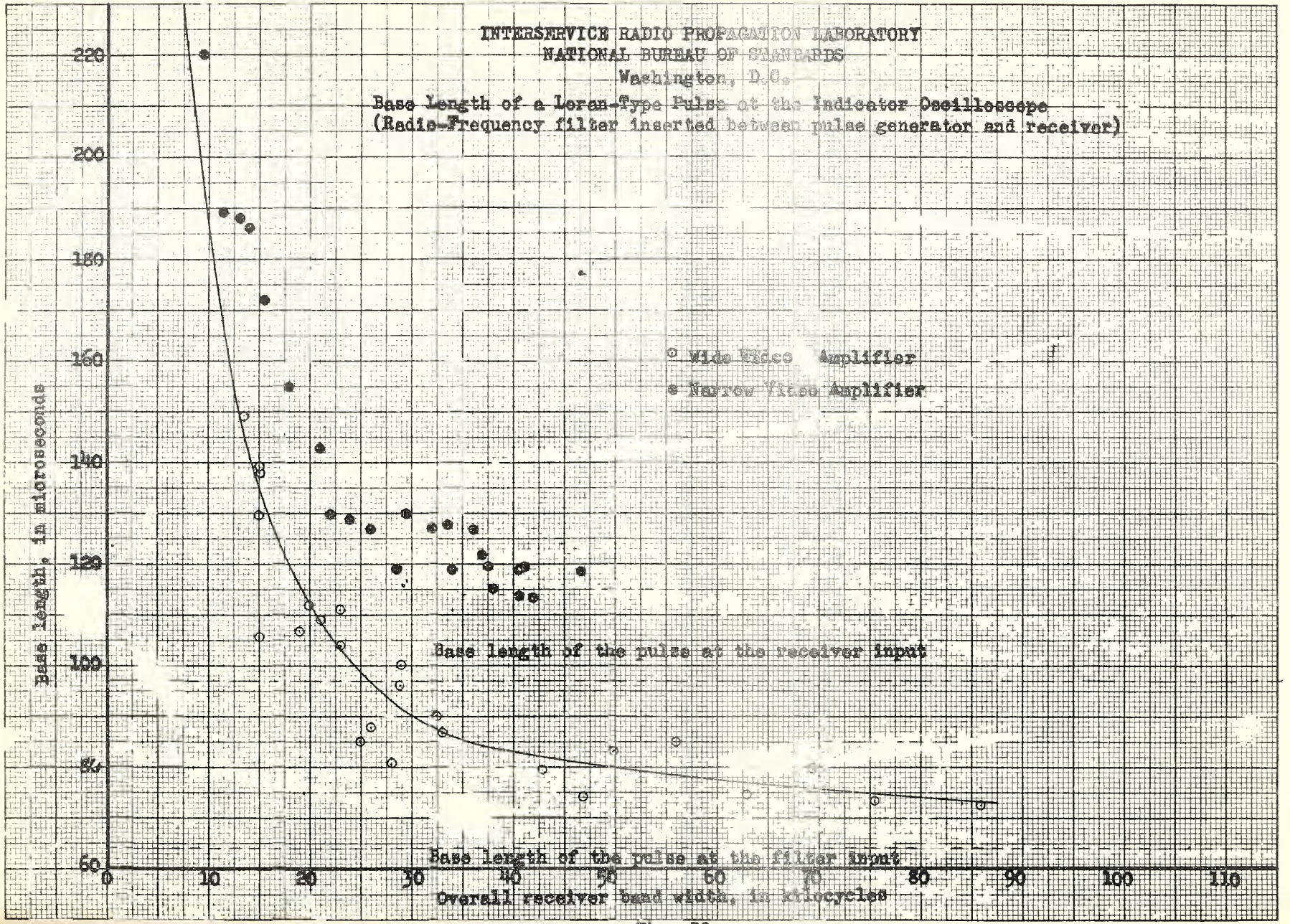
INTERSERVICE RADIO PROPAGATION LABORATORY
NATIONAL BUREAU OF STANDARDS
Washington, D.C.
Base Length of a Loran-Type Pulse at the Indicator Oscilloscope
(Radio-Frequency filter inserted between pulse generator and receiver)
Wide Video Amplifier
Narrow Video Amplifier
Base length of the pulse at the receiver input
Base length of the pulse at the filter input
Base length, in microseconds
Overall receiver band width, in kilocycles
220
200
180
160
140
120
100
80
60
0
10
20
30
40
50
60
70
80
90
100
110

Fig. 30

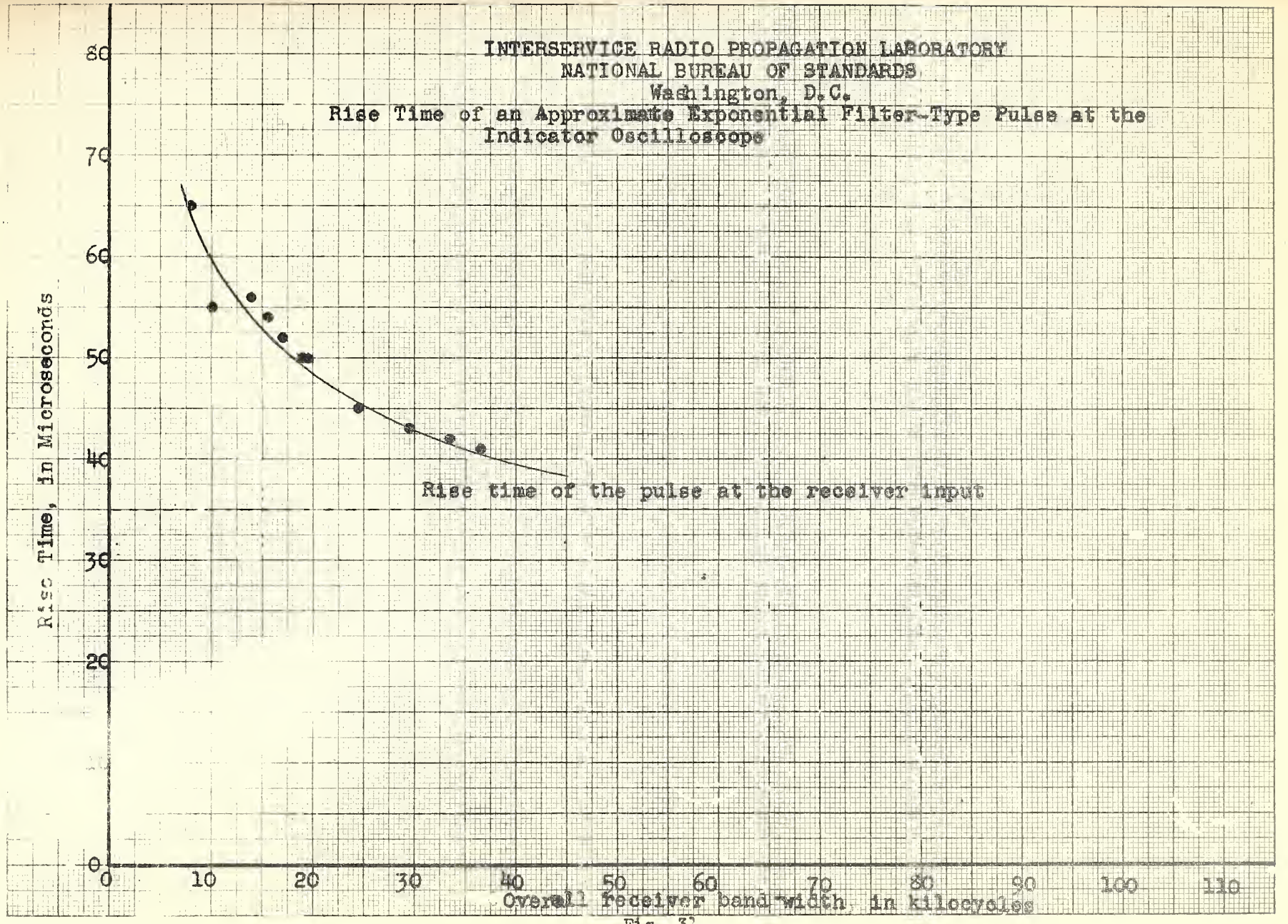
INTERSERVICE RADIO PROPAGATION LABORATORY
NATIONAL BUREAU OF STANDARDS
Washington, D.C.
Rise Time of an Approximate Exponential Filter-Type Pulse at the Indicator Oscilloscope
Rise Time, in Microseconds
Rise time of the pulse at the receiver input
Overall receiver band-width in kilocycles
0
10
20
30
40
50
60
70
80
90
100
110

Fig. 31

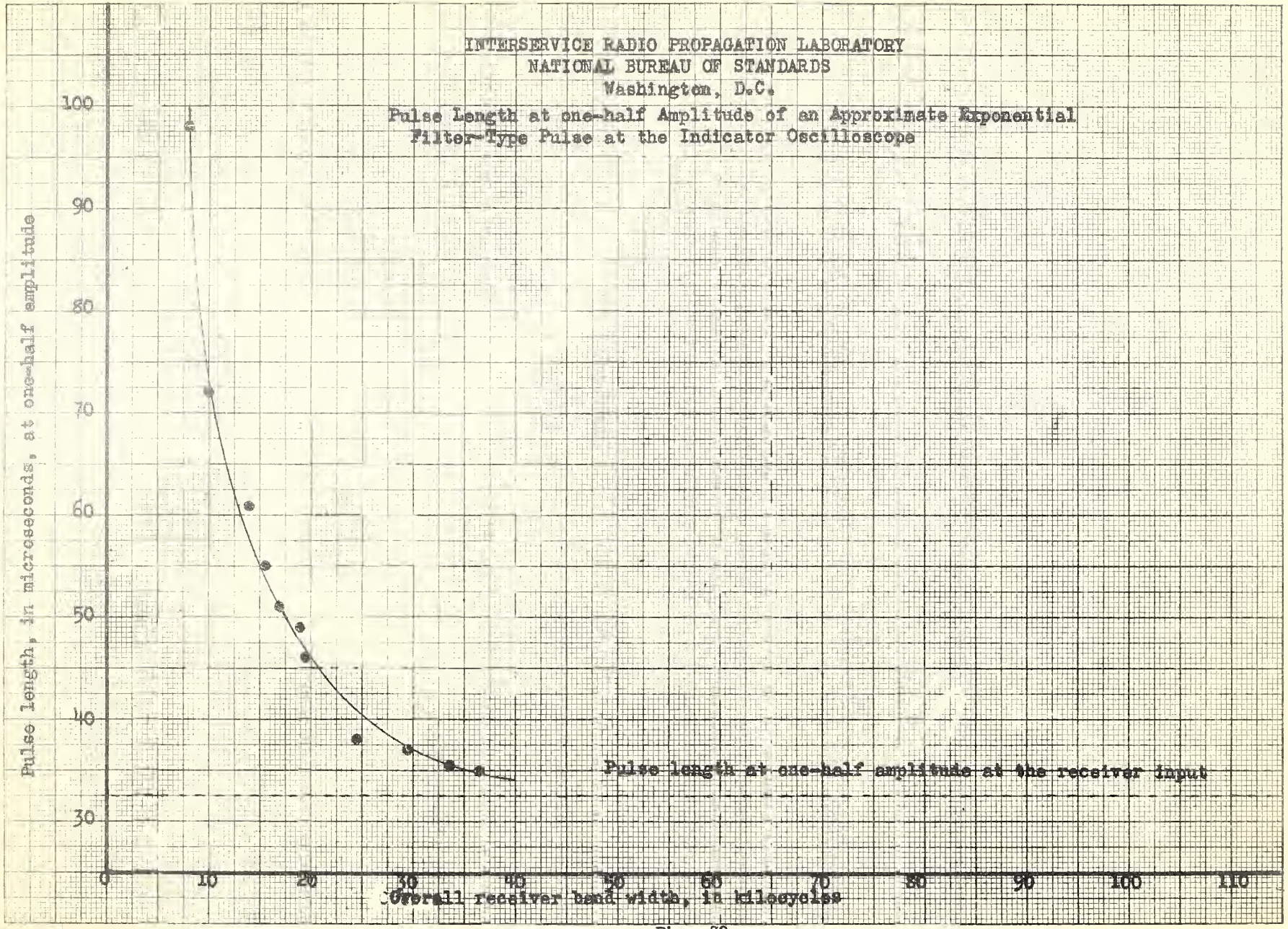
INTERSERVICE RADIO PROPAGATION LABORATORY
NATIONAL BUREAU OF STANDARDS
Washington, D.C.
Pulse Length at one-half Amplitude of an Approximate Exponential Filter-Type Pulse at the Indicator Oscilloscope
Pulse length, in microseconds, at one-half amplitude
100
90
80
70
60
50
40
30
0
10
20
30
40
50
60
70
80
90
100
110
Overall receiver band width, in kilocycles
Pulse length at one-half amplitude at the receiver input

Fig. 32

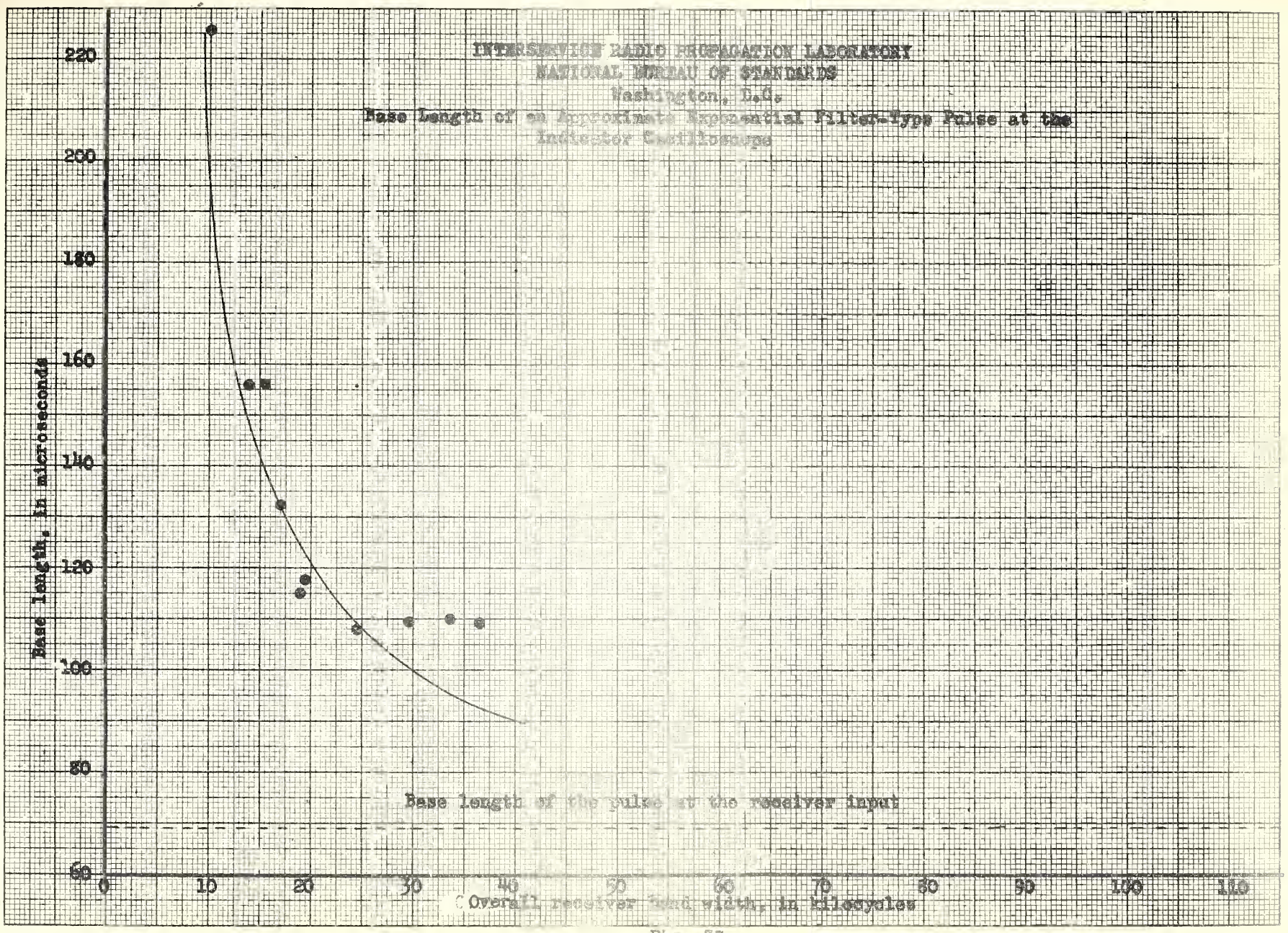
INTER-SERVICE RADIO PROPAGATION LABORATORY
NATIONAL BUREAU OF STANDARDS
Washington, D.C.
Base Length of an Approximate Exponential Filter-Type Pulse at the Indicator Oscilloscope
Base length, in microseconds
220
200
180
160
140
120
100
80
60
0
10
20
30
40
50
60
70
80
90
100
110
Base length of the pulse at the receiver input
Overall receiver band width, in kilocycles

Fig. 33

INTERSERVICE RADIO PROPAGATION LABORATORY
NATIONAL BUREAU OF STANDARDS
Washington, D.C.

Comparison of Pulses Obtained at the Oscilloscope of the Indicator with Different Adjustments of the Receiver Intermediate-Frequency Amplifier to Obtain the Same Band Widths Using a Loran-Type Pulse.

Intermediate-frequency amplifier tuned circuits damped with resistors.	No damping in intermediate-frequency amplifier.
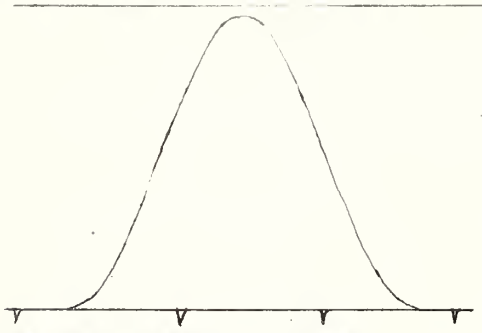	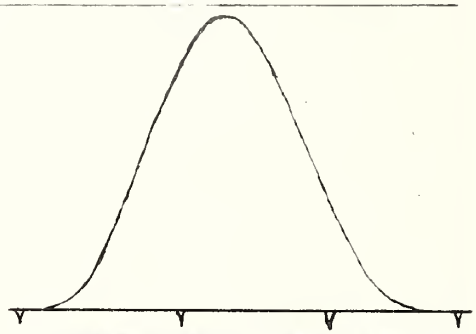
overall band width 15 kc	overall band width 15 kc
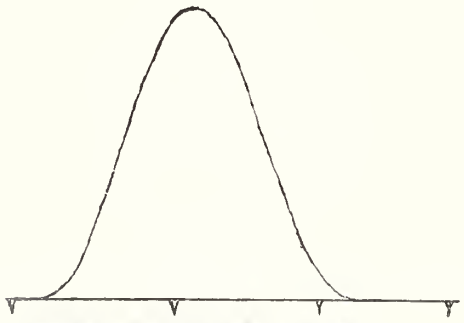	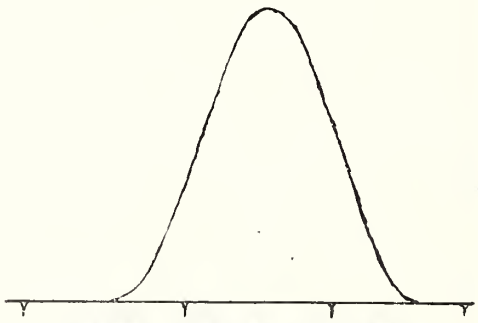
overall band width 20 kc	overall band width 21 kc
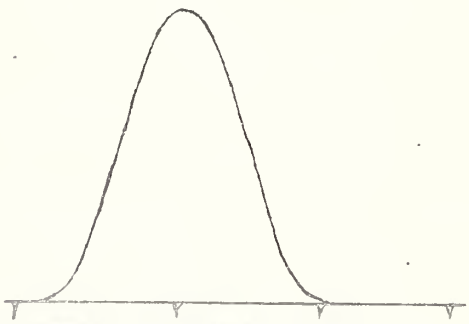	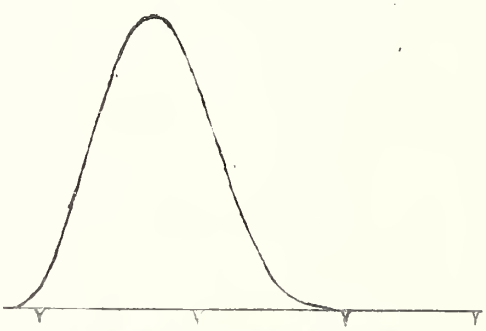
overall band width 25 kc	overall band width 23 kc

Fig.

INTERSERVICE RADIO PROPAGATION LABORATORY
NATIONAL BUREAU OF STANDARDS
Washington, D.C.

Comparison of Pulses Obtained at the Oscilloscope of the Indicator with Different Adjustments of the Receiver Intermediate-Frequency Amplifier to Obtain the Same Band Widths Using a Loran-Type Pulse.

Intermediate-frequency amplifier tuned circuits damped with resistors.	No damping in intermediate-frequency amplifier.
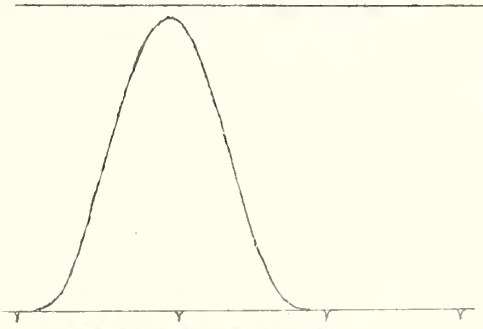 overall band width 29 kc	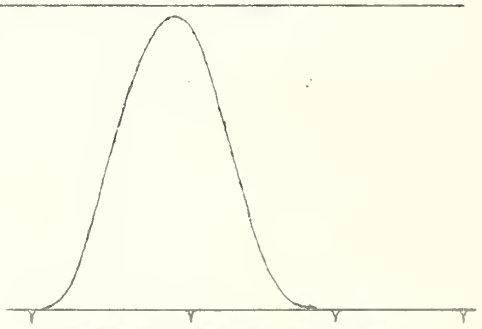 overall band width 29 kc
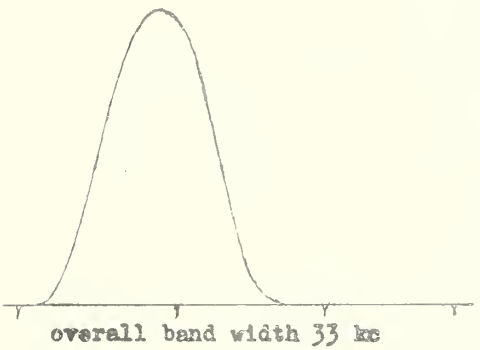 overall band width 33 kc	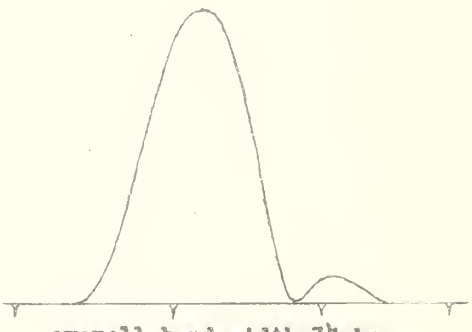 overall band width 34 kc

Fig. 34 (continued)

INTERSERVICE-RADIO PROPAGATION LABORATORY
NATIONAL BUREAU OF STANDARDS
Washington, D.C.

Comparison of Pulses Obtained at the Oscilloscope of the Indicator with Different Adjustments of the Receiver Intermediate-Frequency Amplifier to Obtain the Same Band Widths, Using a Loran-Type Pulse with Radio-Frequency Filter Inserted between Pulse Generator and Receiver

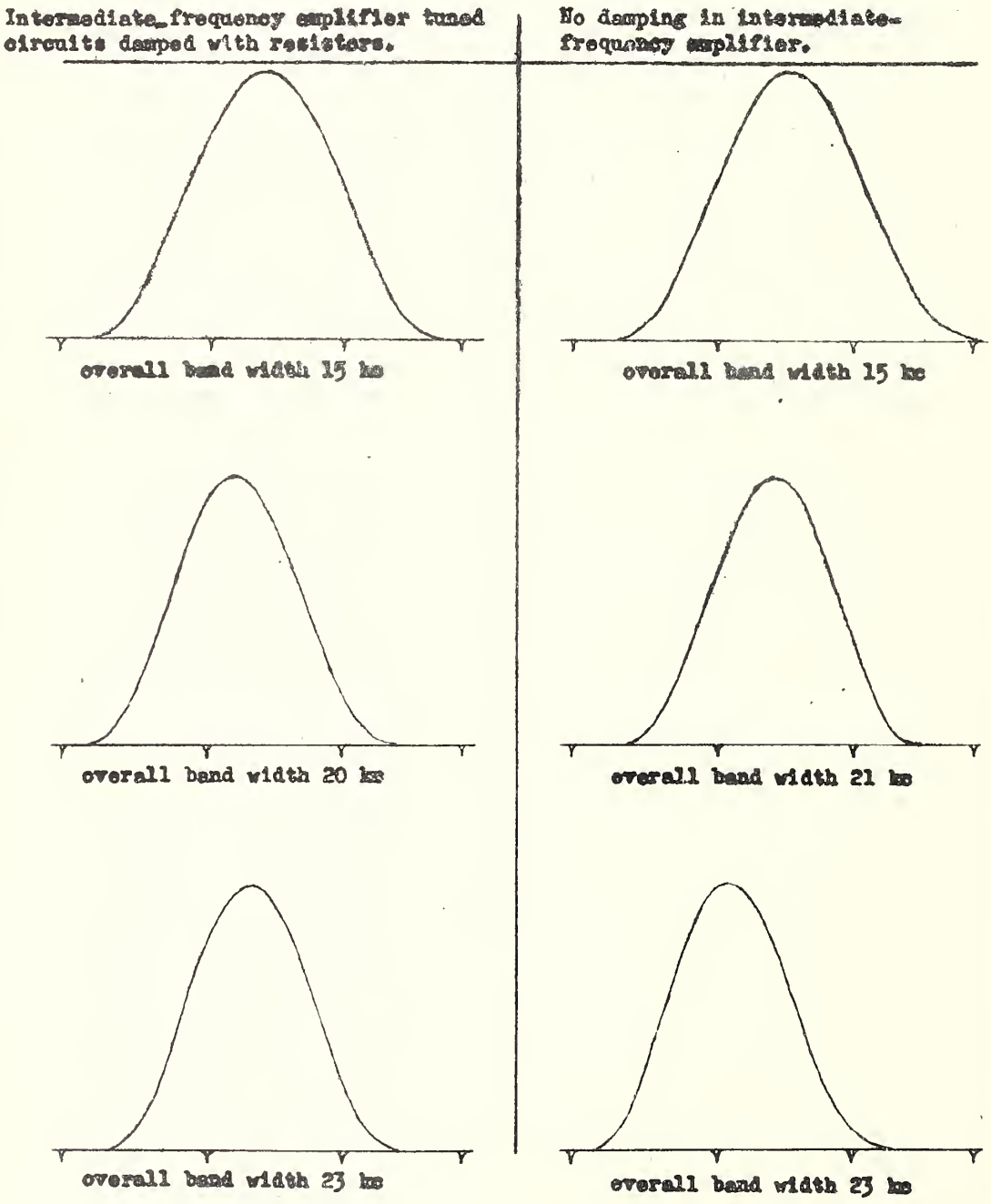

Fig. 36

INTERSERVICE RADIO PROPAGATION LABORATORY
NATIONAL BUREAU OF STANDARDS
Washington, D.C.

Comparison of Pulses Obtained at the Oscilloscope of the Indicator with Different Adjustments of the Receiver Intermediate-Frequency Amplifier to Obtain the Same Band Widths, Using a Loran-Type Pulse with Radio-Frequency Filter Inserted between Pulse Generator and Receiver.

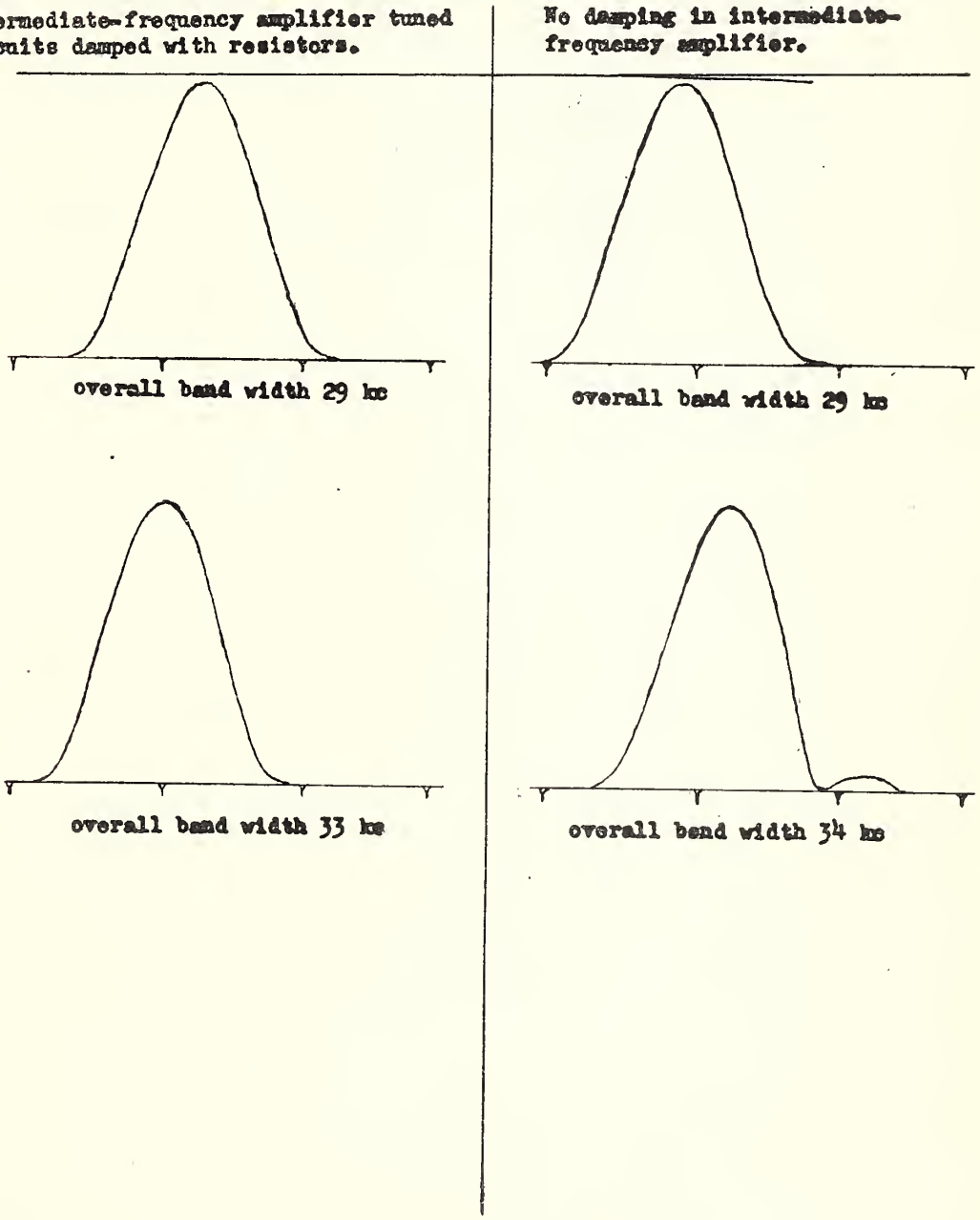

Fig. 35 (continued)

INTERSERVICE RADIO PROPAGATION LABORATORY
NATIONAL BUREAU OF STANDARDS
Washington, D.C.

Comparison of the Rise Time of a Loran-Type Pulse at the Indicator Oscilloscope with Different Adjustments of the Receiver Intermediate-Frequency Amplifier to Obtain the Same Band Widths.

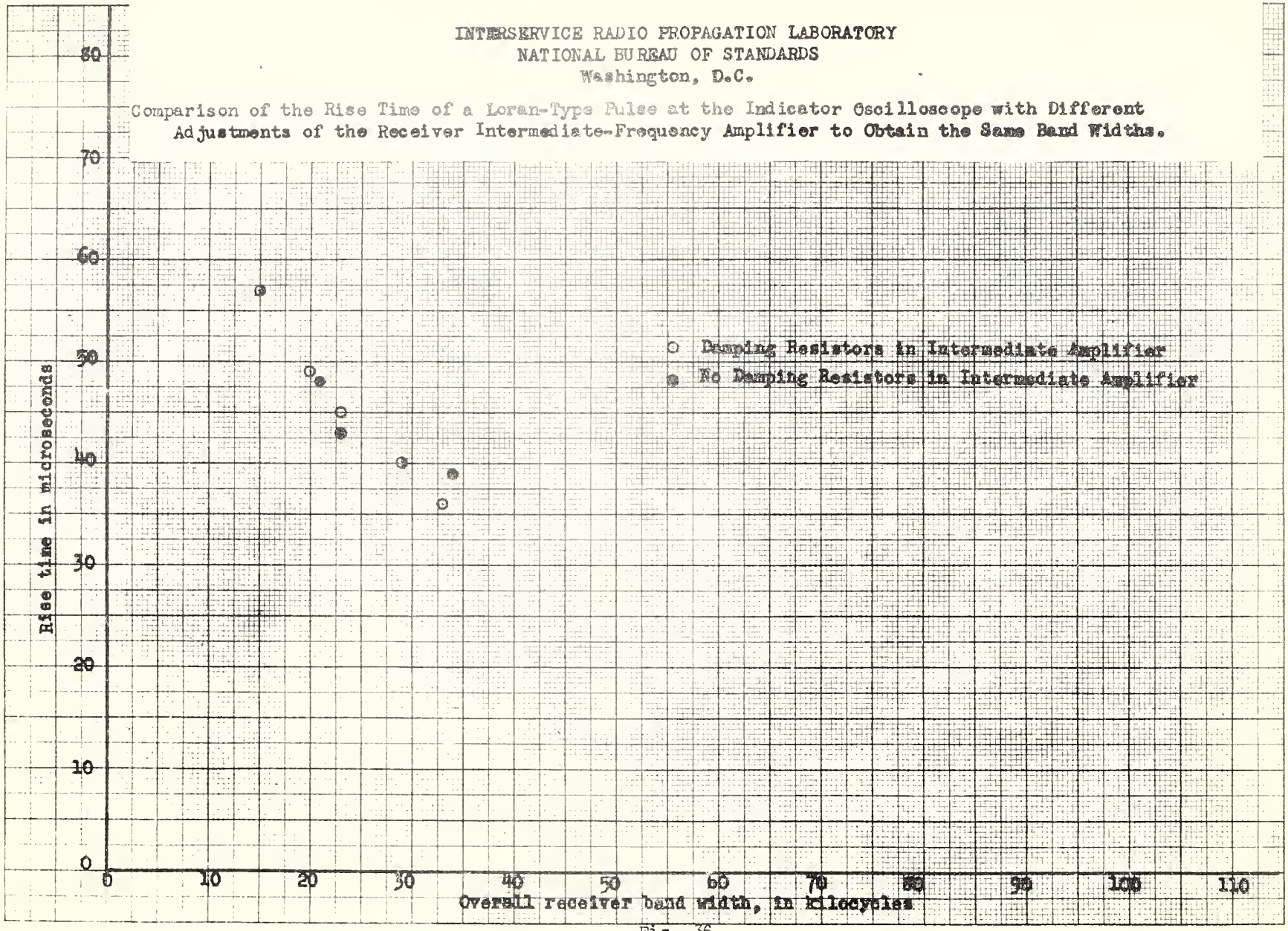

Fig. 36

INTERSERVICE RADIO PROPAGATION LABORATORY
NATIONAL BUREAU OF STANDARDS
Washington, D.C.

Comparison of the Pulse Length at One-Half Amplitude of a Loran-Type Pulse at the Indicator Oscilloscope with Different Adjustments of the Receiver Intermediate-Frequency Amplifier to Obtain the Same Band Widths.

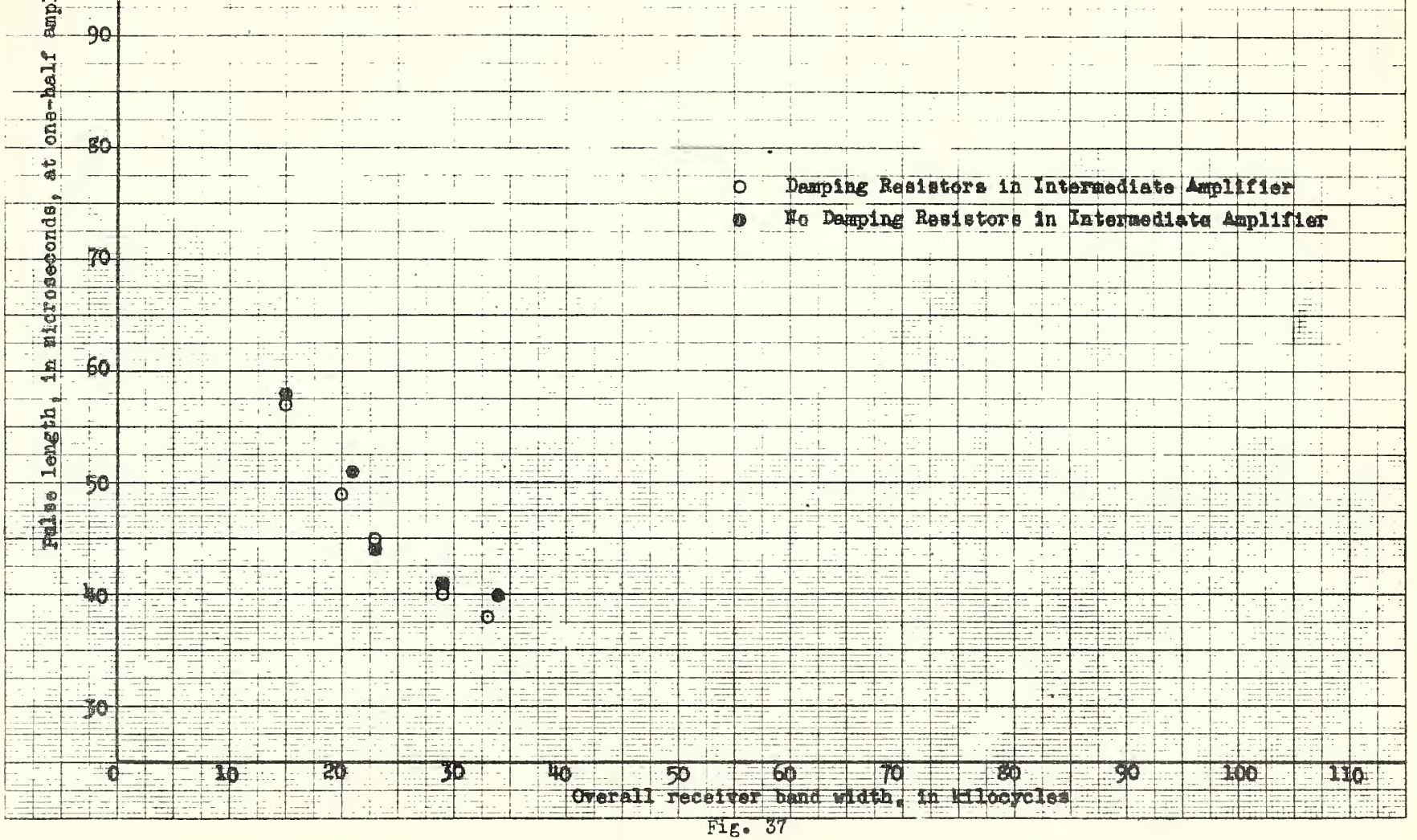

Fig. 37

INTERSERVICE RADIO PROPAGATION LABORATORY
NATIONAL BUREAU OF STANDARDS
Washington, D.C.

Comparison of the Base Length of a Loran-Type Pulse at the Indicator Oscilloscope with Different Adjustments of the Receiver Intermediate-frequency Amplifier to Obtain the Same Band Widths.

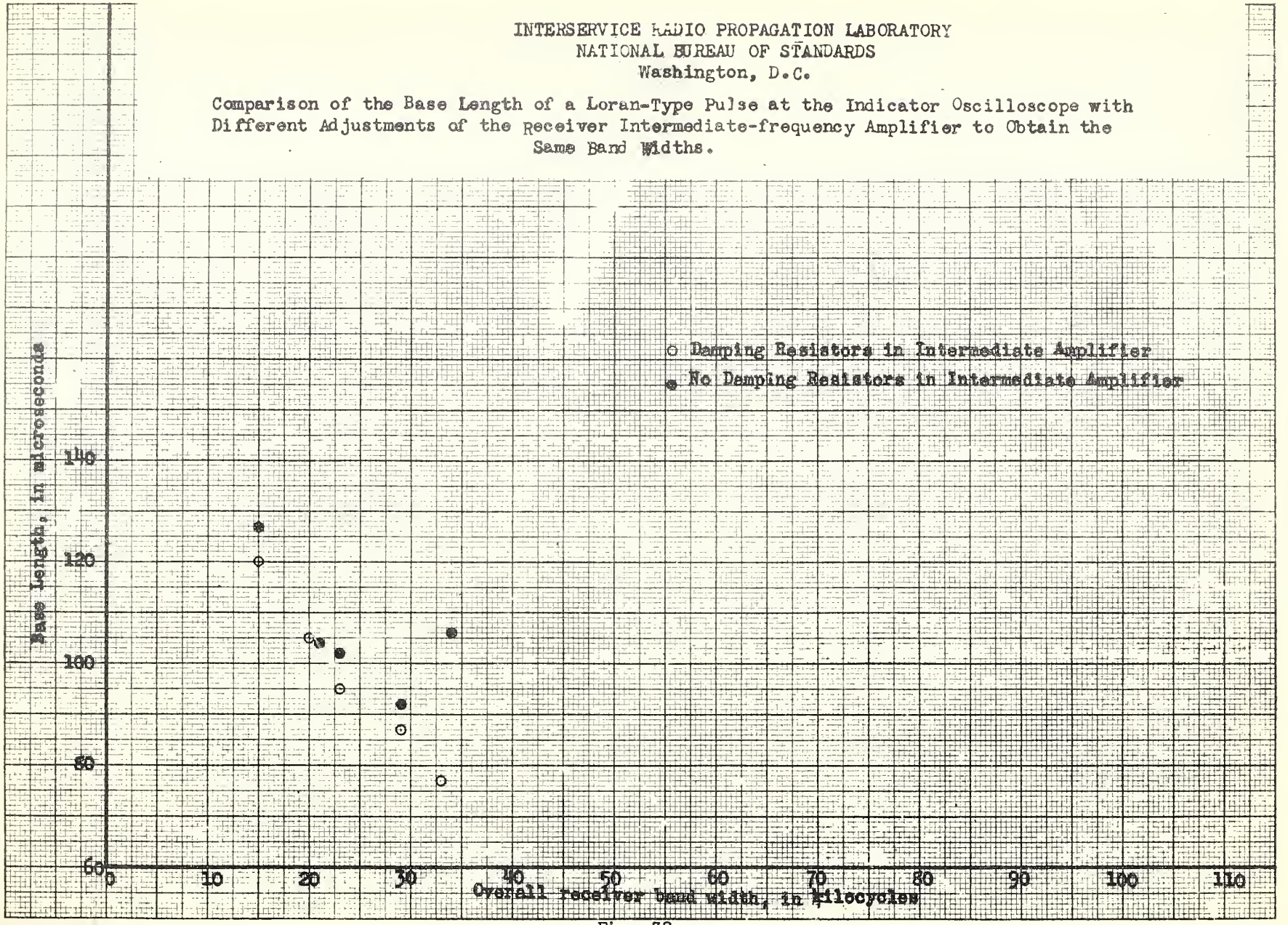

Fig. 38

INTERSERVICE RADIO PROPAGATION LABORATORY
NATIONAL BUREAU OF STANDARDS
Washington, D.C.

Comparison of the Rise Time of a Loran-Type Pulse at the Indicator Oscilloscope (Radio-Frequency Filter Inserted between Pulse Generator and Receiver) with Different Adjustments of the Receiver Intermediate-Frequency Amplifier to Obtain the Same Band Widths.

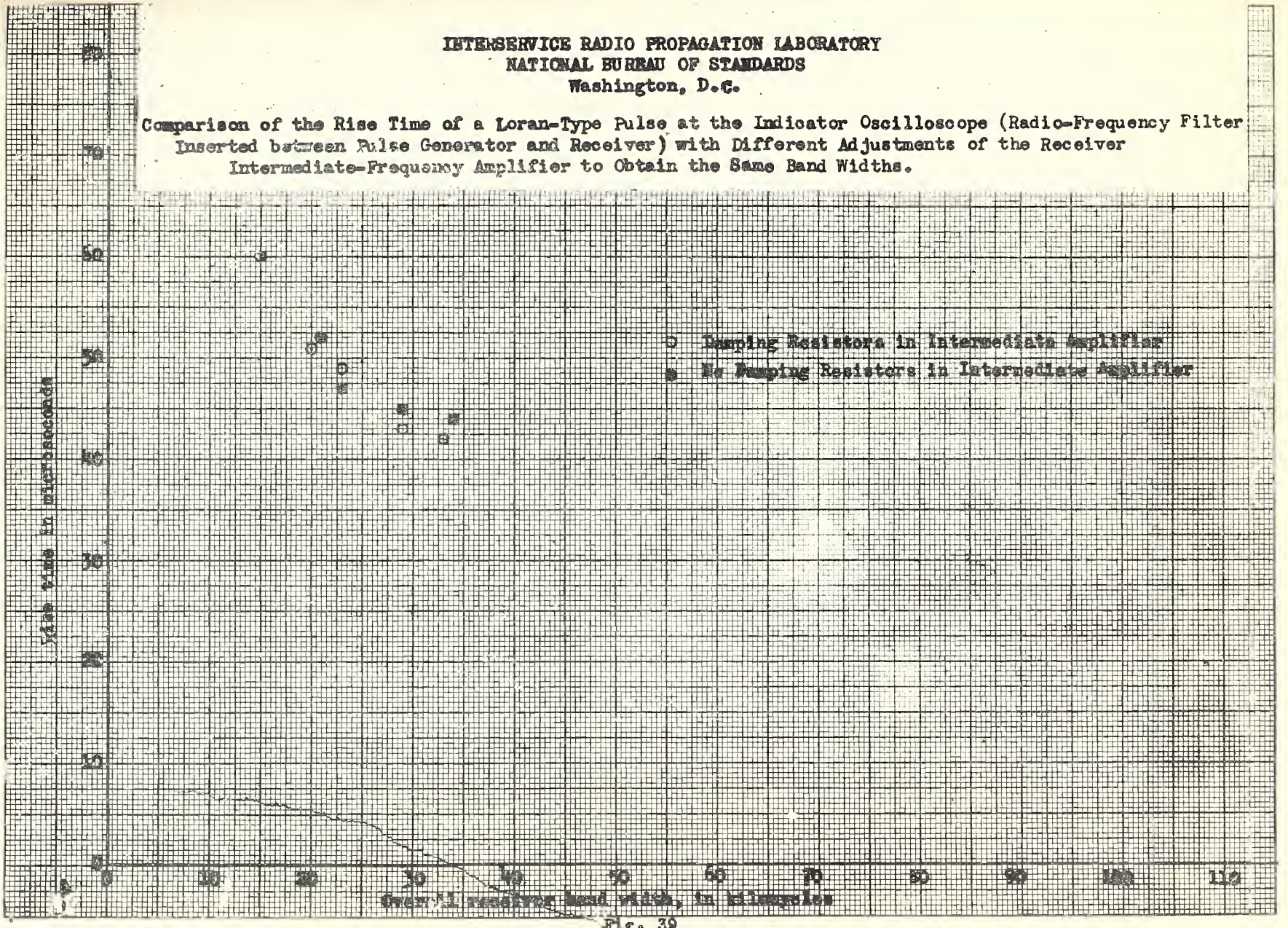

Fig. 39

INTERSERVICE RADIO PROPAGATION LABORATORY
NATIONAL BUREAU OF STANDARDS
Washington, D.C.

Comparison of the Pulse Length at One-Half Amplitude of a Loran-Type Pulse at the Indicator Oscilloscope (Radio-Frequency Filter Inserted between Pulse Generator and Receiver) with Different Adjustments of the Intermediate-Frequency Amplifier to Obtain the Same Band Widths.

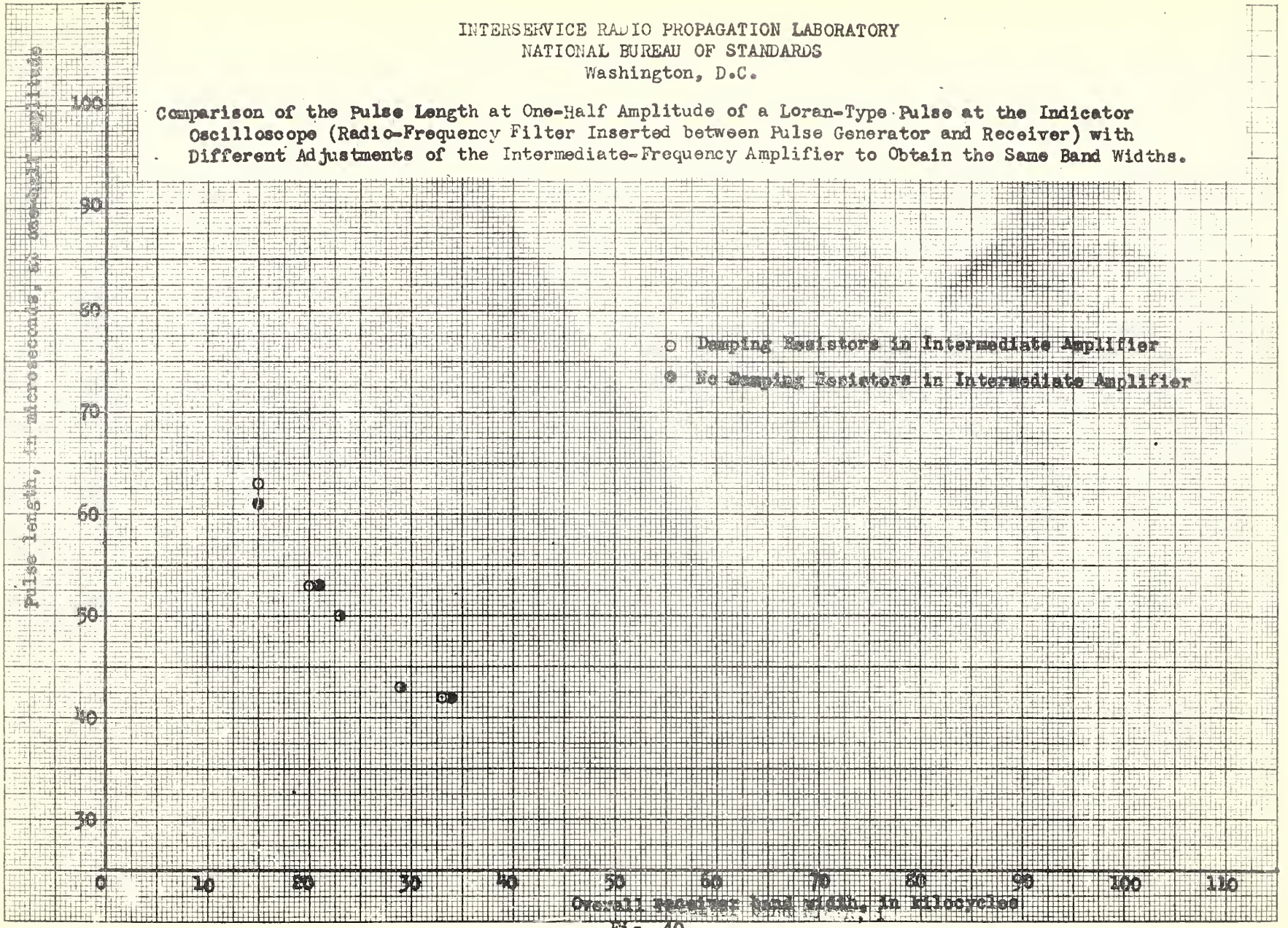

Fig. 40

INTERSERVICE RADIO PROPAGATION LABORATORY
NATIONAL BUREAU OF STANDARDS
Washington, D.C.

Comparison of the Base Length of a Loran-Type Pulse at the Indicator Oscilloscope (Radio-Frequency Filter Inserted between Pulse Generator and Receiver) with Different Adjustments of the Receiver Intermediate-Frequency Amplifier to Obtain the Same Band Widths.

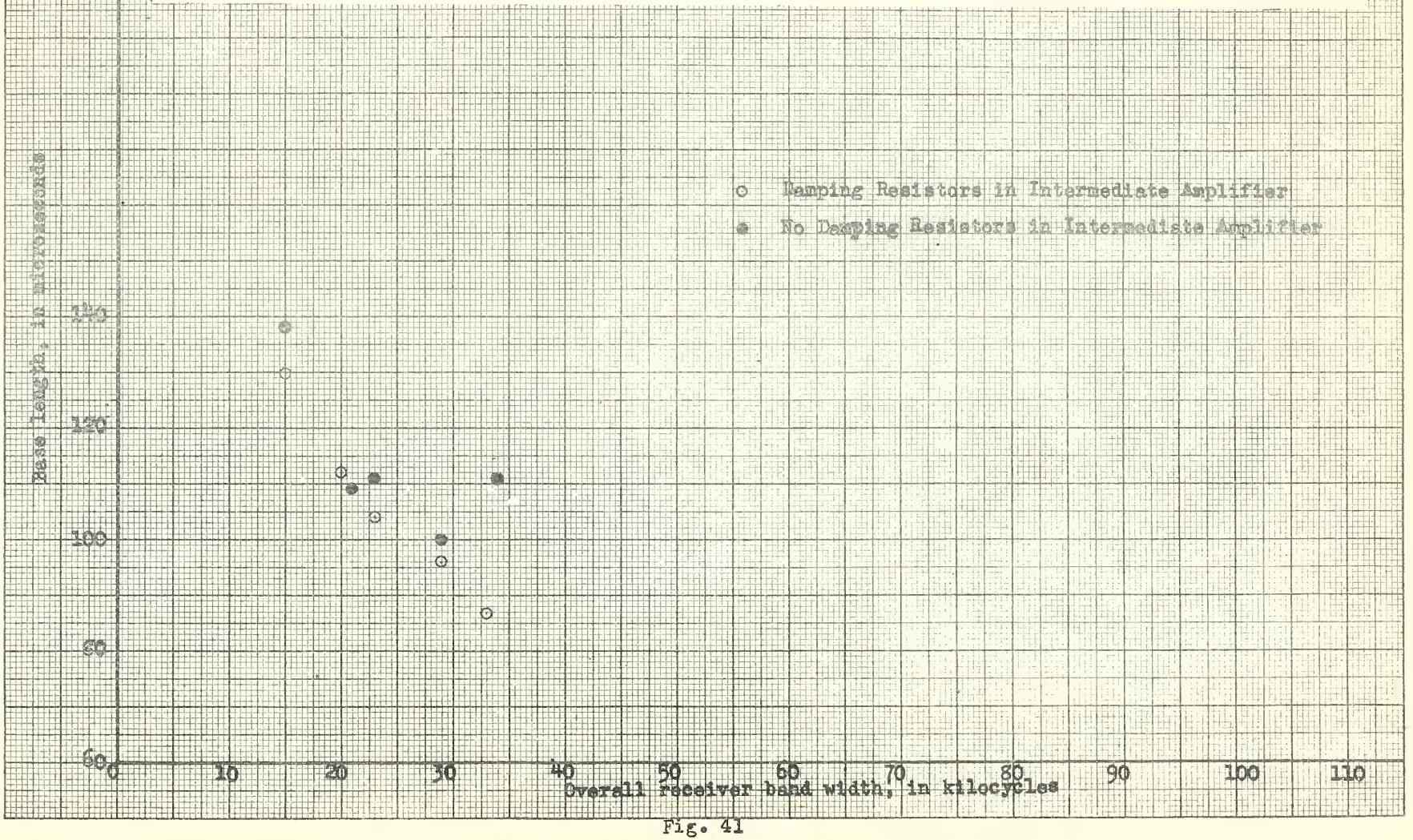

Fig. 41

INTERSERVICE RADIO PROPAGATION LABORATORY
NATIONAL BUREAU OF STANDARDS
Washington, D.C.

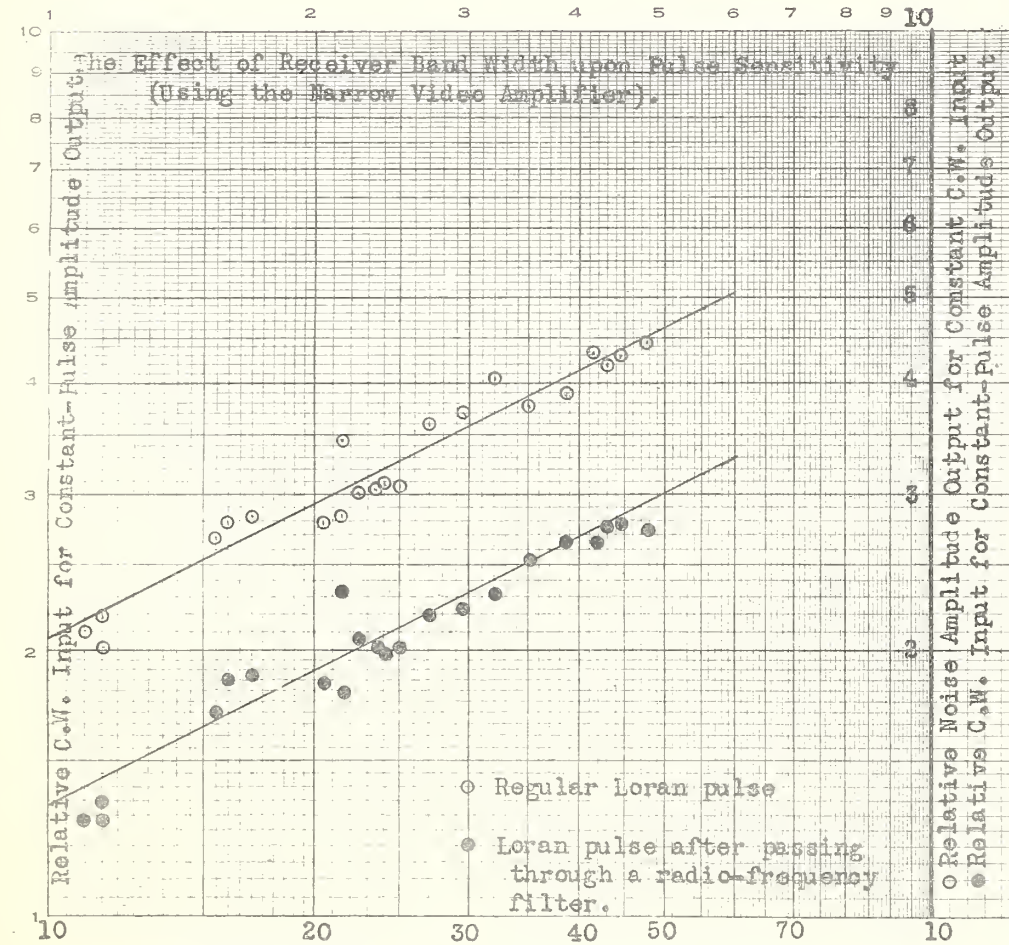

Fig. 42

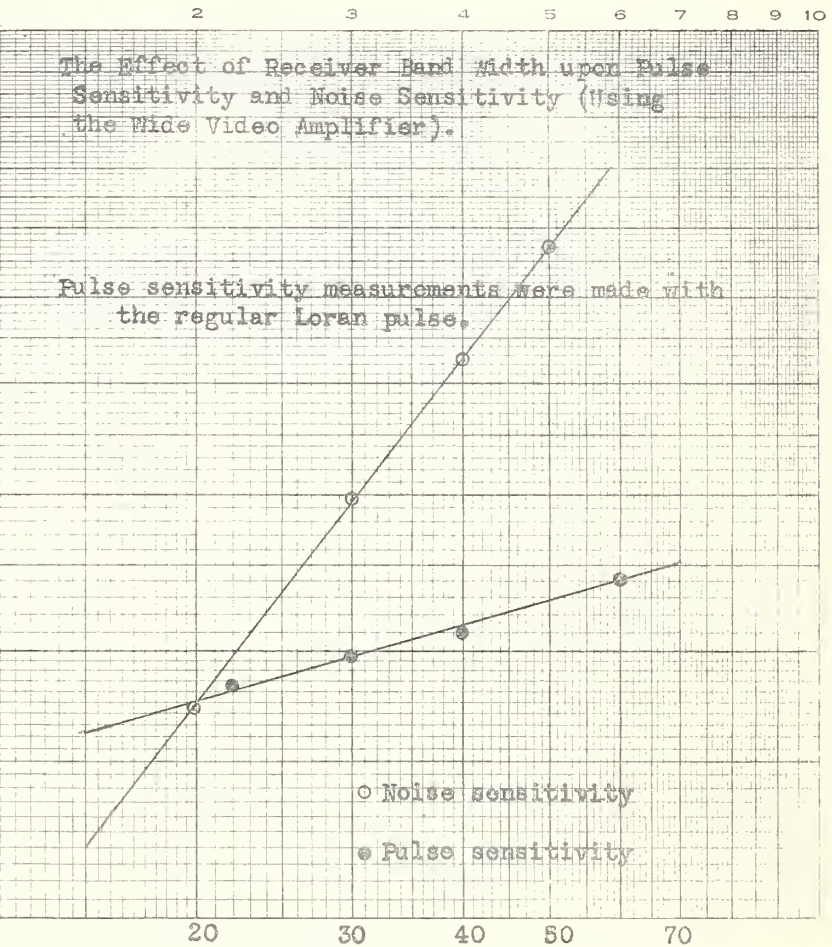

Fig. 43

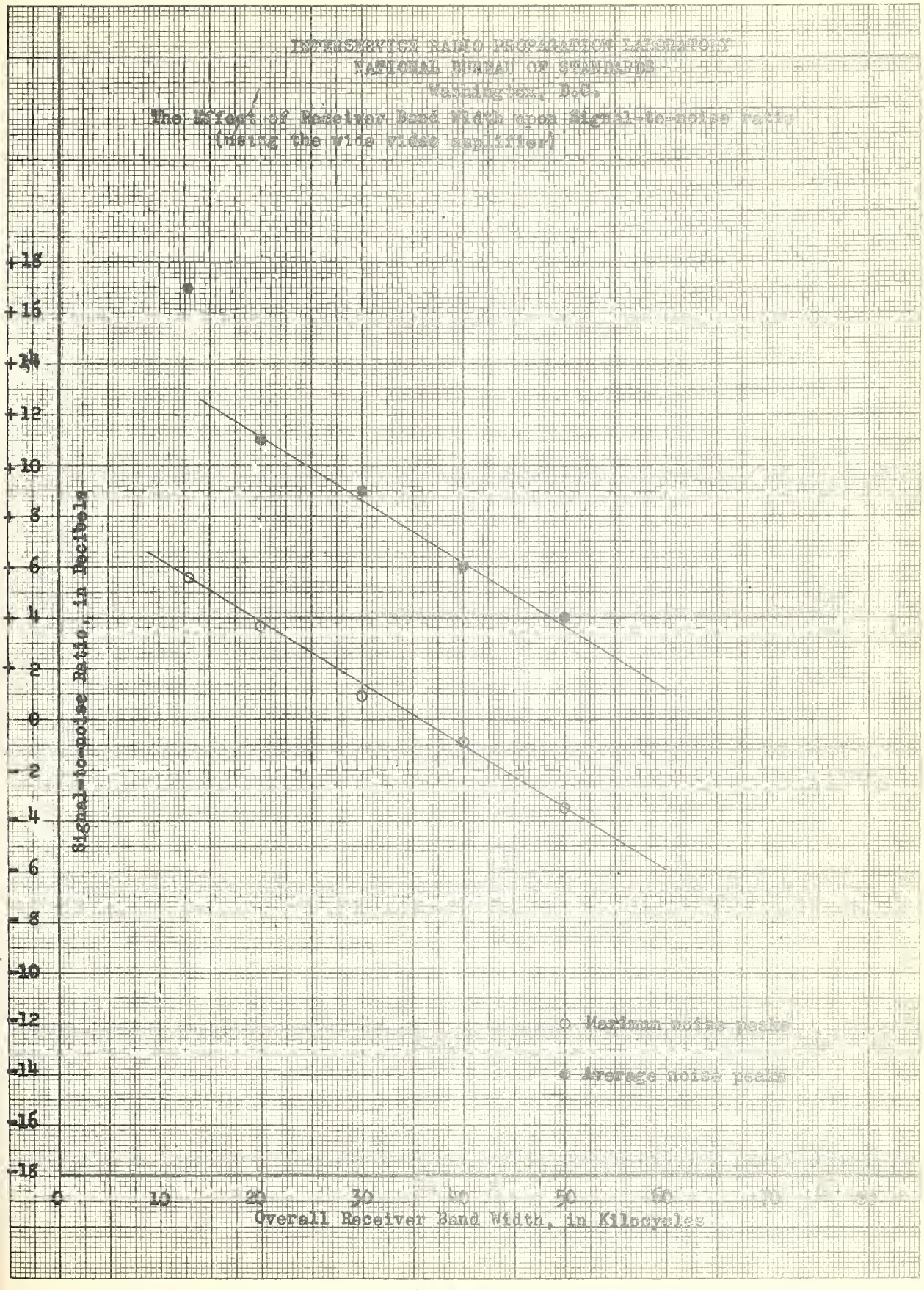
INTERSERVICE RADIO PROPAGATION LABORATORY
NATIONAL BUREAU OF STANDARDS
Washington, D.C.
The Effect of Receiver Band Width upon Signal-to-noise ratio
(Using the wide video amplifier)
+18
+16
+14
+12
+10
+8
+6
+4
+2
0
-2
-4
-6
-8
-10
-12
-14
-16
-18
Signal-to-noise Ratio, in Decibels
0
10
20
30
40
50
60
70
80
90
Overall Receiver Band Width, in Kilocycles
Maximum noise peaks
Average noise peaks

Fig. 44

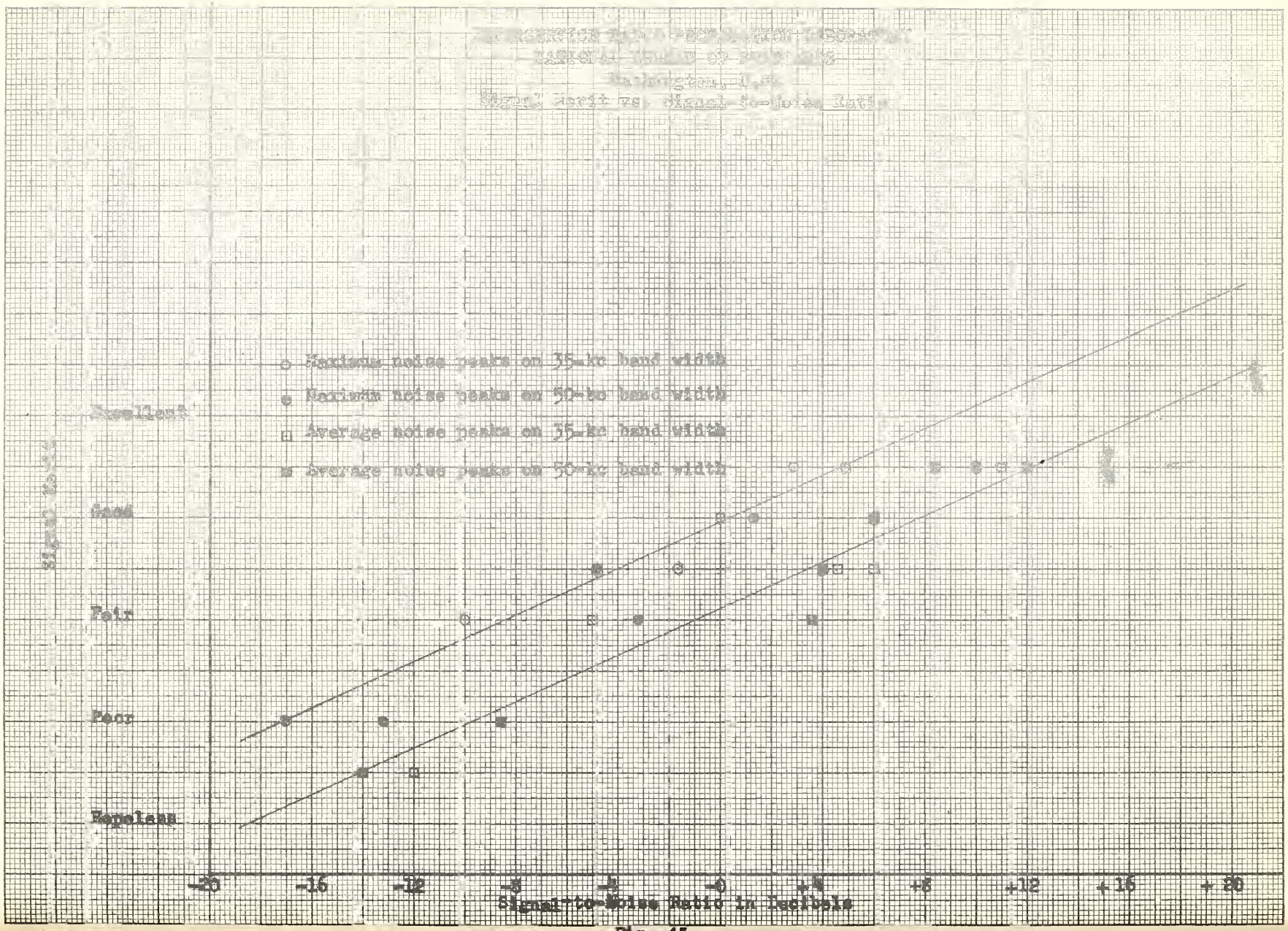
Maximum noise peaks on 75-kc band width
Maximum noise peaks on 50-kc band width
Average noise peaks on 75-kc band width
Average noise peaks on 50-kc band width
Excellent
Good
Fair
Poor
Unreliable
-20
-16
-12
-8
-4
-0
+4
+8
+12
+16
+20
Signal-to-Noise Ratio in Decibels

Fig. 45